The University of Manitoba

SOME APPLICATIONS OF EXPERIMENTAL AND THEORETICAL NUCLEAR SPIN-SPIN COUPLING CONSTANTS TO THE STUDY OF MOLECULAR STRUCTURE

by

Roderick Ernest Wasylishen

A Thesis

Submitted to

the Faculty of Graduate Studies and Research

The University of Manitoba

In Partial Fulfillment

of the Requirements of the Degree

DOCTOR OF PHILOSOPHY

Winnipeg, Manitoba

June, 1972

ACKNOWLEDGMENTS

I would like to express my gratitude to Dr. Ted Schaefer for his guidance and friendship during my tenure at Manitoba. It has been a privilege and pleasure to work with him and his group.

I would also like to thank Dr. Ludger Ernst and Dr. Brian Rowbotham for many interesting discussions and for the preparation of the aniline-^{15}N derivatives. I am grateful to Dr. Rowbotham for his assistance with some of the computer programming and to Dr. Ernst, who analyzed the n.m.r. spectra of all the aniline-^{15}N derivatives described here. In addition, thanks are due to Dr. Frank Hruska, Dr. Don Wood, Dr. C.E. Burchill, Mr. Jim Peeling, Mr. Bruce Goodwin, and Mr. Tom McCaig for advice on various matters.

I would especially like to thank my wife for typing this manuscript and for bearing with the author over the past four years.

The encouragement of my parents during my years at university is also gratefully acknowledged.

Finally I would like to thank the University of Manitoba and the National Research Council of Canada for financial assistance.

THESIS AND PUBLICATIONS

A study of benzene solvent-induced shifts in the proton magnetic resonance spectra of some substituted benzenes. M.Sc. Thesis. University of Manitoba. 1970.

Proton magnetic resonance spectrum of 2,6-dichlorobenzaldoxime. Signs and magnitudes of long-range spin-spin couplings. Degree of nonplanarity. T. Schaefer and R. Wasylishen. Can. J. Chem. 47, 3707 (1969).

Hydrogen bonding and long-range proton coupling constants in some ortho disubstituted aniline derivatives. Intramolecular proton exchange and degree of nonplanarity of the amino group. R. Wasylishen and T. Schaefer. Can. J. Chem. 48, 1263 (1970).

Signs of long-range amino proton-ring proton coupling constants in N-ethyl-4-chloro-2-nitroaniline. T. Schaefer and R. Wasylishen. Can. J. Chem. 48, 1343 (1970).

Benzene solvent-induced shifts of the proton magnetic resonance spectra of some benzene derivatives. Importance of charge effects. R. Wasylishen, T. Schaefer, and R. Schwenk. Can. J. Chem. 48, 2885 (1970).

Proton magnetic resonance spectrum of parafluorotoluene. Sigma and pi electron contributions to $J_p^{H,F}$. R. Wasylishen and T. Schaefer. Can. J. Chem. 49, 94 (1971).

Proton magnetic resonance of the methyl derivatives of 2-fluoropyridine. Sigma and pi electron contributions to spin-spin coupling constants. J.B. Rowbotham, R. Wasylishen, and T. Schaefer. Can. J. Chem. 49, 1799 (1971).

Nuclear magnetic resonance spectra, conformations, spin coupling mechanisms, and INDO molecular orbital calculations for the monofluorobenzaldehydes and some derivatives. R. Wasylishen and T. Schaefer. Can. J. Chem. 49, 3216 (1971).

Free energy barrier to rotation of the amino group in 2-aminoacetophenone. R. Wasylishen and T. Schaefer. Can. J. Chem. 49, 3575 (1971).

Proton magnetic resonance spectrum of 2-chloroaniline-^{15}N. Long range coupling constants to amino protons from all ring protons. R. Wasylishen and T. Schaefer. Can. J. Chem. 49, 3627 (1971).

Proton magnetic resonance spectra, conformational preferences and approximate molecular orbital calculations for the syn and anti 2-furanaldoximes. R. Wasylishen and T. Schaefer. Can J. Chem. 50, 274 (1972).

INDO molecular orbital calculations on the conformational dependence of long-range spin-spin coupling of methyl protons in toluene, p-fluorotoluene and the xylenes. Can. J. Chem. in press.

Long-range spin-spin coupling constants from amino protons and ^{15}N to ring protons in aniline-^{15}N and some derivatives. INDO molecular orbital calculations. R. Wasylishen, J.B. Rowbotham, L Ernst, and T. Schaefer. Can. J. Chem. in press.

INDO MO calculations of the conformational dependence of the vicinal $^{13}C,H$ spin-spin coupling constants in propane. R. Wasylishen and T. Schaefer. Can. J. Chem. in press.

INDO molecular orbital calculations of nitrogen-proton spin-spin coupling constants over two and three bonds. Effects of lone-pair orientation, of dihedral angles and of protonation. R. Wasylishen and T. Schaefer. Can. J. Chem. in press.

ABSTRACT

This thesis is concerned with some applications of experimental and theoretical nuclear spin-spin coupling constants to the study of molecular structure.

In Part I precise analyses of the proton and some fluorine magnetic resonance spectra in acetone solution are reported for the three monofluorobenzaldehydes as well as for 2-chloro-6-fluorobenzaldehyde and for 4-fluoro-2-nitrobenzaldehyde. The conformational dependence of the coupling parameters allows the measurement of energy differences between the O-cis and O-trans conformations. The energy differences are in better agreement with the INDO predictions than they are with energies derived from i.r. data. Dipole moments are computed reliably and their measurement is suggested as a good guide to conformational preferences for molecules of this kind. The spin-spin coupling constants between the aldehyde proton and the ring protons and fluorine nuclei are computed for benzaldehyde and the three monofluorobenzaldehydes by the INDO and CNDO molecular orbital approximations. In many instances the agreement between calculated and observed couplings is quantitative.

In Part II a complete analysis (8-spins) is given of the proton magnetic resonance spectrum of aniline-^{15}N, of the spectra of some haloanilines-^{15}N and of 2-aminoacetophenone-^{15}N. Intermolecular exchange of the amino protons is slow enough for observation of their spin-spin coupling to the ring protons. The magnitudes of the coupling constants between amino protons and ^{15}N or ring protons are a measure

of the geometry of the amino group. This is not true of the couplings between ^{15}N and the ring protons. Long-range couplings computed in the CNDO/2 and INDO approximations of molecular orbital theory show points of agreement with experiment. For example, their signs and magnitudes are consistent with a nonplanar but not with a planar conformation of aniline. Couplings from ^{15}N to ring protons are also computed for nitrobenzene.

In Part III molecular orbital theory at the INDO level of approximation is used to calculate the Fermi contact contribution to two-bond and three-bond nitrogen-proton coupling constants for a wide variety of compounds. The dependence of calculated N,H coupling constants upon the spatial orientation of the nitrogen lone-pair is examined for selected molecules. For both saturated and unsaturated compounds the calculated $^{2}J(^{15}N,H)$ is large and negative when the lone-pair is oriented cis to the proton, and is small and of either sign when the lone-pair lies trans to the proton. Calculated $^{3}J(N,H)$ depends both on the orientation of the nitrogen lone-pair and on the HCCN dihedral angle. Computed $^{2}J(N,H)$ and $^{3}J(N,H)$ generally follow the experimentally known substituent and structural effects. It is suggested that observed phosphorus-proton coupling constants in tervalent phosphorus compounds are dependent on lone-pair orientation in a manner analogous to the corresponding nitrogen-proton coupling constants. The influence of the nitrogen lone-pair orientation on geminal proton-proton coupling constants in methylamine is computed and compared with experiment. Calculated barriers to pyramidal inversion and methyl group rotation are in reasonable agreement with available experimental data.

In Part IV the conformational dependence of the nuclear spin-spin coupling from methyl protons to ring protons, to the fluorine nucleus, and to protons of other methyl groups in toluene, p-fluorotoluene, and the xylenes is computed by the finite perturbation technique in the INDO approximation of molecular orbital theory. The calculated coupling over six bonds to the proton in the para position agrees quantitatively with experiment and its predicted dependence on the rotational angle of the methyl group supports a commonly assumed π electron mechanism for the transmission of spin information between the nuclei. Similar remarks apply to the fluorine nucleus in p-fluorotoluene. The couplings over five and four bonds to the protons in the meta and ortho positions display a more complex angular dependence and the former can be interpreted in terms of a dominant σ electron mechanism. The coupling between protons in different methyl groups in the ortho and meta xylenes is calculated as rather larger than the values observed in their derivatives and in the main shows the behavior expected from a π electron mechanism. Those conformations of ortho xylene in which the coupled protons are in close proximity yield computed values plausibly attributable to "direct" and/or "through-space" mechanisms. The preferred conformation of the methyl group in toluene is predicted to have a C-H bond eclipsing the plane of the aromatic ring and the calculated barriers to rotation of 0.013 kcal/mol in toluene and of 0.014 kcal/mol in p-fluorotoluene are in quantitative accord with microwave data.

TABLE OF CONTENTS

LIST OF TABLES

LIST OF FIGURES

INTRODUCTION

Scope

Indirect nuclear spin-spin interactions were first observed in 1951 by Gutowsky and McCall (1) and by Hahn and Maxwell (2). The interaction energy between two nuclei in the liquid phase, where rapid tumbling is present, has been found experimentally to have the form

$$E_{ij} = h\, J_{ij} \vec{I}_i \cdot \vec{I}_j$$

where J_{ij} is defined as the coupling constant between nuclei i and j, $\vec{I}_i$ is the total spin angular momentum of nucleus i, and h is Planck's constant. Typically the energy involved in nuclear spin-spin coupling is relatively small - at most a few erg/mol, and often much less.

For fluids Ramsey and Purcell (3) proposed that nuclear spins interact through magnetic polarization of the spins of nearby molecular electrons. The theory of these nuclear spin - nuclear spin interactions, as originally formulated by Ramsey (4), is based on three types of interactions between the electron and nuclear spins: (i) a magnetic dipole-dipole interaction, (ii) an orbital-dipole interaction between the magnetic fields due to the orbital motion of the electrons and the nuclear magnetic dipole, and (iii) a Fermi contact interaction between the electron and nuclear spins. If protons are involved the Fermi contact term seems to be predominant.

Because nuclear spins interact via intervening electrons it is not surprising that the signs and magnitudes of nuclear spin-spin coupling constants are dependent on molecular structure. One of the best known relationships between molecular structure and J is

given by the Karplus equation (5, 6), which relates the three-bond proton-proton coupling constant, $^{3}J(H,H)$, in the saturated HCCH fragment to the dihedral angle. This and other relationships between molecular structure and coupling constants have been reviewed (7-13) and will not be discussed further in this section.

In practice, the utilization of spin-spin coupling constants for the determination of molecular structure involves two separate problems, viz., the determination of their signs and magnitudes, and the deduction of structural relationships from them. The first problem, that of spectral analysis, has been discussed in several excellent reviews (14-18) and will not concern us here. It should be pointed out, however, that with the advent of high resolution n.m.r. spectrometers operating at magnetic fields up to 70.5 kG (7.05 tesla) and the availability of computer programs (17, 19) for analyzing complex spectra, reliable spin-spin coupling constants are now readily available. In order to deduce useful empirical relationships between observed coupling constants and molecular structure, the experimentalist must obtain accurate coupling constants from a set of model compounds of known geometry. Often it is difficult to obtain a satisfactory model system since the conformations of interest may not be stable, or the required compounds may not exist or be readily available.

The potential value of a reliable method for the calculation of coupling constants is obvious. It would allow the experimentalist to anticipate the effects of various bond angles, bond lengths, and substituents on coupling constants. Until recently the calculation of

coupling constants has not been particularly encouraging.[1] Most calculations have been very tedious and involve several questionable approximations. Recently Pople's group (22, 23) has demonstrated that reliable proton-proton coupling constants over two and three bonds can be calculated using SCF-MO theory and INDO wavefunctions (24). Although the calculations were not quantitative, experimental trends were reproduced. It was felt that the semiempirical MO method of Pople et al. (22) showed promise and that it should be further tested on a wide variety of molecules.

In Part I of this dissertation the long-range ring proton - aldehyde proton coupling constants are measured in the monofluorobenzaldehydes and compared with the values calculated using the method of Pople, McIver, and Ostlund (22). In addition the experimental results are used to deduce the conformational preference of the aldehyde group. In Part II the effect of structural changes on observed and calculated ^{15}N-H and H-H coupling constants in aniline and some aniline derivative are considered. In Part III nitrogen-proton spin-spin coupling constants are calculated over two and three bonds for a wide variety of compounds. The effects of lone-pair orientation, of dihedral angles, and of nitrogen protonation on these coupling constants are examined. Finally in Part IV the conformational dependence of long-range spin-spin coupling constants of methyl protons in toluene,

---

[1] For a review of work prior to 1968 which is concerned with the theory and calculation of nuclear spin-spin coupling the reader is referred to references 20 and 21.

p-fluorotoluene, and the xylenes is discussed.

Prior to Part I a brief discussion of the method used for the calculation of coupling constants may be helpful.

Calculation of Coupling Constants

All coupling constants calculated in this thesis were calculated using the finite perturbation technique (22) and semiempirical SCF-MO theory. Both CNDO/2 and INDO wave functions were employed (24). In the finite perturbation formalism the calculation of the Fermi contact contribution to a nuclear spin coupling, J_{AB}, involves the calculation of an open-shell molecular orbital wave function under the influence of the perturbation

$$h_B = (8\pi/3)\beta\mu_B S_B^2(0)$$

due to the presence of a nuclear moment μ_B. In this theory, the implementation of the perturbation simply involves the addition of the contact perturbation h_B to the diagonal matrix element representing the s orbital of atom B of the Fock matrix corresponding to electrons of α spin. This term is subtracted from the corresponding element of the Fock matrix for electrons of β spin. This perturbation, h_B, at atom B, has the effect of introducing a very small spin density, ρ^{spin}, throughout the molecular electron system. The nuclear spin-spin coupling constant, J_{AB}, is then proportional to the value of the spin density $\rho^{spin}_{S_A S_A}$ transmitted to the second nucleus, A. This may be represented schematically as shown in 1 [2] and by Equation 1,

---

[2] In Appendix 1 the transmission of unpaired spin density in the toluene molecule is discussed.

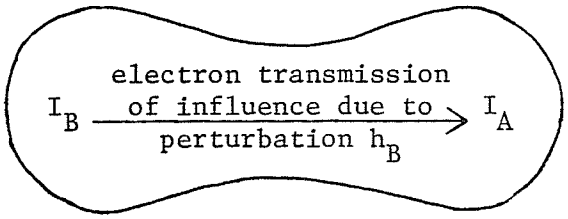

1

$$J_{AB} = (\text{constant}) \left[\partial \rho^{\text{spin}}_{S_A S_A}(h_B)/\partial h_B \right] h_B=0 \qquad (1)$$

where $\rho^{\text{spin}}_{S_A S_A}(h_B)$ is the diagonal element of the spin density matrix corresponding to the valence s orbital. Using the method of finite differences, Pople, McIver, and Ostlund (22) have shown that the derivative in Equation 1 can be approximated by $\rho^{\text{spin}}_{S_A S_A}(h_B)/h_B$. The complete expression for the coupling constant J_{AB} (in Hz) is approximated by the expression

$$J_{AB} = \hbar/2 \left[(8\pi/3)\beta \right]^2 \gamma_A \gamma_B S_A{}^2(0)\, S_B{}^2(0) \left[\rho_{S_A S_A}(h_B)/h_B \right]. \qquad (2)$$

The error in the approximation has a minimum when h_B is approximately 10^{-3} hartrees (22). γ_A and γ_B are the magnetogyric ratios of nuclei A and B; β is the Bohr magneton and $S_A{}^2(0)$ and $S_B{}^2(0)$ are the valence s-orbital electron densities of atom A and atom B at their respective nuclei.

Pople et al. (22) make the reasonable assumption that the valence s-orbital densities $S_A{}^2(0)$ and $S_B{}^2(0)$ are invariant from molecule to molecule and depend only on the nature of the atoms A and

B. The valence s-orbital densities used here are the semiempirical ones given in reference 22. All coupling constants are calculated using Equation 2 with the same integral parameterization as used previously by Pople et al. (22-24).

As all other terms in Equation 2 are taken as constant, it is the sensitivity of the spin density in the orbital S_A to the presence of the perturbation h_B which determines the spin-spin coupling constants. Because h_B is small, the spin densities are extremely small and therefore the spin density matrix must be known very accurately in the calculation of coupling constants. For example, for nitrogen-proton coupling constants, $J(^{14}N,H) = 141174.7016 \times \rho^{spin}_{H_S H_S}$ Hz when $h_N = 10^{-3}$ hartrees. In order to obtain reasonably accurate coupling constants the usual energy criterion for convergence of the SCF iteration was not used. Instead, either the coupling constants were printed out after each SCF cycle and/or the following criterion was used

$$10^{-4} \leqslant \rho^{old}_{ii} - \rho^{new}_{ii} / \rho^{old}_{ii} \qquad (3)$$

for all i. With this criterion one can estimate the accuracy of the calculated coupling constants since J_{AB} is directly proportional to ρ^{spin}_{AA}/h or ρ^{spin}_{BB}/h depending on whether A or B is perturbed. For example, consider the accuracy of a calculated $J(^{14}N,H)$ with a magnitude of 14.12 Hz. If the convergence criterion given by Equation 3 is satisfied then the change in $J(^{14}N,H)$ in one SCF cycle is less than 0.00141 Hz. In cases where the coupling constants were printed out after each SCF cycle, convergence was usually considered complete when coupling constants did not change by more than 0.01 Hz in 10 SCF cycles. The SCF procedure was limited to a maximum of 100 cycles

because of the expence of these calculations.

The input data for a calculation required the cartesian coordinates of all atoms, the total charge, and the multiplicity of the molecule. Since the calculated coupling constants were often very sensitive to the molecular geometry, an attempt was made to use the best available structural parameters. The atomic coordinates were usually calculated from these structural parameters with the aid of the "Model-Builder" program MBLD (25). The sources of the structural parameters or atomic coordinates are given in the appropriate tables and are discussed in the text.

All calculations were carried out on an IBM 360/65 computer.

REFERENCES FOR THE INTRODUCTION

1. H.S. Gutowsky and D.W. McCall. Phys. Rev. 82, 748 (1951).
2. E.L. Hahn and D.E. Maxwell. Phys. Rev. 84, 1246 (1951).
3. N.F. Ramsey and E.M. Purcell. Phys. Rev. 85, 143 (1952).
4. N.F. Ramsey. Phys. Rev. 91, 303 (1953).
5. M. Karplus. J. Chem. Phys. 30, 11 (1959).
6. M. Karplus. J. Am. Chem. Soc. 85, 2870 (1963).
7. L.M. Jackman and S. Sternhell. Applications of nuclear magnetic resonance spectroscopy in organic chemistry. 2nd Edition. Pergamon Press, Oxford, 1969.
8. S. Sternhell. Quart. Rev. 23, 236 (1969).
9. M. Barfield and B. Chakrabarti. Chem. Rev. 69, 757 (1969).
10. A.A. Bothner-By. Advan. Mag. Res. 1, 195 (1965).
11. G.R. Bedford. Ann. Rev. NMR Spectroscopy, 4, 1 (1971).
12. H. Booth. Prog. NMR Spectroscopy, 5, 149 (1969).
13. F.A.L. Anet and R. Anet. In Determination of organic structures by physical methods. Edited by F.C. Nachod and J.J. Zuckerman. Academic Press, New York, N.Y., Vol. 3, p.343, 1971.
14. J.D. Swalen. Prog. NMR Spectroscopy, 1, 205 (1966).
15. Y.K. Pan and M.T. Rogers. Rev. Pure and Appl. Chem. 18, 17 (1968).
16. E.D. Bishop. Ann. Rev. NMR Spectroscopy, 1, 91 (1968).
17. C.W. Haigh. Ann. Rev. NMR Spectroscopy, 4, 311 (1971).
18. R.J. Abraham. Analysis of high resolution NMR spectra. Elsevier Publishing Company, Amsterdam, 1971.

19. Quantum Chemistry Program Exchange Catalog and Procedures, Vol. VII (1972), Indiana University Chemistry Department, Bloomington, Indiana.

20. J.N. Murrell. Prog. NMR Spectroscopy. 6, 1 (1971).

21. M. Barfield and D.M. Grant. Advan. Mag. Res. 1, 149 (1965).

22. J.A. Pople, J.W. McIver, Jr., and N.S. Ostlund. J. Chem. Phys. 49, 2960, 2965 (1968).

23. G.E. Maciel, J.W. McIver, Jr., N.S. Ostlund, and J.A. Pople. J. Am. Chem. Soc. 92, 4151, 4497, 4506 (1970).

24. J.A. Pople and D.L. Beveridge. Approximate molecular orbital theory. McGraw-Hill Book Company, New York, N.Y., 1970.

25. Program 135. Quantum chemistry program exchange. Indiana University, Bloomington, Indiana.

PART I

Nuclear Magnetic Resonance Spectra, Conformations, Spin Coupling Mechanisms, and INDO Molecular Orbital Calculations for the Monofluorobenzaldehydes and some Derivatives

INTRODUCTION

The spin-spin coupling constants over six bonds between ring protons and methyl protons in toluene derivatives are dominated by π electron contributions, which are also important in the analogous couplings to ortho and meta ring protons (1). In benzaldehyde, on the other hand, the coupling between the aldehydic protons and the para ring protons is not sensibly different from zero (2) but the coupling over five bonds to the meta protons is strongly stereospecific and is probably dependent on a σ electron mechanism (3-5).

The spin-spin coupling constants between fluorine nuclei and methyl protons in derivatives of the fluorotoluenes depend primarily on a π electron mechanism, their signs being opposite to the analogous ring proton - methyl proton couplings in the toluenes. The sign opposition has its reasonable origin in the signs of the hyperfine interaction constants: $Q_{CF} > 0$ and $Q_{CH} < 0$ (6). In brief, $^{4,6}J^{H,CH_3}_{o,p} < 0$, $^{4,6}J^{F,CH_3}_{o,p} > 0$, $^{5}J^{H,CH_3}_{m} > 0$, $^{5}J^{F,CH_3}_{m} < 0$, $^{5}J^{H,CHO}_{m} > 0$, $^{6}J^{H,CHO}_{p} = 0$, where left superscripts give the number of bonds intervening between the coupled nuclei, indicated in the right superscript. In the right subscripts, o, m, and p signify ortho, meta, and para positions of the substituents relative to the fluorine or proton ring positions.

A recent sign determination gave $^{6}J^{F,CHO}_{p} < 0$ in p-fluorobenzaldehyde (7) suggesting a negative Q value for an aldehyde group coplanar with the ring if this is indeed a π electron coupling. On the other hand, the sign sequence of fluorine-proton couplings in pentafluorobenzaldehyde (8) is evidently the same as in the fluoro-

toluene derivatives (6) but with a much larger magnitude of $^{5}J_{m}^{F,CHO}$ than of $^{5}J_{m}^{F,CH_3}$. A resolution of this apparent contradiction and a base for the more general study of the coupling mechanisms in benzaldehyde derivatives (9) demands reliable coupling data for the three monofluorobenzaldehydes. A careful analysis of the p.m.r. spectra of these compounds, as well as of two of their derivatives,is reported here. Fluorine spectra are reported where necessary.

The model in which σ and π electron mechanisms for the couplings are separately considered is very successful for the toluene (1), fluorotoluene (6, 10), and fluoropicoline (11) derivatives.[1] In this model, ring substituents affect spin couplings between ring protons and between ring protons and ring fluorine substituents, primarily via a polarization of the σ system (12, 13); while their effect on long-range couplings between side-chain nuclei and ring protons or fluorine substituents is much less marked. It is of interest to discover whether such a simple model can also be used in discussing the couplings in benzaldehyde derivatives. Therefore, INDO and CNDO molecular orbital methods (13 -15)are used to compute the long-range couplings between the aldehyde proton and the ring protons and fluorine nuclei. The differences between the couplings found by the two methods are an indication of the π electron contribution to the couplings (14).

Conformational preferences are deduced from the observed long-range couplings over five bonds.

---

[1] See Part IV.

EXPERIMENTAL

The compounds were obtained commercially and were used without further purification, except for the nitro derivative from which ferromagnetic dust had to be removed. Thirty mol percent solutions in acetone-d_6, containing tetramethylsilane (TMS) as an internal reference, were degassed by the freeze-pump-thaw technique. Other solvents that were tried gave very tightly coupled spectra and made an accurate analysis difficult at 100 MHz. At 60 MHz even the acetone solutions did not allow completely reliable analyses in one or two cases.

The p.m.r. spectra were recorded in the frequency sweep mode on an HA100-D spectrometer at a probe temperature of 30 ± 1°C. The calibration procedure is described for m-fluorobenzaldehyde and applies to the other compounds. The ring proton peak positions were determined by reading manual and sweep oscillator frequencies at intervals of less than 3 Hz, each peak being calibrated at least five times. Proton resonance peaks were normally less than 0.12 Hz wide at half-height. The aldehyde proton peaks were calibrated ten times. The average standard deviations of the measured peak frequencies were 0.017 Hz for the protons and 0.019 Hz for the aldehyde protons (this compares with an r.m.s. error of 0.019 Hz in the analysis, see below). Sweep rates were 0.01 Hz/s.

Some spectra were also recorded at 60 MHz on a DA60-I spectrometer at a probe temperature of 31 ± 1°C. Fluorine resonance spectra were measured on an A56-60 spectrometer at a probe temperature of 32 ± 1°C. When the solutions were prepared it was not considered

that fluorine spectra would be required and therefore no internal fluorine reference material was present. At any rate, the observed fluorine spectra were needed only to confirm the sign of certain coupling constants. The fluorine resonance peaks were normally less than 0.20 Hz wide at half-height.

Certain decoupling and tickling experiments were carried out in the usual way (16).

RESULTS AND DISCUSSION

1. Analysis of Spectra

a) p-Fluorobenzaldehyde

The proton resonance is the $[AB]_2X$ part of an $[AB]_2XR$ spectrum and was analyzed using the computer program LAOCN3 (17) in a manner similar to the analysis recently described for p-fluorotoluene (10). Of the 128 calculated transitions with intensity greater than 0.01, 106 were assigned to experimental peaks. The r.m.s. error was 0.012 Hz when all parameters were allowed to vary in the iteration. The probable error in all parameters was less than or equal to 0.003 Hz. The final parameters are given in Table 1. Extensive tickling experiments (16) confirmed the negative sign of $^6J_p^{F,CHO}$.

b) 2-Nitro-4-fluorobenzaldehyde

The analysis of the proton resonance spectrum using LAME (18) was straightforward except that the peaks from the ring proton ortho to the nitro group were somewhat broadened by incompletely relaxed coupling to the quadrupolar ^{14}N nucleus. This means that the shift of this proton, H_3, is precise to only ± 0.1 Hz and that $J_o^{H3,F}$ is known to only ±0.1 Hz. All of the 48 transitions for H_1, H_5, and H_6 were assigned. The r.m.s. error between observed and calculated transitions was 0.007 Hz. Three elements in the correlation matrix were greater than 0.05 and these lay between 0.05 and 0.17. The probable error was 0.004 Hz or less for all but the two parameters above and the error in the small $^6J_p^{H,CHO}$ is realistically put at 0.02 Hz. Final parameters are tabulated in Table 1.

TABLE 1. Spectral parameters in Hz for 30 mol % solutions in acetone-d_6

Parameter*	Compound				
	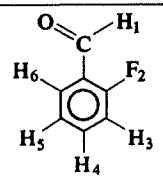	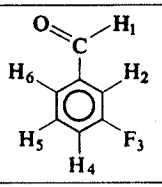	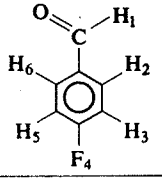	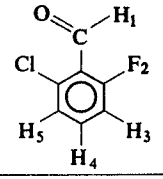	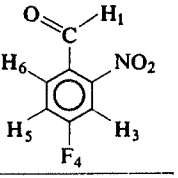
ν_1	1030.934	1002.39±0.02	1000.540	1038.202	1024.562
ν_2	—	757.556	797.565	—	—
ν_3	724.058	—	728.877	721.070	785.5
ν_4	767.844	738.907	—	763.131	—
ν_5	731.790	758.945	728.877	732.659	765.262
ν_6	782.816	773.587	797.565	—	801.501
$^3J_{o}^{HH}$	[8.417(3,4) 7.389(4,5) 7.757(5,6)]	[8.268(4,5) 7.594(5,6)]	8.561	[8.474(3,4) 8.159(4,5)]	8.657
$^4J_{m}^{HH}$	[1.010(3,5) 1.885(4,6)]	[2.732(2,4) 1.431(2,6) 1.026(4,6)]	[2.207(2,6) 2.612(3,5)]	0.976	2.528
$^5J_{p}^{HH}$	0.401	0.428	0.396	—	0.329
$^3J_{o}^{HF}$	10.804	[8.879(2,3) 8.575(3,4)]	8.689	10.467	[7.720(4,5) 8.2±0.1]
$^4J_{m}^{HF}$	[5.404(2,4) 7.091(2,6)]	5.352	5.502	5.849	5.601
$^5J_{p}^{HF}$	−0.183	0.232	—	−1.068	—
$^4J_{o}^{H,CHO}$	−0.152	−0.005(1,2)†; −0.116(1,6)	−0.123	—	−0.06±0.02
$^5J_{m}^{H,CHO}$	[0.739(1,5) 0.122(1,3)]	0.391	0.442	[0.273(1,5) 0.539(1,3)]	[0.658(1,5) 0.132(1,3)]
$^6J_{p}^{H,CHO}$	−0.005†	0.015†	—	−0.010†	—
$^4J_{o}^{F,CHO}$	−0.378	—	—	−1.080	—
$^5J_{m}^{F,CHO}$	—	1.845±0.02	—	—	—
$^6J_{p}^{F,CHO}$	—	—	−0.442	—	< |0.05|

*Chemical shifts, ν, are relative to internal TMS at 100 MHz.
†Not necessarily different from zero, there being no *direct* experimental evidence for their presence. Unless otherwise indicated, the probable errors are normally less than or equal to 0.005 Hz (see text)

c) o-Fluorobenzaldehyde, ABCDXR

Of 183 transitions calculated to have intensity greater than 0.01, 156 were assigned to experimental peaks, yielding an r.m.s. error of 0.018 Hz when all parameters were allowed to vary in the LAOCN3 analysis. The probable errors in the parameters was less than or equal to 0.005 Hz. Parameters are given in Table 1.

No splittings attributable to $^5J_p^{HF}$ were observed in the H_5 resonance region. However, after assigning all the transitions in the low-field H_5 region a negative value of J_p^{HF} was obtained on iteration. The negative sign was clearly confirmed by comparison of the observed ^{19}F resonance spectrum with calculated spectra using various sign combinations (see Figure 1). Weak irradiation experiments confirmed the negative sign of $^4J_o^{F,CHO}$, as did the observed ^{19}F spectrum. In Figure 2 the calculated and observed ring proton spectra are compared. With the exception of a few obvious impurity peaks agreement is good. The ring proton resonance spectrum was not sensitive to the sign of $^4J_o^{F,CHO}$.

The observed and calculated spectra at 100 and 60 MHz of the aldehyde proton are given in Figure 3. The correct signs of all the long-range couplings to the aldehyde proton are easily found from Figure 3 even in the absence of double resonance experiments. The effective T_2 in the calculated spectra in Figure 3 was deliberately increased beyond the value indicated by the observed spectrum at 100 MHz because it makes comparisons more obvious without vitiating any conclusions.

Figure 1. The observed and calculated ^{19}F magnetic resonance spectra at 56 MHz of a 30 mol % solution of o-fluorobenzaldehyde in acetone. The calculated spectra use the spectral parameters in Table 1 and different sign combinations for $^{4}J_{o}^{F,CHO}$ and $^{5}J_{p}^{H,F}$. The calculated spectrum with both signs negative is the correct one.

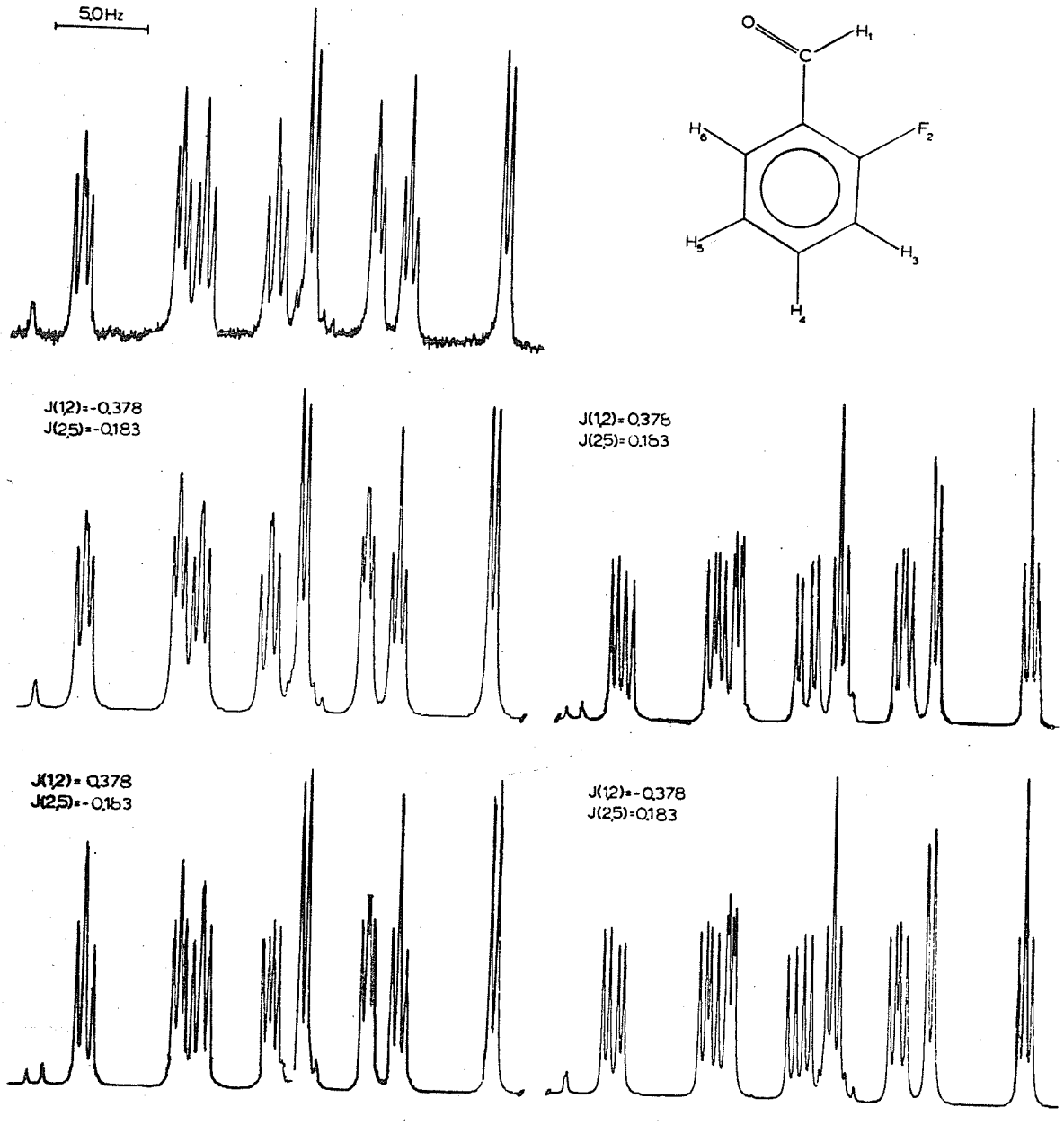
5,0 Hz
O
C
H1
H6
F2
H5
H3
H4
J(1,2)=-0,378
J(2,5)=-0,183
J(1,2)=0,378
J(2,5)=0,183
J(1,2)=0,378
J(2,5)=-0,183
J(1,2)=-0,378
J(2,5)=0,183

Figure 2. The observed and calculated ring proton magnetic resonance spectra at 100 MHz of a 30 mol % solution of o-fluorobenzaldehyde in acetone. The calculated spectrum uses the parameters in Table 1. The experimental spectrum shows the presence of a small amount of impurity.

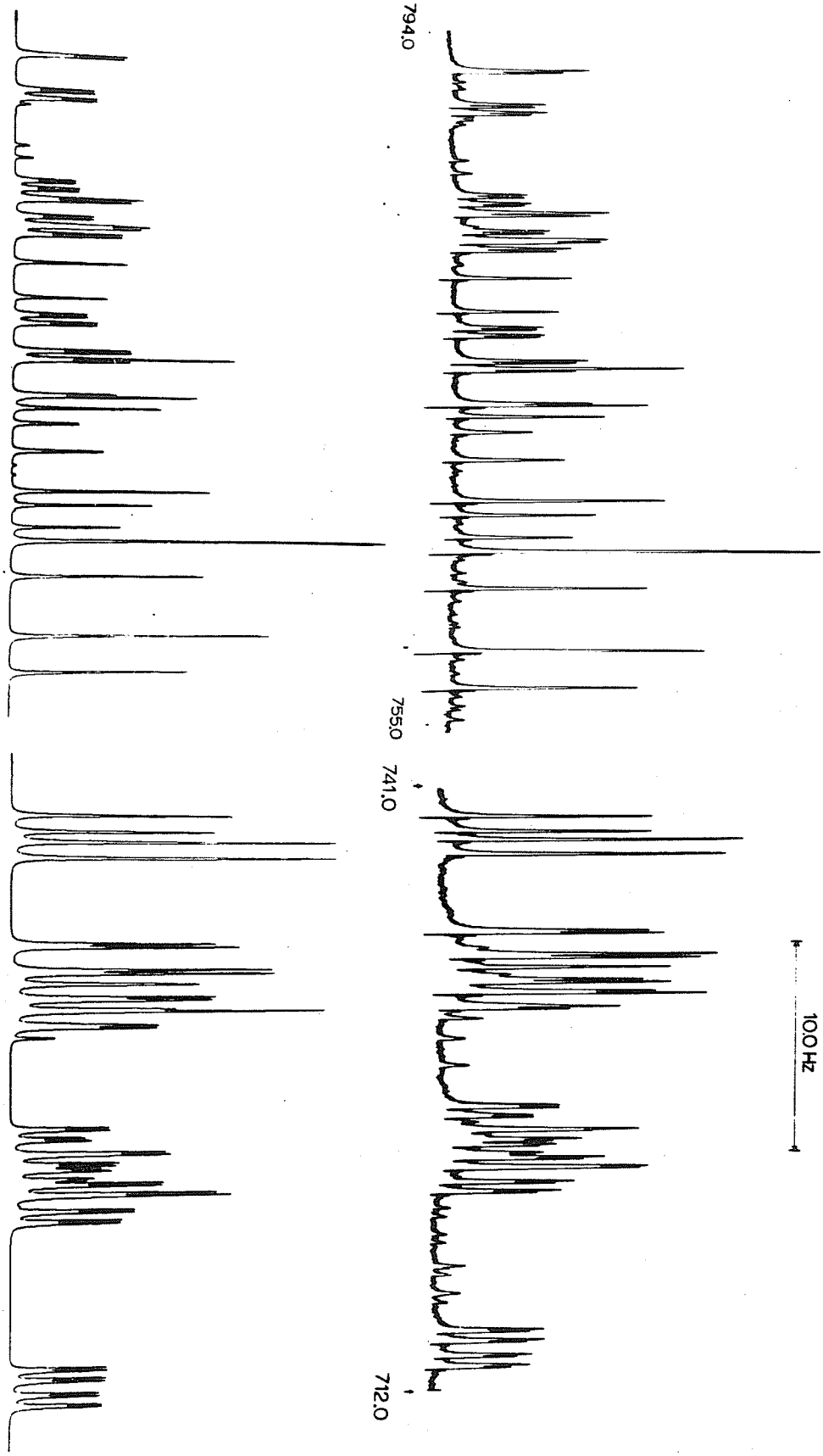
794.0
755.0
741.0
712.0
10.0 Hz

Figure 3. The aldehyde proton magnetic resonance of o-fluorobenzaldehyde as a 30 mol % solution in acetone. In a the observed spectrum is shown at 100 MHz while in f the observed spectrum appears at 60 MHz. In b to e and g to j the spectra calculated with the coupling parameters in Table 1 and with the following couplings involving the aldehyde proton are shown; b and g are clearly the correct sign combinations so that the signs of all these couplings can be directly obtained from the aldehyde proton resonance.

100 MHz 60 MHz	b g	c h	d i	e j
$^4J_{o}^{F,CHO}$	-0.378	0.378	-0.378	-0.378
$^5J_{m}^{H_3,CHO}$	0.122	0.122	0.122	-0.122
$^5J_{m}^{H_5,CHO}$	0.739	0.739	0.739	0.739
$^4J_{o}^{H_6,CHO}$	-0.152	-0.152	0.152	-0.152

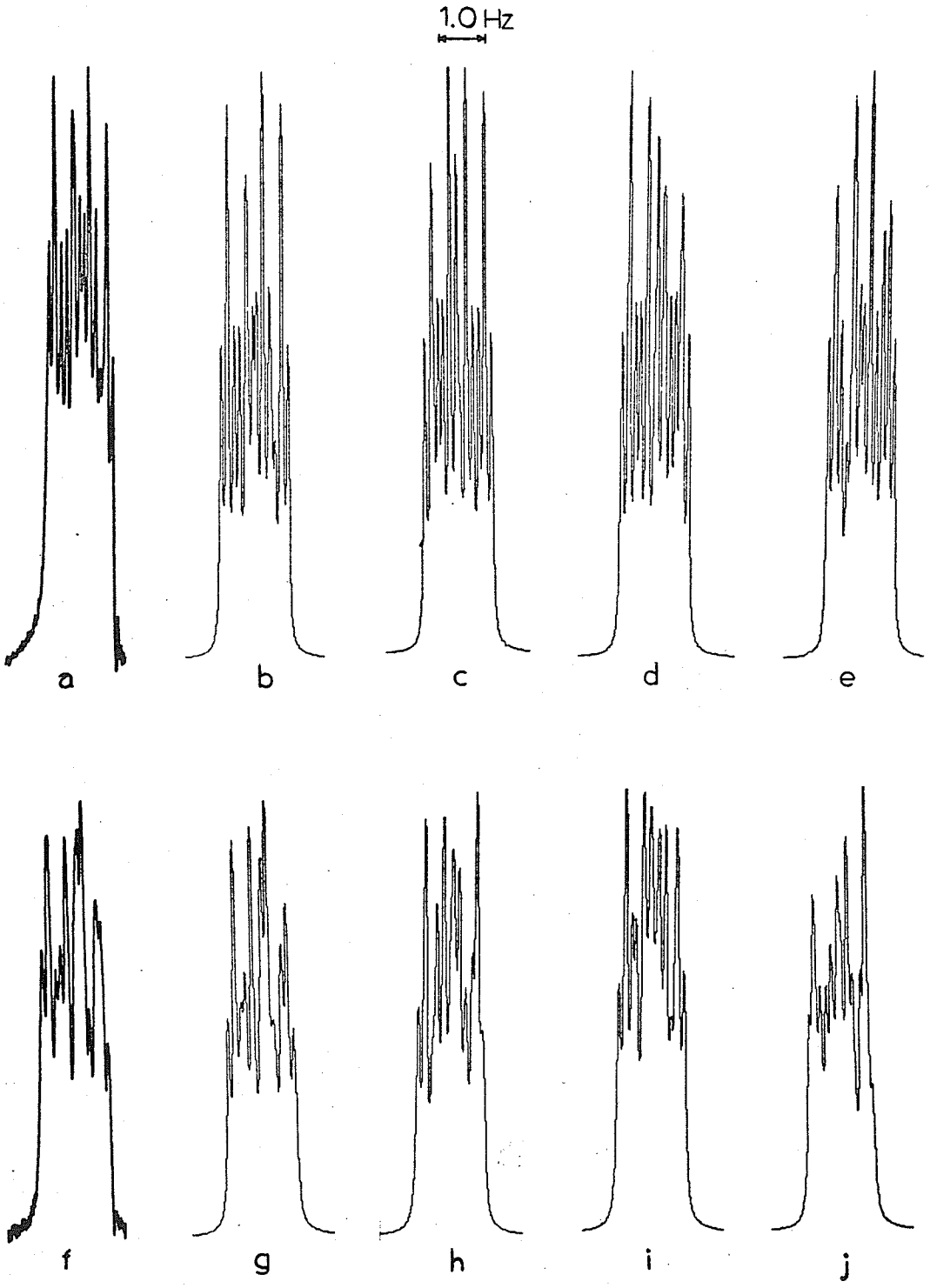
1.0 Hz
a
b
c
d
e
f
g
h
i
j

d) m-Fluorobenzaldehyde, ABCDXR

The chemical shift between H_2 and H_5 is only about 0.015 p.p.m., presenting some analysis problems. In a preliminary experiment the ring proton spectrum was calibrated twice while decoupling the aldehyde proton. Several trial and error calculations with LAOCN3, followed by some iterative runs, finally yielded the correct relative chemical shifts of H_5 and H_2. The coupling parameters so obtained agreed to within about 0.02 Hz with the results of the complete analysis which is discussed below.

Proper calibration procedures on the complete proton spectrum, and assignment of 126 of the 137 ring proton transitions with intensities greater than 0.01, gave the parameters in Table 1. The r.m.s. error was 0.019 Hz and the probable errors varied between 0.003 and 0.006 Hz (two values). No agreement between calculated and observed ring proton spectra could be obtained unless $^4J_o^{H_6,CHO}$ was -0.116 Hz. Observed splittings in the H_6 region could not be predicted if this coupling was held at 0.00 Hz in the iteration and, furthermore, the small doublet splittings (0.1 Hz) in the H_6 region between 795 to 810 Hz (see Figure 4) disappeared when the aldehyde protons were irradiated. One might note that at 60 MHz these splittings are not observable. In Figure 4 the calculated and observed ring proton spectra are compared. Apart from a few obvious, weak impurity peaks, the agreement is quite satisfactory.

The aldehyde proton resonance displayed asymmetry about its midpoint[2]

---

[2] Because of multiple degeneracies in the aldehyde proton resonance the estimated error in the shift of the aldehyde proton and in $^5J_m^{F,CHO}$ is 0.02 Hz.

Figure 4. The observed and calculated ring proton magnetic resonance spectra at 100 MHz of a 30 mol % solution of m-fluorobenzaldehyde in acetone. The calculated spectrum uses the parameters in Table 1. There are present a few impurity peaks, their presence becoming obvious only when proper assignments of peak position are complete.

There are one or two peaks which appear unresolved in the calculated spectrum, a consequence of the Lorentzian line shape. A calculated spectrum in which the right hand half of the peaks is "brought down" more sharply than for a Lorentzian, thereby simulating spectrometer conditions, showed better agreement with the observed spectrum for these peaks.

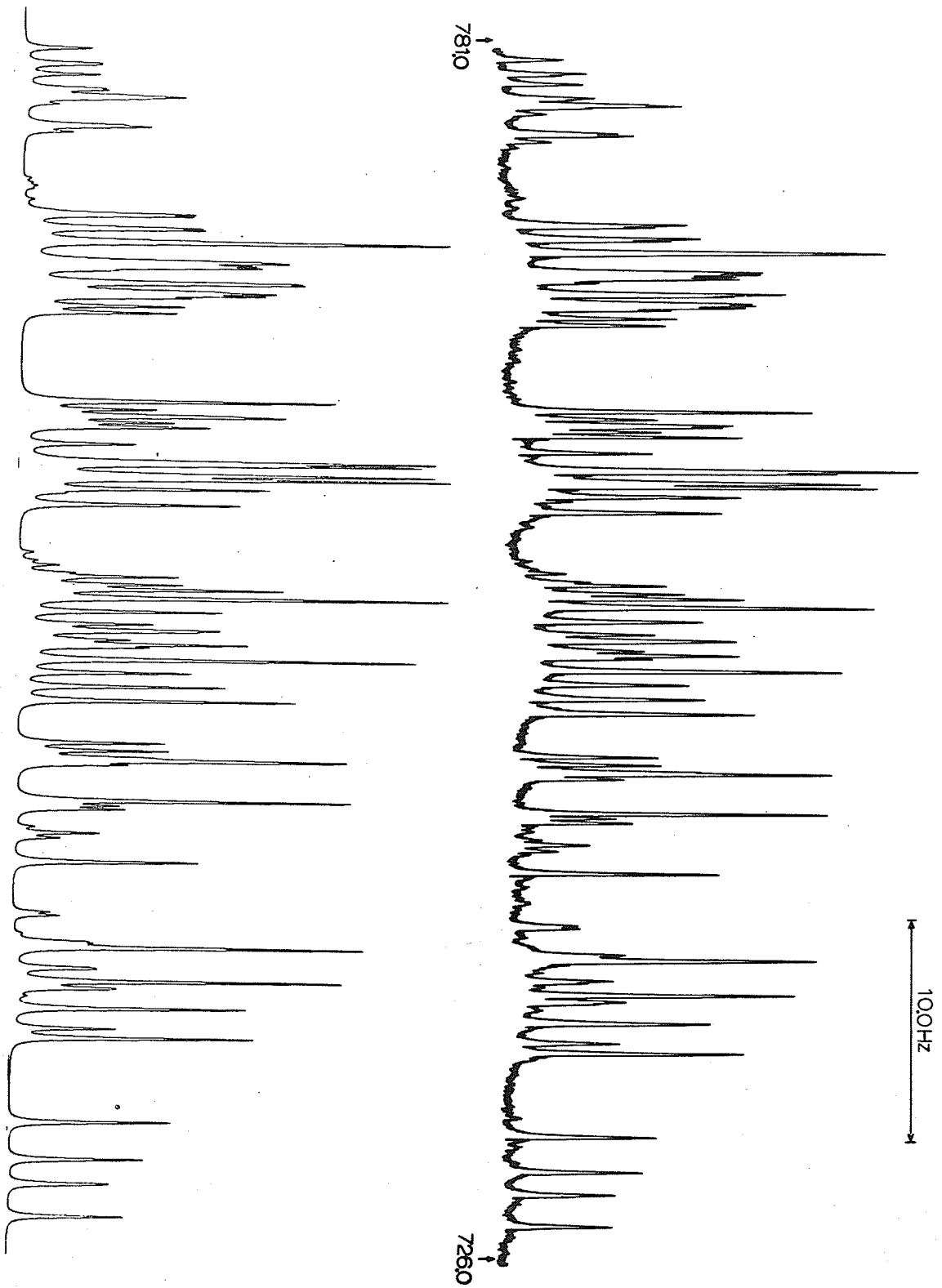
781.0
726.0
10.0Hz

and could be reproduced only by a positive value of $^5J_m^{F,CHO}$. Because a negative value could be inferred from previous work (8) it was felt necessary to compare the ^{19}F spectrum with those calculated for different signs of $^5J_m^{F,CHO}$. In Figure 5 the various sign combinations of $^5J_m^{F,CHO}$ and $^5J_p^{HF}$ very clearly demonstrate the positive sign of these two couplings. A positive $^5J_p^{HF}$ had previously been known only in fluorobenzene itself (19) and was negative in those derivatives studied to date (10).

Finally, it might be mentioned that the near degeneracy of the H_2 and H_5 chemical shifts allows the presence of $^4J_o^{H_6,CHO}$ to go undetected at 60 MHz.

e) 2-Fluoro-6-chlorobenzaldehyde

The analysis of the proton resonance spectrum as an ABCX part of an ABCXR spectrum by LAOCN3 was straightforward. The negative signs of $^5J_p^{HF}$ and $^4J_o^{F,CHO}$ were confirmed by double irradiation experiments. The r.m.s. error was 0.010 Hz and probable errors were 0.004 Hz or less. Parameter values are given in Table 1.

2. The Chemical Shifts

The chemical shifts are solvent dependent (20) and will not be discussed in detail. The relative shifts of the ring protons are consistent with the predictions (21) based on mesomeric and inductive interactions of the substituents with the aromatic ring, as modified by magnetic anisotropy effects from the carbonyl group at the ortho proton (21), for example, and by the sizeable reaction field (22) shifts caused by the polar solvent. The shifts of the aldehydic

Figure 5. The observed and calculated ^{19}F magnetic resonance spectra at 56 MHz of a 30 mol % solution of m-fluorobenzaldehyde in acetone. The calculated spectra use the spectral parameters in Table 1 and different sign combinations for $^5J_{m}^{F,CHO}$ and $^5J_{p}^{HF}$. There is no doubt that the calculated spectrum with both signs positive is the correct one.

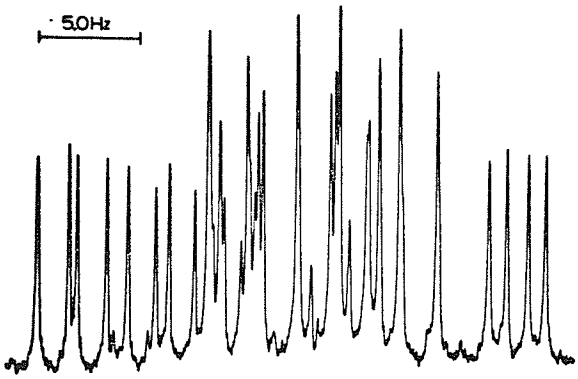

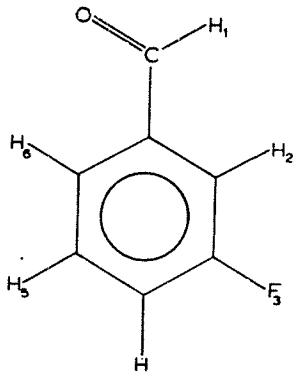

J(1,3) = 1.845
J(3,6) = 0.232

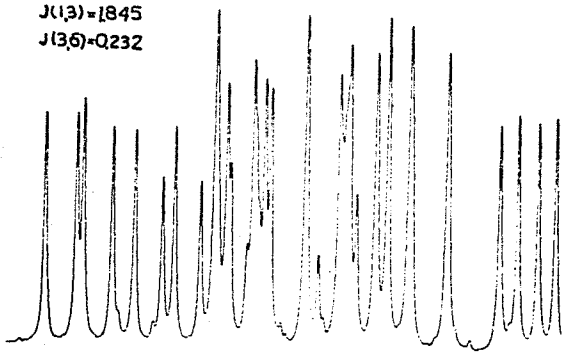

J(1,3) = 1.845
J(3,6) = -0.232

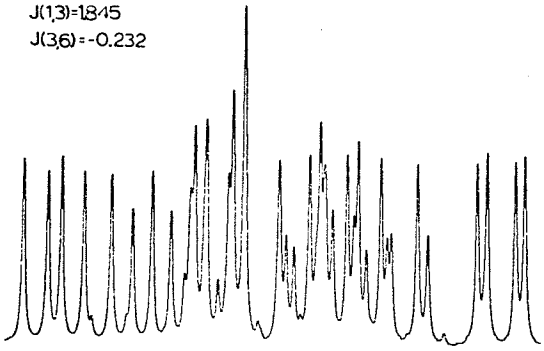

J(1,3) = -1.845
J(3,6) = -0.232

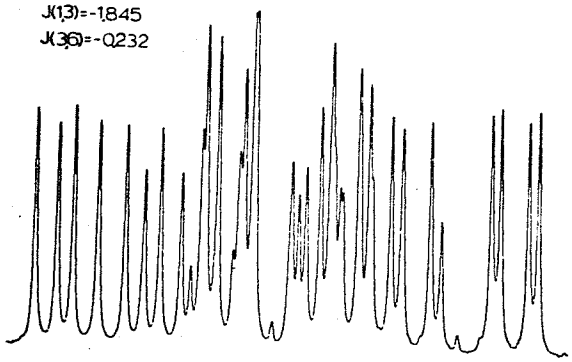

J(1,3) = -1.845
J(3,6) = 0.232

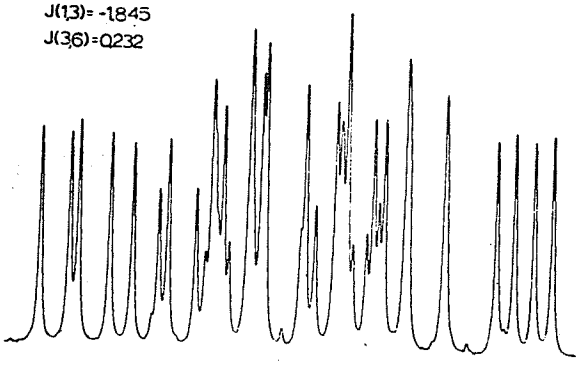

protons show some evidence for deshielding effects caused by steric interactions (21, 23) with ortho substituents.

3. The Spin-Spin Coupling Constants in the Ring

a) The Proton-Proton Couplings

Taking J_o^{HH} as 7.54, J_m^{HH} as 1.38, and J_p^{HH} as 0.63 Hz in benzene (24) the additivity of substituent effects on these couplings was examined by using the parameters for fluorobenzene in acetone solution (19) and for benzaldehyde in CCl_4 solution (25). The agreement between predicted and observed proton-proton couplings was excellent for p-fluorobenzaldehyde, deviations ranging between 0.00 and 0.04 Hz for the four values. For m-fluorobenzaldehyde agreement was also good, the average deviation for six values being less than 0.04 Hz. The biggest deviation was 0.07 Hz for one of the J_o^{HH} couplings.

In o-fluorobenzaldehyde the mean deviation between predicted and observed couplings was 0.07 Hz (six values), not quite large enough to decide whether the substituent effect of the aldehyde group depends on its conformation (24). The INDO calculations suggest no conformational dependence (13). In later sections it is shown that m-fluorobenzaldehyde probably exists almost equally in the O-cis and O-trans conformations whereas o-fluorobenzaldehyde exists predominantly in the O-trans conformation indicated in Table 1.

For 2-fluoro-6-chlorobenzaldehyde and 2-nitro-4-fluorobenzaldehyde the average deviation rises to 0.27 and 0.11 Hz, respectively. A saturation phenomenon (26) is indicated for three substituents in that the deviations of the calculated from the observed couplings are

in the direction expected if the effect of a substituent has been decreased by the presence of the other two substituents. The saturation phenomenon is evidently most marked when the three substituents are placed 1, 2, 3 on the ring.

b) The Proton-Fluorine Couplings

The substituent effect of the aldehyde group on these coupling constants has not been previously measured. Considering the aldehyde group as more electronegative than hydrogen, the observed changes in these couplings are, with one exception, in the direction found by Goldstein and co-workers (27) for a series of fluorobenzene derivatives. The exception is $J_o^{H_2,F}$ in m-fluorobenzaldehyde where a decrease of 0.4 Hz relative to its value in fluorobenzene is observed instead of a predicted increase (27). It is noted that, in contrast to ring proton-proton couplings, ring proton-fluorine couplings are measurably solvent dependent (28) so that a further uncertainty is present here.

For fluorobenzene in acetone solution $^5J_p^{HF} = 0.3$ Hz and the methyl group replacement technique (6, 29) implies that σ and π contributions to this coupling are of opposite sign, resulting in a value near zero (10). Therefore, the small negative value of J_p^{HF} (-0.18 Hz) in o-fluorobenzaldehyde and the small positive value in m-fluorobenzaldehyde (0.23 Hz) are in agreement with the known regularities, as is the larger negative value (-1.07 Hz) in 2-fluoro-6-chlorobenzaldehyde.

4. Spin-Spin Couplings to the Aldehydic Protons

a) To Meta Protons over Five Bonds, $^5J_m^{H,CHO}$, and Conformational Preferences

In benzaldehyde $^5J_m^{H,CHO}$ is 0.38 Hz (2), an average of the two couplings in 1. In a series of 4-substituted derivatives of 1 a maximum increase of 0.1 Hz is found for strongly electron donating groups like OCH_3 but $^5J_m^{H,CHO}$ is never less than 0.38 Hz, even for electron attracting groups (3). The coupling is stereospecific. In 2-hydroxybenzaldehyde (9), 2-aminobenzaldehyde,[3] 2-hydroxy-3-methoxybenzaldehyde (5a), all of which correspond to 2 because of hydrogen

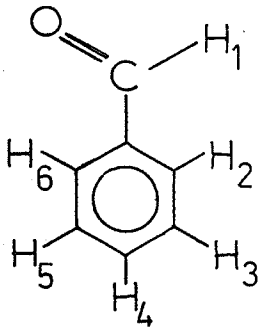

1

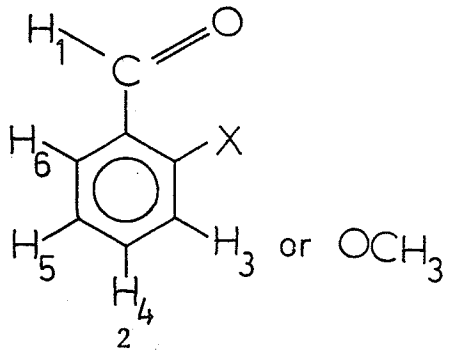

2

bonding of the carbonyl group to X, $^5J_m^{H_5,CHO}$ is undetectably small. When X = OCH_3 or Br, the aldehyde group adopts a conformation in which the carbonyl oxygen and X are trans to one another. In these two cases $^5J_m^{H_3,CHO}$ is not detectably different from zero while $^5J_m^{H_5,CHO}$ is 0.84 and 0.77 Hz for X = OCH_3 and Br, respectively (9).

Consideration of all of these data strongly suggests that in benzaldehyde $^5J_m^{H_3,CHO}$ = 0.00Hz while $^5J_m^{H_5,CHO}$ = 0.76 Hz when numbering as in 1, in good agreement with theoretical models (30).

---

[3] R. Wasylishen. Unpublished work.

Note particularly that the coupling increases in 2-methoxybenzaldehyde compared to 2-bromobenzaldehyde in a manner analogous to the 4-substituted derivatives, but that $^{5}J_{m}^{H3,CHO}$ (non zig-zag) does not increase above zero.

To a very good approximation, therefore, the accurate data in Table 1 can be used to derive the proportions of the two possible conformations of each of the compounds in acetone solution.

i) o-Fluorobenzaldehyde

One has the two possible conformations, 3 and 4, called O-cis and O-trans, respectively. On the assumption that the 1,5 coupling

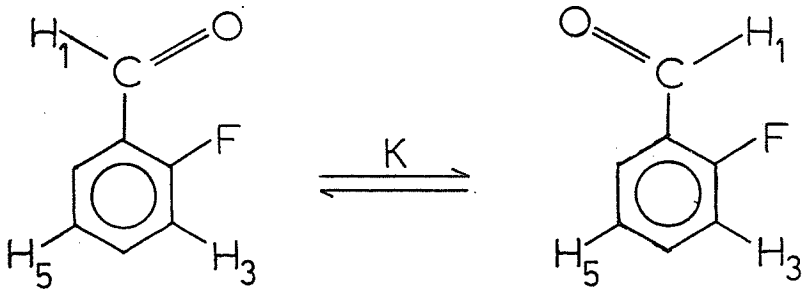

3 4

in 3 is zero the data in Table 1 give the populations as $P_3 = 0.14$ and $P_4 = 0.86$ or $K = 6.1$. Hence the free energy difference at 31 °C is 1.1 kcal/mol, O-trans more stable. This conclusion differs markedly from that reached by far i.r. torsional data in the gas phase (31), $K = 1.6$, or from that obtained by i.r. intensity measurements in solution (32), 32% trans, $K < 1$. On the other hand, the INDO calculations yield an energy difference of 0.94 kcal/mol, O-trans more stable, The entropy difference between 3 and 4 is presumably small and although the polar acetone will somewhat favor the more

polar O-cis form, the agreement between INDO and this result is still remarkably good.[4] The only other conformational data on this system are for the radical anion, where only one conformation is observed, assigned to the O-trans form (33).

There is no evidence that 4, the predominant isomer, is non-planar; while 3 would have a maximum out-of-plane twist of 20° of the carbonyl group (34), the available coupling data on 2,6-dichloro- and 2,6-dinitro-benzaldehydes imply no measurable change in $^{5}J_{m}^{H,CHO}$ for this degree of nonplanarity (34).

ii) m-Fluorobenzaldehyde

$^{5}J_{m}^{H,CHO}$ is 0.39 Hz, strongly implying a zero free energy difference between the two conformations. INDO computes an energy difference of 0.16 kcal/mol, O-trans more stable. The acetone solvent favors the O-cis form and therefore the agreement is quite close, INDO having K = 1.3 for zero entropy difference between conformations. In contrast, torsional frequency measurements in the gas phase (31) have K = 10, O-cis more stable. Band intensity measurements in the i.r. suggest 70% O-trans in nonpolar solvents (32), while other i.r. data for chloroform solutions give K = 2.3, O-cis more stable (31). The radical anion of this moledule contains comparable populations of two isomers (33).

iii) 2-Fluoro-6-chlorobenzaldehyde

The procedure yields a free energy difference of 0.41 kcal/mol, O-trans to chlorine being more stable. The coupling constant data on

---

[4] Note that the assumption of a zero $^{5}J_{m}$ in the non zig-zag conformation (1,5 in 3) puts a lower limit on $K=P_4/P_3$ and, therefore, on the free energy difference.

2,6-dichlorobenzaldehyde (34) suggest a maximum twist of 20° of the carbonyl group from the plane of the ring when it lies cis to chlorine. In that compound $^{5}J_{m}^{H,CHO}$ is 0.40 Hz implying the validity of the population analysis above, i.e., a small twist of the carbonyl group does not noticeably affect $^{5}J_{m}^{H,CHO}$.

iv) 2-Nitro-4-fluorobenzaldehyde

The free energy difference obtained from the coupling constants is 0.87 kcal/mol, O-trans to the nitro group more stable. Note that the sum of the coupling constants is 0.79 Hz, almost the same as in benzaldehyde and in 2,6-dinitrobenzaldehyde, 0.78 Hz (34). The INDO energy difference is 1.64 kcal/mol, O-trans to nitro more stable. But the calculation was done for completely planar conformations so that 1.64 kcal/mol is very much of an upper limit. The O-cis to nitro form must have strong steric hindrance between the N — O and C = O bonds. Previous measurements on 2,6-dinitrobenzaldehyde (34) indicate a maximum twist of 25° of the carbonyl group out of the plane of the ring. No doubt the nitro group will also twist out of plane. The INDO calculations on nonplanar forms are not encouraging for standard geometries. The failure of the CNDO/2 method to predict the barriers in some conjugated systems has recently been discussed by Gropen and Seip (35).

v) Suggested Dipole Moment Measurements

The INDO computations on 2-fluoro- and 3-fluorobenzaldehydes predict dipole moments of 4.32 (2.95) and 3.47 (1.13) D, respectively, the O-trans moment being given in brackets. For benzaldehyde INDO calculates 2.75 D, measured values ranging from 2.8 to 3.0 D in

solution (36). For p-fluorobenzaldehyde the calculated value is 1.87 D, observed being 1.98 D (36). The good agreement encourages the measurement of the dipole moments of the other two isomers as a check on the conformational information reported here. Small long-range couplings can be measured accurately and if this is done, relatively reliable conformational information can be obtained (complete analyses of good high resolution spectra is absolutely essential, however).

b) To Fluorine over Four Bonds, $^{4}J_{o}^{F,CHO}$, and Five Bonds, $^{5}J_{o}^{F,CHO}$

The population analyses in previous sections can be used in calculation values of $^{4}J_{o}^{F,CHO}$ when the C — H bond of the aldehyde group lies cis, J_c, and when it lies trans, J_t, to the fluorine. Thus for o-fluorobenzaldehyde write $0.14\ J_t + 0.86\ J_c = 0.38$ Hz (Table 1) while for 2-fluoro-6-chlorobenzaldehyde write $0.66\ J_t + 0.34\ J_c = 1.08$ Hz. Then $^{4}J_{c}^{F,CHO}$ is -0.2 and $^{4}J_{t}^{F,CHO}$ is -1.6 Hz. This result is insensitive to the assumptions concerning $^{5}J_{m}^{F,CHO}$. An assumption that it is 0.1 Hz in the non zig-zag path yields $^{4}J_{c}^{F,CHO}$ as -0.4 and $^{4}J_{t}^{F,CHO}$ as -1.4 Hz.

For 2,6-difluorobenzaldehyde one predicts $^{4}J_{o}^{F,CHO}$ to be -0.9 Hz. For pentafluorobenzaldehyde there is a report of +1.0 Hz for this coupling (8), a reasonable magnitude but a questionable sign. In ortho fluoro derivatives of benzalchloride a negative sign and a similar stereochemical dependence is found for $^{4}J_{o}^{F,CHCl_2}$ (37).

In m-fluorobenzaldehyde $^{5}J_{m}^{F,CHO}$ is +1.84 Hz. There is a reported value of -1.3 Hz for this coupling in pentafluorobenzaldehyde (8) and must be the mean of its values in O-cis and O-trans conformations with respect to one meta fluorine substituent. The population analysis implies 1.84 Hz as the average value for the two equally

populated O-cis and O-trans forms of m-fluorobenzaldehyde. If $^{5}J_{m}^{F,CHO}$ has a conformational dependence similar to that of $^{5}J_{m}^{H,CHO}$ then $^{5}J_{m}^{F,CHO}$ lies between +3 and 4 Hz in the O-cis form of m-fluorobenzaldehyde (as actually calculated by INDO, see below). If -1.3 Hz is the correct value in pentafluorobenzaldehyde, a very large substituent effect exists in this molecule.

c) INDO and CNDO-MO Calculations of J

These were carried out on an IBM 360/65 system, using standard geometries (14). As many as 76 cycles in the SCF procedure were necessary to obtain convergence of the calculated coupling constants to 0.01 Hz; as few as 50 were sufficient for CNDO. As a check the proton couplings in benzene were calculated and agreed to within less than 0.01 Hz with the values quoted in reference 14. The $J(^{13}C - H)$ value in benzaldehyde was calculated as 159.08 Hz, in exact agreement with the value given in reference 38.

In Table 2 the calculated coupling constants to the aldehyde proton are reported for the planar conformations of benzaldehyde and the three fluorobenzaldehydes. In view of the expense of these calculations, they were not done for the other two compounds in Table 1. In Table 3 the observed and calculated coupling constants are compared. All conformations are planar, benzaldehyde and p-fluorobenzaldehyde naturally having two equally populated forms, while the fractional populations of the o-fluorobenzaldehyde and m-fluorobenzaldehyde were taken from section 4a above.

i) Calculated Couplings in Table 2

Inasmuch as the INDO approximation considers one-centre exchange integrals (14) it includes the π electron contribution, expected to be

TABLE 2

Calculated aldehyde proton coupling constants in Hz in the planar conformations of benzaldehyde and the three fluorobenzaldehydes

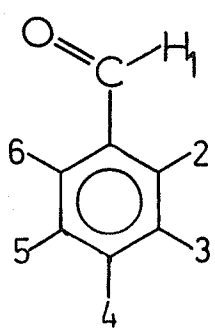
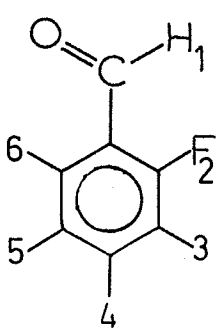
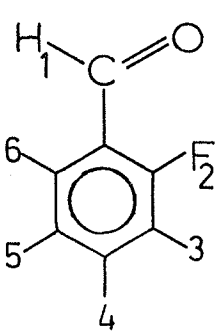
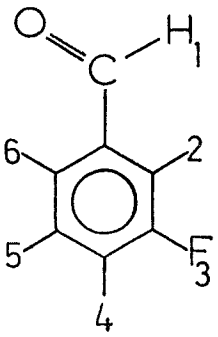
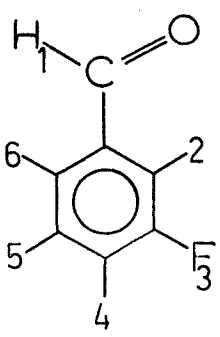
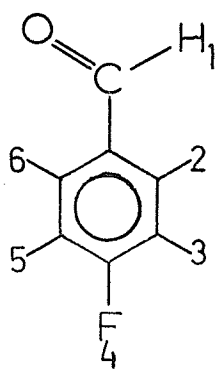

Coupling constant (Hz)	INDO	CNDO	INDO	CNDO	INDO	CNDO	INDO	CNDO	INDO	CNDO	INDO	CNDO
$^4J(1,2)$	0.21	0.53	0.11	0.31	0.38	0.50	0.20	0.52	-0.30	0.36	0.18	0.52
$^4J(1,6)$	-0.41	0.28	-0.37	0.30	0.16	0.51	-0.43	0.27	0.08	0.49	-0.40	0.27
$^5J(1,3)$	0.20	0.02	0.21	0.03	1.60	0.93	-0.36	0.07	3.47	2.55	0.19	0.02
$^5J(1,5)$	1.60	0.90	1.55	0.88	0.20	0.02	1.61	0.89	0.24	0.02	1.51	0.86
$^6J(1,4)$	-0.29	0.00	-0.29	0.00	-0.28	0.00	-0.31	0.00	-0.34	-0.01	0.53	0.08

TABLE 3

Comparison of calculated and observed aldehydic proton coupling constants on the basis of deduced conformational* preferences in benzaldehyde and its monofluoro derivatives

		$^{4}J_{H,CHO}$		$^{5}J_{H,CHO}$		$^{6}J_{H,CHO}$	$^{4,5,6}J_{F,CHO}$
		o		m		o	o,m,p
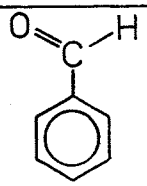	Expt1	-0.10		0.38		-0.03	—
	INDO	-0.10		0.90		-0.29	—
	CNDO	0.40		0.46		0.00	—
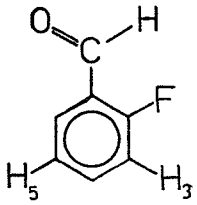			H_5		H_3		
	Expt1	-0.15	0.74		0.12	0.00	-0.39
	INDO	-0.30	1.36		0.40	-0.29	0.14
	CNDO	0.33	0.76		0.16	0.00	0.34
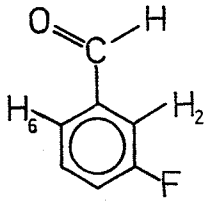		H_2	H_6				
	Expt1	-0.01	-0.12	0.39		0.00	1.84
	INDO	-0.05	-0.17	0.92		-0.32	1.56
	CNDO	0.44	0.38	0.46		-0.01	1.31
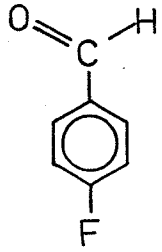	Expt1	-0.12		0.44		—	-0.44
	INDO	-0.11		0.85		—	0.53
	CNDO	0.40		0.44		—	0.08

* Benzaldehyde is planar in the gas phase (39) and it is assumed that it and p-fluorobenzaldehyde are planar in solution. The fractional contributions of the O-cis and O-trans forms of the o- and m-fluorobenzaldehydes are taken from section 4a, as derived from the five-bond proton-proton coupling constants. All data are in Hz.

negative over four or six bonds and positive over five bonds. The expectation is borne out by, for example, the two sets of data for benzaldehyde in Table 2. However, it is probable that calculations using standard geometries somewhat overestimate the π electron contributions to $^{5}J_{m}^{H,CHO}$ (see below). The data in Table 2 may well be of interest in the study of those molecules in which the carbonyl group is fixed by intramolecular hydrogen bonding. Note that the presence of the fluorine substituents has a negligible effect on the calculated magnitudes of $^{5}J_{m}^{H,CHO}$ and $^{6}J_{p}^{H,CHO}$ and probably constitutes support for the conformational arguments in section 4a. The insensitivity to substituent and solvent effects of the long-range couplings between protons on a side-chain and ring protons is experimentally known for a variety of benzene derivatives (3, 6, 10).

ii) Observed and Calculated Couplings in Table 3

A stringent comparison between observed and calculated values can be made for benzaldehyde and p-fluorobenzaldehyde. INDO is in excellent agreement with the observed $^{4}J_{o}^{H,CHO}$ data while CNDO yields rather too large values, indicating the importance of π electron contributions (for that matter, INDO is also in striking agreement with the two different observed $^{4}J_{o}^{H,CHO}$ values in m-fluorobenzaldehyde).

On the other hand, CNDO agrees quantitatively with the $^{5}J_{m}^{H,CHO}$ measurements while INDO overestimates their magnitude substantially, suggesting that π electron contributions to $^{5}J_{m}^{H,CHO}$ are very small. This suggestion is verified by the observations on appropriate compounds that a methyl group, replacing the ring or aldehyde proton, does not couple to the remaining proton. It should couple if a π

electron contribution were important (29). Furthermore, the five-bond coupling is not known for the anti-zig-zag arrangement and (in Table 2) CNDO calculates less than 0.03 Hz for this situation while INDO finds 0.2 Hz, which would be easily observed. In ring-substituted styrenes, Barfield et al. (40) have also found INDO to overestimate $^5J_{\underline{H},\underline{CH}CH_2}^{m}$ for the planar zig-zag arrangement. They attribute the disagreement between $^5J_{\underline{H},\underline{CH}CH_2}^{m}$ calculated and observed to an overestimate of the σ electron effect by INDO.

CNDO predicts a vanishing $^6J_p^{H,CHO}$, as observed for all molecules in Table 3, while INDO overestimates this coupling by -0.3 Hz.

The agreement between calculated and observed H, F couplings in Table 3 is not terribly good, an exception being $^5J_m^{F,CHO}$ in the INDO approximation. Both methods calculate a positive $^6J_p^{F,CHO}$ in p-fluorobenzaldehyde, contrasting with the negative observed value. Similar disagreements for H, F couplings in other molecules are mentioned by Pople and co-workers (14).

In general the agreement between theory and experiment for the present molecules is impressive and the use of the combined CNDO and INDO theories in conjunction with precise experimental, long-range coupling data is suggested as an improved tool in conformational studies.

d) Calculations of J for nonplanar Conformations

It has been argued (41) that, as the carbonyl group twists about the C — C bond in benzaldehyde $^6J_p^{H,CHO}$ should become large and negative, displaying an extremum when the carbonyl group lies perpendicular to the ring plane. Similarly, $^6J_p^{F,CHO}$ in p-fluorobenzaldehyde should become large and positive (7). In Table 4 the computed long-

range couplings of the aldehydic proton in benzaldehyde and p-fluorobenzaldehyde are presented for conformations in which the plane of the carbonyl group lies perpendicular to the aromatic plane. The INDO calculations bear out the previous predictions as expected if, in the qualitative model (7, 39), the coupling to the para position now goes mainly via a π electron mechanism. The synthesis of the 2,6-di-t-butyl derivatives is suggested.

TABLE 4

Computed ring proton - aldehyde proton coupling constants in benzaldehyde and p-fluorobenzaldehyde for perpendicular orientations of the carbonyl group

		$^4J_{H,CHO}$ o	$^5J_{H,CHO}$ m	$^6J_{H(F),CHO}$ p
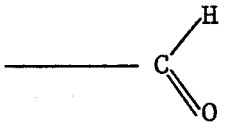	INDO	-0.43	1.01	-0.76
	CNDO	0.48	0.19	0.01
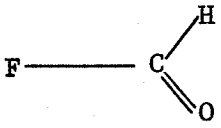	INDO	-0.49	0.98	1.45
	CNDO	0.46	0.17	0.13

Finally, it may be remarked that the presence of a substituent distorts the benzene ring and it would be of interest to perform a systematic series of calculations in which such a distortion is introduced.

ADDENDUM

While this thesis was in preparation, Bock and Tomchuk (42) measured the dipole moments of the three monofluorobenzaldehydes in benzene at 25 °C. For 2-fluoro-, 3-fluoro-, and 4-fluorobenzaldehyde they observed 3.07, 2.63, and 2.03 D respectively. Assuming the calculated dipole moments (section 4av) are correct, the observed values indicate that the O-trans conformation is the most stable one for 2-fluorobenzaldehyde and that m-fluorobenzaldehyde exists in benzene (a nonpolar solvent) in roughly equal proportions of O-trans and O-cis conformations.

REFERENCES FOR PART I

1. C.J. Macdonald and W.F. Reynolds. Can. J. Chem. 48, 1002 (1970).
2. R.J. Kostelnik, M.P. Williamson, D.E. Wisnosky, and S.M. Castellano. Can. J. Chem. 47, 3313 (1969).
3. S.S. Danyluk, C.L. Bell, and T. Schaefer. Can. J. Chem. 47, 4005 (1969).
4. D.G. Kowalewski and V.J. Kowalewski. Mol. Phys. 9, 331 (1965).
5. (a) S. Forsén, B. Akermark, and T. Alm. Acta Chim. Scand. 18, 2313 (1964). (b) G.J. Karabatsos and F.M. Vane. J. Am. Chem. Soc. 85, 3886 (1963).
6. D.J. Blears, S.S. Danyluk, and T. Schaefer. J. Chem. Phys. 47, 5037 (1967).
7. T. Schaefer and S.S. Danyluk. Can. J. Chem. 47, 4289 (1969).
8. R.R. Dean and W. McFarlane. J. Chem. Soc. B, 509 (1969).
9. D.G. DeKowalewski and S. Castellano. Mol. Phys. 16, 567 (1969).
10. R. Wasylishen and T. Schaefer. Can. J. Chem. 49, 94 (1971).
11. J.B. Rowbotham, R. Wasylishen, and T. Schaefer. Can. J. Chem. 49, 1799 (1971).
12. S. Castellano and R. Kostelnik. J. Am. Chem. Soc. 90, 141 (1968).
13. G.E. Maciel, J.W. McIver, Jr., N.S. Ostlund, and J.A. Pople. J. Am. Chem. Soc. 92, 4506 (1970).
14. D.L. Beveridge and J.A. Pople. Approximate molecular orbital theory. McGraw-Hill Book Company, New York, N.Y., 1970.
15. Program 141. Quantum chemistry program exchange. Indiana University, Bloomington, Indiana.

16. R. Freeman and W.A. Anderson. J. Chem. Phys. 37, 2053 (1962).

17. S. Castellano and A.A. Bothner-By. Mellon Institute Publication, Pittsburgh, Pennsylvania, 1967.

18. (a) C.W. Haigh and J.M. Williams. J. Mol. Spectrosc. 32, 398 (1969). (b) C.W. Haigh. In Annual reports on NMR spectroscopy. Vol. 4., p. 311. Edited by E.F. Mooney. Academic Press, New York, 1971.

19. J.E. Loemker and J.H. Goldstein. Spectrosc. Lett. 1, 153 (1968).

20. T. Schaefer and W.G. Schneider. J. Chem. Phys. 32, 1218 (1960).

21. K. Hayamizu and O. Yamamoto. J. Mol. Spectrosc. 29, 183 (1969).

22. A.D. Buckingham. Can. J. Chem. 38, 300 (1960).

23. T. Schaefer, W.F. Reynolds, and T. Yonemoto. Can J. Chem. 41, 2969 (1963).

24. S. Castellano and R. Kostelnik. Tetrahedron Lett. 5211 (1967).

25. W. Brügel. Nuclear magnetic resonance spectra and chemical structure. Academic Press. New York, N.Y., 1967.

26. T. Schaefer, G. Kotowycz, H.M. Hutton, and J.W.S. Lee. Can. J. Chem. 46, 2531 (1968).

27. J.E. Loemker, J.M. Read, Jr., and J.H. Goldstein. J. Phys. Chem. 72, 991 (1968).

28. H.M. Hutton, B. Richardson, and T. Schaefer. Can. J. Chem. 45, 1795 (1967).

29. R. Hoffman and S. Gronowitz. Arkiv Kemi, 16, 471 (1960).

30. M. Barfield and B. Chakrabarti. Chem. Rev. 69, 757 (1969).

31. F.A. Miller, W.G. Fately, and R.E. Witkowski. Spectrochim. Acta, 23A, 891 (1967).

32. A.R. Katritzky, M.V. Sinnott, T.T. Tidwell and R.D. Topsom. J. Am. Chem. Soc. 91, 628 (1969).

33. A. Hudson and J.W.E. Lewis. Mol. Phys. 19, 241 (1970).

34. C.L. Bell, S.S. Danyluk, and T. Schaefer. Can. J. Chem. 47, 3529 (1969).

35. O. Gropen and H.M. Seip. Chem. Phys Lett. 11, 445 (1971).

36. A.L. McClellan. Tables of experimental dipole moments. W.H. Freeman and Company, San Francisco, California, 1963.

37. H.M. Hutton, J.B. Rowbotham, B.H. Barber, and T. Schaefer. Can. J. Chem. 49, 2033 (1971).

38. G.E. Maciel, J.W. McIver, Jr., N.S. Ostlund, and J.A. Pople. J. Am. Chem. Soc. 92, 1 (1970).

39. R.K. Kakar, E.A. Rinehart, C.R. Quade, and T. Kojima. J. Chem. Phys. 52, 3803 (1970).

40. M. Barfield, C.J. Macdonald, I.R. Peat, and W.F. Reynolds. J. Am. Chem. Soc. 93, 4195 (1971).

41. C.L. Bell, S.S. Danyluk, and T. Schaefer. Can J. Chem. 47, 3529 (1969).

42. E. Bock and E. Tomchuk. Can J. Chem. (to be published).

PART II

Long-Range Spin-Spin Coupling Constants from Amino Protons and ^{15}N to Ring Protons in Aniline-^{15}N and Some Derivatives. INDO Molecular Orbital Calculations

INTRODUCTION

The one-bond ^{15}N-H spin-spin coupling constants in aniline-^{15}N and many of its derivatives have been discussed in detail (1-4). Ring substituents which diminish electron density on the nitrogen atom cause an increase in the magnitude of these coupling constants, apparently implying an alteration in the geometry of the amino group and describable as a change in hybridization of the nitrogen atom. The chemical shifts of the amino protons (5-8) and of ^{15}N are interpreted in a similar manner (1).

Long-range coupling constants between ring protons and protons on sidechain functions such as methyl (9-13), formyl (14-17), hydroxyl (18, 19) and amino (20, 21) groups are stereospecific. Such couplings for the amino protons therefore offer another approach to the study of the geometry of this moiety. The couplings are less than 1 Hz in magnitude and this approach has until recently (22-24) been hampered by the facile intermolecular exchange of the amino protons in solutions of aniline and its derivatives. The mean lifetime before exchange must be increased to the order of seconds before these long-range couplings become observable in a slow-passage experiment. In this part of the thesis these parameters are described for aniline-^{15}N itself and also for some of its derivatives.

The spin-spin interactions between ^{15}N and the ring protons are also measured. Other workers have observed their magnitudes only for protons situated ortho to the amino group (1).

In addition, the long-range coupling constants involving the $^{15}NH_2$ fragment are calculated by the finite perturbation technique (25) in the INDO molecular orbital approximation (26). A comparison of calculated with observed couplings leads to inferences about the comformation of the amino group in aniline.

EXPERIMENTAL

1. Preparation of Compounds

Acetanilide-^{15}N was prepared by the addition of 5.3 ml of acetic anhydride to a solution of 4.2 g of aniline-^{15}N (96.5 atom % ^{15}N from Azote et Produits Chimiques, Toulouse) in 2.4 ml of acetic acid. After the mixture solidified, 50 ml of water were added and the product was filtered off and dried at 60 °C/0.01 torr for three hours, m.p. 114-116 °C. The mass spectrum was consistent with that expected on the basis of the mass spectrum from a commercial sample of acetanilide.

To prepare 2-aminoacetophenone-^{15}N, a solution of 5.00 g of acetanilide-^{15}N in 120 ml of absolute ethanol was irradiated for eighteen hours at 254 nm while bubbling dry nitrogen through the solution. Steam distillation and extraction of the distillate gave 0.12 g of a mixture of 2-aminoacetophenone-^{15}N and acetanilide-^{15}N. This mixture was submitted to dry column chromatography: silica gel, column length 80 cm, diameter 2.5 cm, eluant ethyl acetate/cyclohexane 95:5, v:v. The yield[1] of pure 2-aminoacetophenone-^{15}N was 0.10 g, 2%. Extraction of the residue from the steam distillation yielded 4.4 g (88%) of starting material.

A three:two mixture of 4-bromo-2-chloroaniline-^{15}N and 2-chloro-4,6-dibromoaniline-^{15}N was obtained by the addition of bromine to 0.2 g of 2-chloroaniline-^{15}N (96.47 atom % ^{15}N from Merck, Sharp and Dohme

---

[1] Elad (27) obtained a 20% yield of 2-aminoacetophenone by using a high pressure mercury vapor lamp.

of Canada) in 5ml of acetic acid. When a slight color remained, 10 ml of water were added and the precipitate was collected. An analogous bromination of aniline-^{15}N yielded a two:one mixture of 2,4-dibromoaniline-^{15}N and 2,4,6-tribromoaniline-^{15}N.

2. Preparation of Samples for Spectral Work

All samples (solvents and concentrations given in Table 5) were degassed by the freeze-pump-thaw technique. Internal tetramethylsilane was added as reference material. Intermolecular exchange of the amino protons was retarded by adding basic alumina to the sample tubes before sealing and some of the solutions were stored over NaOH pellets for several hours.

The reaction of equimolar quantities of aniline-^{15}N and D_2O yielded a mixture containing the ^{15}NHD group among others. The mixture was dried over NaOH pellets and was transferred to a sample tube containing basic alumina and sufficient toluene-d_8 to yield a 15 mol % solution of nonexchanging amine. The sample was degassed and the proton magnetic resonance spectrum indicated equimolar amounts of the $^{15}NH_2$ and ^{15}NHD moieties.

3. Proton Magnetic Resonance Spectra

Spectra were recorded in the frequency sweep mode on an HA100-D spectrometer at sweep rates of 0.01 and 0.02 Hz/sec at sweep widths of 1 Hz/cm. They were calibrated by reading sweep and manual oscillator frequencies at intervals of a few Hz, and double and triple resonance experiments (28, 29) yielded the signs of the coupling constants.

RESULTS AND DISCUSSION

1. Spectral Analysis

a) Aniline-^{15}N

Two samples were subjected to spectral analysis. In one (17 mol % in benzene-d_6) the rate of intermolecular proton exchange was low enough to allow the observation of the long-range coupling constants between ring and amino protons. In the other (30 mol % in benzene-d_6) the rate of proton exchange was high enough to eliminate the effects of these coupling constants from the observed high resolution spectrum.

Each of the 165 peaks observed in the nonexchanging solution was calibrated at 0.01 Hz/sec. The spectrum was analyzed as an eight spin system by means of the computer program LACX (30). Because so many of the 640 calculated transitions were nearly degenerate it was not sensible to assign more than 380 to observed peaks (348 of the 512 calculated ring proton transitions were assigned). The results given in Tables 5 and 6 were obtained when all parameters were allowed to vary in the final iterative stages. The r.m.s. error was 0.015 Hz and the probable error of all parameters was equal to or less than 0.003 Hz, except that the probable error in $^1J(^{15}N,H)$ was 0.006 Hz. The observed ring proton spectrum, together with the calculated spectrum, is shown in Figure 6. The widths at half-height of non-degenerate peaks in the experimental spectrum are less than 0.11 Hz. The relative signs of all ^{15}N-H coupling constants were determined relative to $^1J(^{15}N,H)$ which was assumed negative (31). In Figure 7,

TABLE 5

Observed coupling constants in Hz between ^{15}N and protons and between amino and ring protons in aniline and some derivatives*

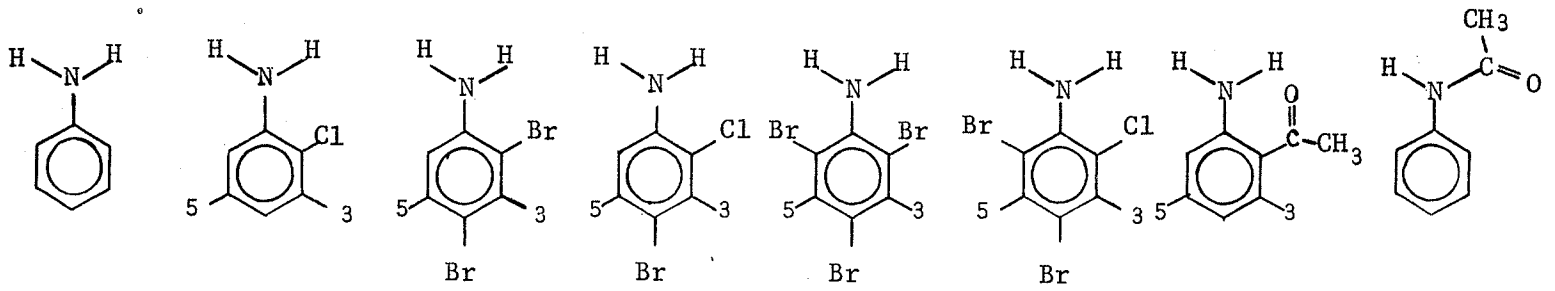

Solvents conc(mol%)		C_6D_6 17	C_6D_6 10	C_6D_6 2	C_6D_6 3	C_6D_6 1	C_6D_6 2	toluene-d_8 15	acetone-d_6 11
$^1J(^{15}N,H)$		-78.875	-82.3	-83.115	-83.148	-85.465	-85.596	-88.6	-91.3 †
$^3J(^{15}N,H_o)$		-1.935	-1.984	-1.873	-1.938	—	—	-2.456	-1.85
$^4J(^{15}N,H_m)$	H_3	-0.476	-0.787	-0.671	-0.706	-0.608	-0.613	-0.834	-0.50
	H_5	-0.476	-0.362	-0.300	-0.308	-0.608	-0.561	-0.305	-0.50
$^5J(^{15}N,H_p)$		0.009	0.166	—	—	—	—	<±0.10	±0.21
^4J_o H,NH		-0.189	-0.122	-0.099	-0.099	—	—	<±0.06	—
^5J_m H,NH	H_3	0.296	0.351	0.283	0.346	0.324	0.356	0.403	—
	H_5	0.296	0.306	0.290	0.324	0.324	0.342	0.305	—
^6J_p H,NH		-0.137	-0.108	—	—	—	—	<±0.06	—

* See text for probable errors of the coupling parameters: they are generally well below 0.01 Hz except for acetanilide-^{15}N where they lie near 0.04 Hz

† In a 9 mol % solution in DMSO.

TABLE 6

Observed proton chemical shifts* and coupling constants† between ring protons in aniline-^{15}N and some derivatives

	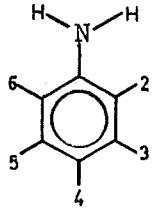	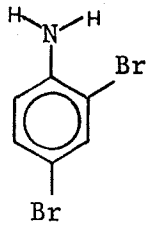	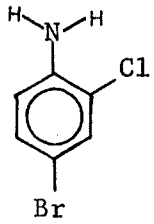	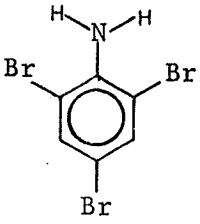	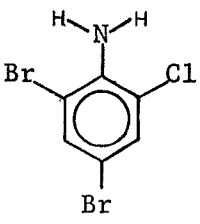	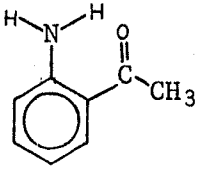	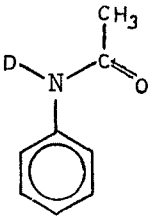
ν_{NH_2}	293.969	323.829	318.240	388.475	381.285	609.0	—
ν_2	635.634	—	—	—	—	215.74(CH_3)	764.41
ν_3	705.018	737.368	720.853	719.413	702.542	732.223	723.72
ν_4	669.189	—	—	—	—	639.008	699.91
ν_5	705.018	689.039	686.455	719.413	716.357	697.127	723.72
ν_6	635.634	584.620	585.411	—	—	621.654	764.41
$^3J_{o\ H,H}$	8.034(2,3)‡	8.561	8.575	—	—	8.092(3,4)	8.19 (2,3)
	7.369(3,4)	—	—	—	—	7.048(4,5) 8.357(5,6)	7.42 (3,4)
$^4J_{m\ H,H}$	1.102(2,4)	2.243	2.242	—	2.145	1.557(3,5)	1.17 (2,4)
	2.496(2,6)						2.42 (2,6)
	1.619(3,5)	—	—	—	—	1.197(4,6)	1.49 (3,5)
$J_{p\ H,H}$	0.496	0.238	0.264	—	—	0.427	0.50

* In Hz at 100 MHz to low field of internal tetramethylsilane; solvent and concentration as in Table 5.
† In Hz, errors as in Table 5.
‡ Numbers in brackets refer to ring positions

Figure 6. The lower part shows the ring proton magnetic resonance spectrum of aniline - ^{15}N as a 17 mol % solution in benzene-d_6 under conditions where long-range coupling between amino and ring protons is clearly observable. In the upper part of the figure the calculated spectrum employs the parameters given in Tables 5 and 6. In the observed spectrum line-widths at half-height of nondegenerate peaks were less than 0.11 Hz.

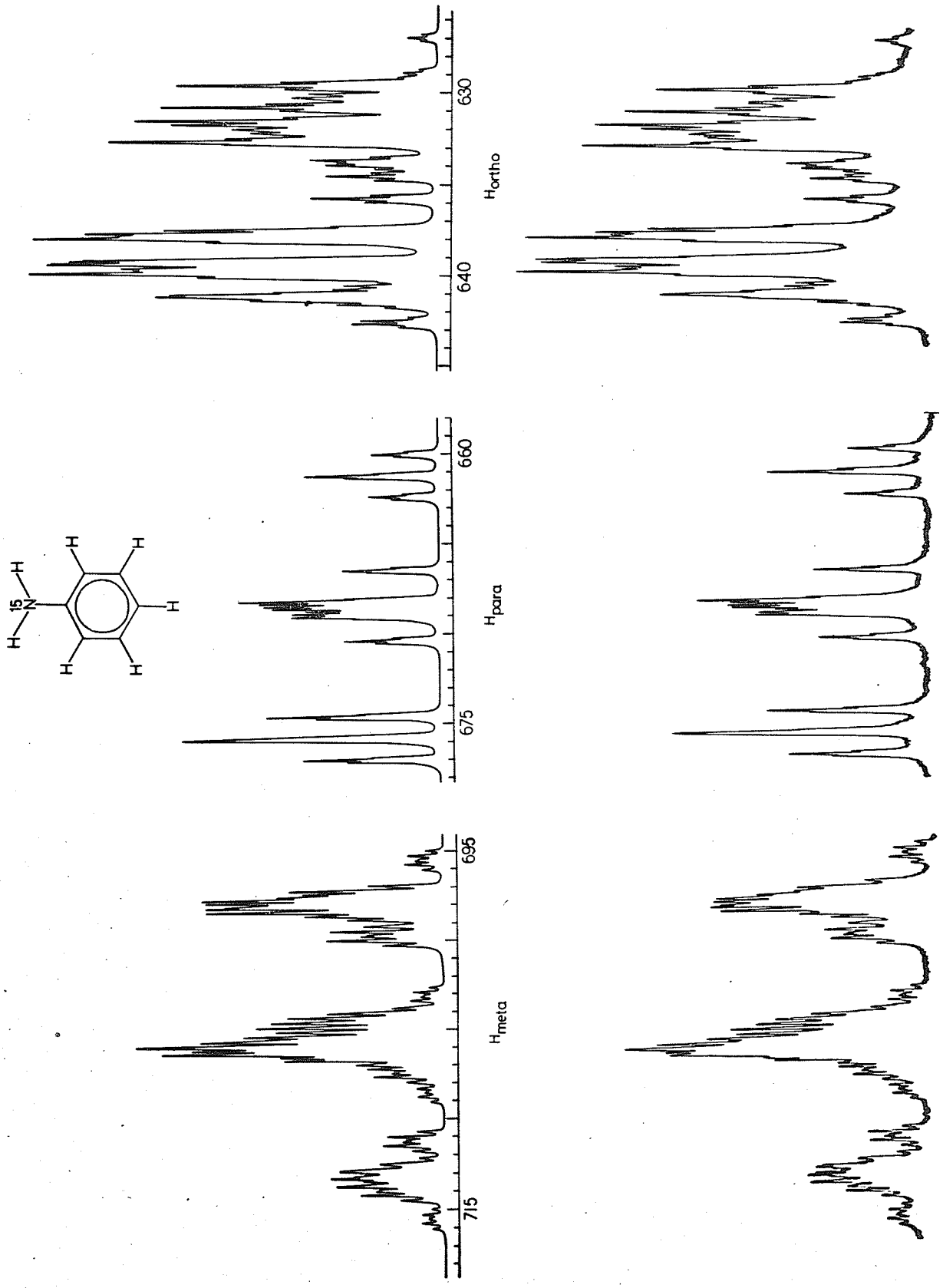
H
H
15N
H
H
H
H
H
H
630
640
660
675
695
715
Hortho
Hpara
Hmeta

the upfield meta proton transitions (701.0 to 694.2 Hz) are shown during irradiation of the low field ^{15}N-H resonance signal (333.408 Hz). Notice that the low field triplets collapse indicating $^{1}J(^{15}N,H)/^{4}J(^{15}N,H) > 0$. In Figure 8 the ortho proton transitions are shown during irradiation of the low field ^{15}N-H doublet. Once again the low field triplets collapse indicating that $^{3}J(^{15}N,H)$ is negative. The signs of the long-range ring proton - amino proton coupling constants were determined as described for 2-chloroaniline (23).

In the spectrum for the exchanging solution, 127 of the 130 transitions of significant intensity calculated by the computer program LAME (30) were assigned to observed peaks. The r.m.s. error was 0.021 Hz in the final iteration and the probable error was less than or equal to 0.008 Hz. Agreement between observed and calculated spectra was excellent. Because all of the coupling constants obtained in this analysis are the same to within 0.01 Hz as those obtained for the non-exchanging sample, the spectra are not reproduced here and the spectral parameters are omitted from the tables.

Only the amino proton resonance peaks were studied for the sample containing $^{15}ND_2$, ^{15}NHD, and $^{15}NH_2$ groups. At 31 ^{o}C the (isotope) shift in the ^{15}NHD group was 0.0235 ± 0.0020 ppm to high field of the $^{15}NH_2$ proton shift, compared to 0.0255 ± 0.0020 ppm in 2-chloroaniline-^{15}N (23). At this temperature the line widths of the ^{15}NHD and $^{15}NH_2$ proton resonance peaks were 1.35 and 0.85 Hz, respectively. Since $\gamma_H/\gamma_D = 6.514$ one can estimate the magnitude of the geminal proton coupling in the amono group, $^{2}J_{g}^{HNH}$, as 1.6 ± 0.6 Hz.

Figure 7. The upfield meta proton transitions (701.0 to 694.2 Hz) for the nonexchanging aniline - ^{15}N solution during strong irradiation of the low field ^{15}N-H resonance signal (333.41 Hz). By comparing this spectrum with that observed for the same region in Figure 6, it is obvious that the low field triplets have collapsed. Thus $^{1}J(^{15}N,H)/^{4}J(^{15}N,H) > 0$.

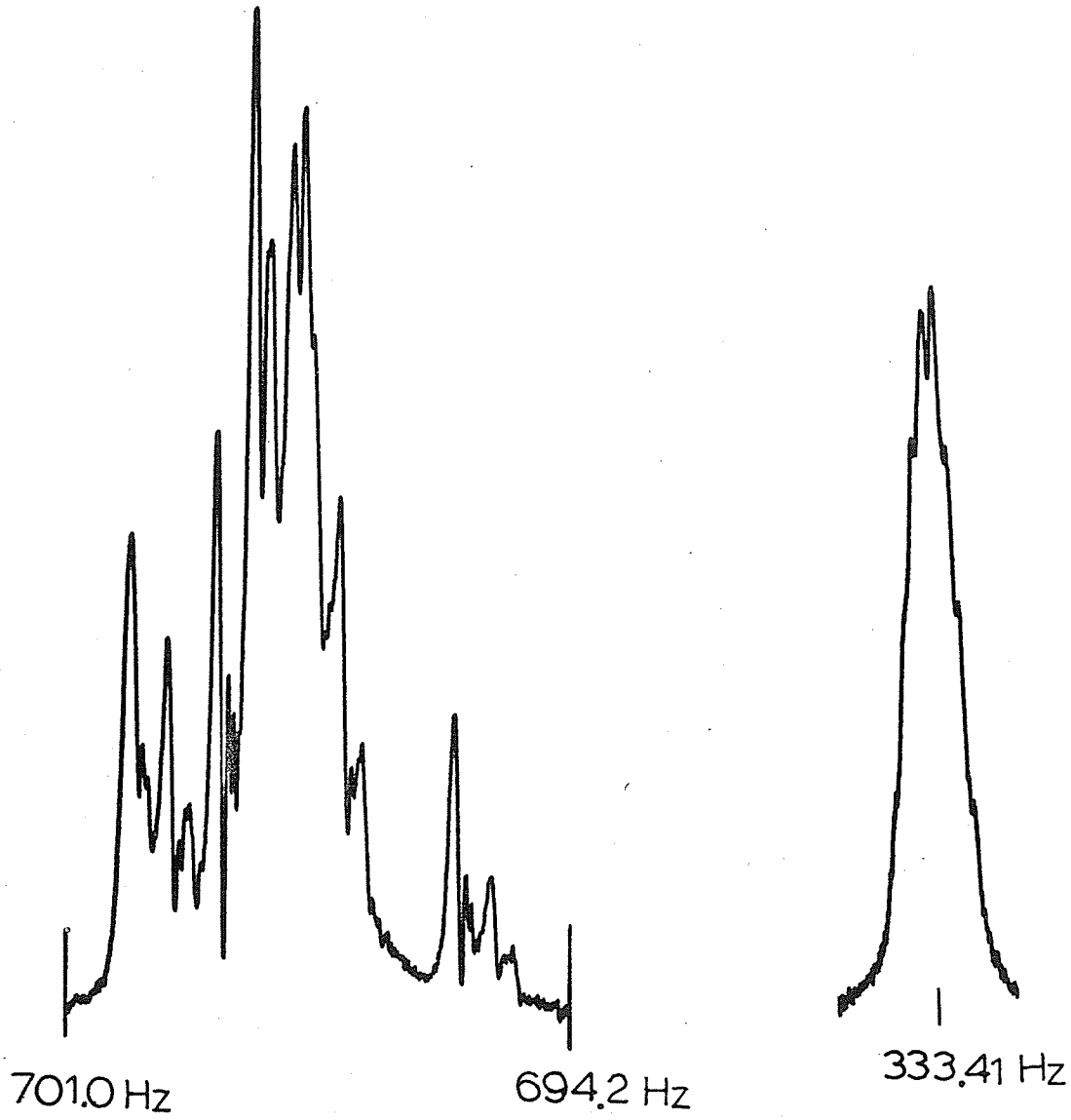
701.0 Hz
694.2 Hz
333.41 Hz

Figure 8. The ortho proton transitions for the nonexchanging aniline - ^{15}N solution during strong irradiation of the low field ^{15}N-H resonance signal. By comparing this spectrum with that observed for the same region in Figure 6, it is obvious that the low field triplets have collapsed. Thus $^{1}J(^{15}N,H)/^{3}J(^{15}N,H) > 0$.

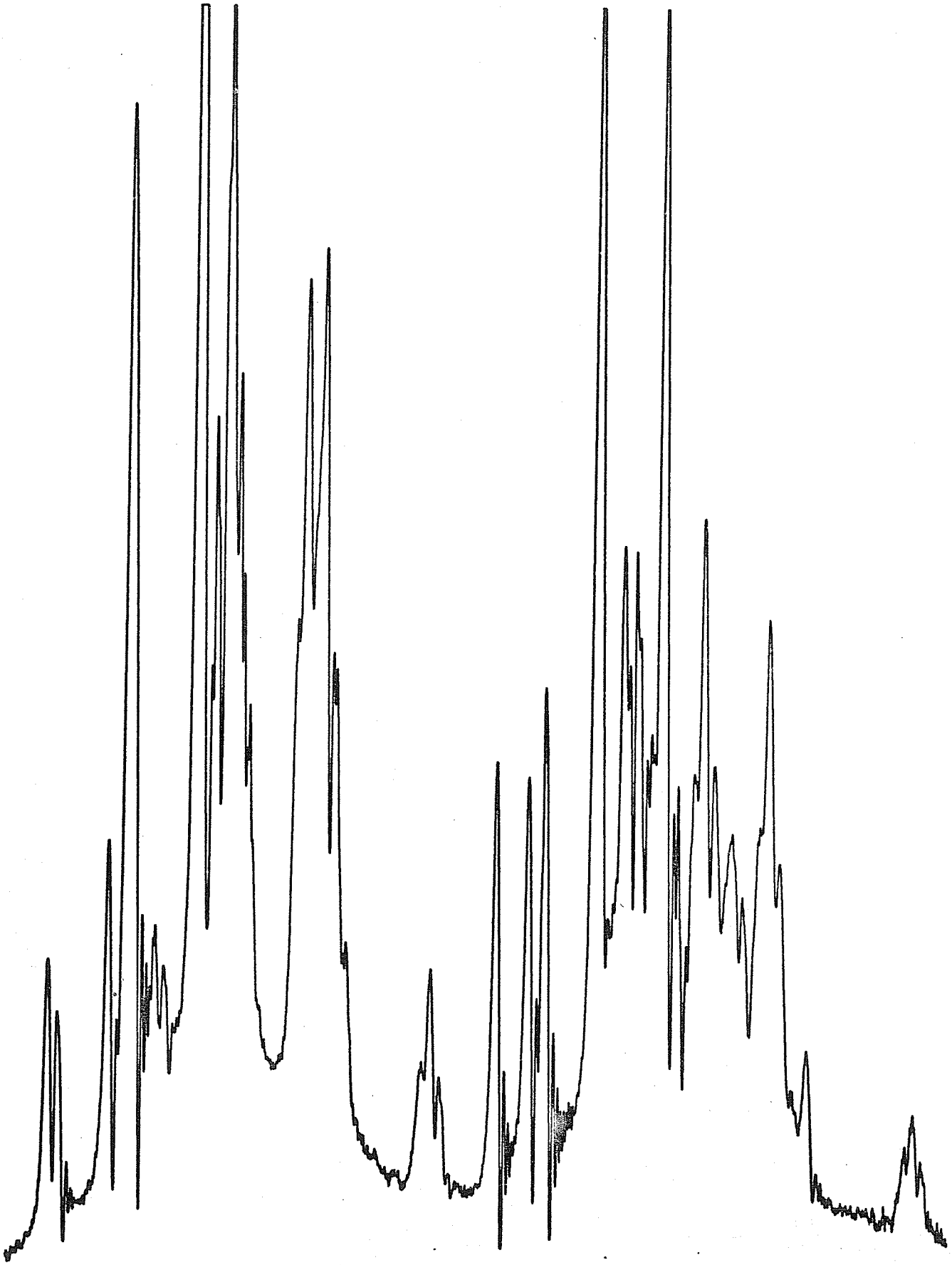

b) 2-Aminoacetophenone-^{14}N and -^{15}N

The derived coupling parameters for the two isotopomers are in close agreement and only those for the sample containing the non-exchanging ^{15}N compound are given in the tables. The methyl protons are coupled to H_6 (ortho to the acetyl group) by ±0.187 Hz.[2] On assigning all of the 264 calculated ring proton transitions to observed peaks the results given in Tables 5 and 6 are obtained. The r.m.s. error was 0.024 Hz and all probable errors were less than or equal to 0.006 Hz.

c) Acetanilide-^{15}ND

Because of its low solubility in benzene, the p.m.r. spectrum of an 11 mol % solution in acetone-d_6 was calibrated and analyzed using the program LACX. When freshly prepared, the amino proton resonance was observable as a doublet. Its disappearance after several weeks is attributed to slow exchange of the amino protons with deuterium in the solvent molecules. The rough analysis gave the results in Tables 5 and 6 and the probable errors were less than or equal to 0.021 Hz but a reasonable error estimate probably lies near 0.04 Hz.

d) Halogenated Derivatives of Aniline-^{15}N

These were studied as dilute solutions in benzene-d_6. The two bromine derivatives were present as a mixture, as were the two bromochloro derivatives. The peaks originating in each compound in the two mixtures were readily distinguishable. All observed peaks, including those of the amino protons, were assigned in the analysis by LAME. The derived parameters, given in Tables 5 and 6, had

---

[2] The value of ±0.187 Hz is obtained by a complete analysis of the spectrum using LAME and does not represent the observed splitting in the methyl proton resonance.

probable errors of less than 0.013 Hz and the r.m.s. error varied between 0.015 and 0.023 Hz. The amino proton - ring proton couplings had probable errors lying between 0.003 Hz and 0.006 Hz (one value).

2. Molecular Orbital Calculations

The coupling constants appearing in Tables 7 and 8 were calculated by the finite perturbation technique (25) in the INDO approximation (26). As many as 100 cycles in the SCF procedure were necessary to obtain convergence to 0.01 Hz. The parameterization is available only for first-row elements. Therefore computations were done only for aniline, 2-aminoacetophenone, acetanilide, and nitrobenzene. Standard geometries (26, 32) were employed to calculate the atomic coordinates in the benzene ring.

For aniline the geometry of the amino group was taken from the microwave results of Lister and Tyler (33). Another calculation on aniline assumed complete planarity of the molecule with C-N and N-H bond lengths equal to those given (33) for the nonplanar molecule. Standard geometries were used in a planar (apart from the methyl protons) model of 2-aminoacetophenone and also for nitrobenzene. The geometry of the sidechain in acetanilide was found in the literature (34-36). The acetamido group was assumed twisted 38° out of the benzene ring plane (36).

According to INDO the nonplanar form of aniline is 11.3 kcal/mol more stable than the planar form. Lister and Tyler (33) suggest an inversion barrier of less than 0.3 kcal/mol. An optimization of the geometry of the amino group at each successive stage of its inversion might well improve the computed value.

The calculated (observed) dipole moments in Debyes are:

TABLE 7

Computed long-range proton-proton coupling constants in Hz in aniline and 2-aminoacetophenone

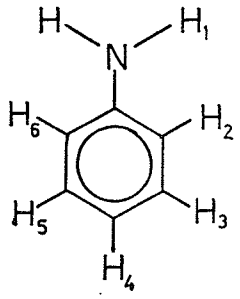

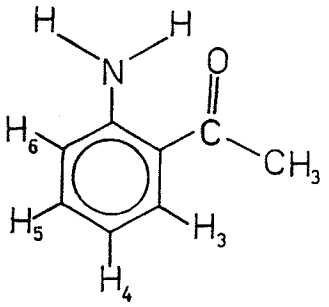

Coupling Constant	Nonplanar CNDO/2	Nonplanar INDO	Planar INDO	Coupling Constant	Planar* INDO
$^4J_o^{H_2,NH_1}$	0.353	0.088	0.686	$^4J_o^{H_6,NH_2}$	0.702
$^4J_o^{H_6,NH_1}$	0.010	-0.727	-0.166	$^4J_o^{H_6,NH_1}$	-0.143
$\langle ^4J_o^{H,NH} \rangle$	0.181	-0.319	0.260	$\langle ^4J_o^{H,NH} \rangle$	0.279
$^5J_m^{H_3,NH_1}$	0.065	0.080	-0.148	$^5J_m^{H_3,NH_1(H_2)}$	-0.211 (0.972)
$^5J_m^{H_5,NH_1}$	0.513	0.983	0.799	$^5J_m^{H_5,NH_1(H_2)}$	0.826 (-0.183)
$\langle ^5J_m^{H,NH} \rangle$	0.289	0.532	0.325	$\langle ^5J_m^{H,NH} \rangle$	0.380(H_3) 0.321(H_5)
$^6J_p^{H,NH}$	0.010	-0.203	0.127	$^6J_p^{H_4,NH_1(H_2)}$	0.187 (0.119)
$^2J_g^{HNH}$	5.704	-0.041	8.231	$^2J_g^{HNH}$	7.61

* $\langle ^5J^{H_3,CH_3} \rangle$ = 0.20 Hz when one C-H bond of the methyl group eclipses the C=O bond and the other two are staggered with respect to the C-H_3 bond of the ring.

TABLE 8

Computed coupling constants in Hz between ^{15}N and protons in some aniline derivatives* and in nitrobenzene

Coupling Constants		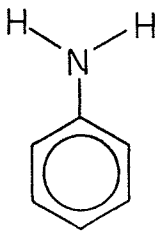	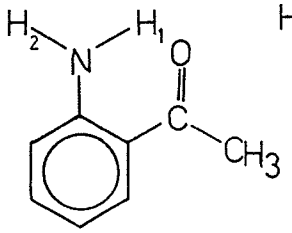	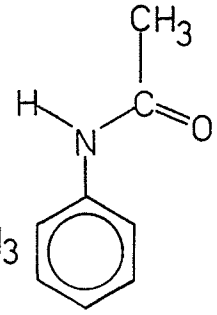	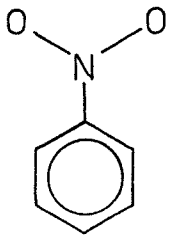
$^1J(^{15}N,H)$	H_1	-59.53†‡	-99.25	-73.48	—
	H_2	-59.53†‡	-87.76	—	—
$^3J(^{15}N,H_o)$		-2.52	-3.90	-3.86§	-3.75
$^4J(^{15}N,H_m)$	H_3	-1.06	-1.10	-1.12	-0.63
	H_5	-1.06	-0.94	-0.77	-0.63
$^5J(^{15}N,H_p)$		0.18	-0.33	-0.62	-0.82

* The nonplanar geometry for aniline and planar geometry for o-aminoacetophenone were employed as described in the text. For acetanilide the calculations were carried out assuming that the planar acetamido group was twisted 38° out of the benzene ring plane (36). Planar geometries assume an HNH angle of 120°.

† For an amino group coplanar with the aromatic ring one finds $^1J(^{15}N,H) = -92.20$ Hz.

‡ CNDO/2 finds -43.0 Hz.

§ This is the average of $^3J(^{15}N,H_2) = -3.461$ and $^3J(^{15}N,H_6) = -4.267$.

aniline, 1.46 (1.56); planar aniline, 1.105; acetanilide, 4.10 (3.88 to 4.02); nitrobenzene, 5.22 (3.93); 2-aminoacetophenone, 1.85 (2.05). Experimental dipole moments are cited from the compilation of McClellan (37).

3. The Coupling between ^{15}N and Amino Protons

a) Experimental Data

Three different linear relationships between the one bond ^{15}N-H coupling and the % s character of the nitrogen bond orbitals have been proposed (2,3, 23). Two (2, 3) are based mainly on the observation for $^{1}J(^{15}N,H)$ of about -75 Hz in ammonium ion (sp^3 hybridization), -90 Hz in amides (sp^2) and about -136 Hz in protonated nitriles (sp). The third (23) used anilinium ion and the geometry of aniline in the gas phase as calibration points. The latter writes % s = -0.59 $^{1}J(^{15}N,H)$ - 17.5 and yields 29% s character in aniline and 52% in sp systems. The former two give 46% and 52% for sp hybridization and 27 and 28% s character for aniline. Clearly, only semiquantitative predictions of the geometry of the amino group in aniline derivatives are possible by these methods. Furthermore, the coupling is solvent dependent (1, 4, 38) and the effective nuclear charge (39) is probably rather different in some of the compounds used for calibration, adding to the uncertainty in the reference points.

Nevertheless, in aniline derivatives containing meta and para substituents (1, 4) electron withdrawing substituents cause an increase in the magnitude of $^{1}J(^{15}N-H)$, interpretable as a decrease in π electron density, a flattening of the pyramid and therefore as a change in hybridization, at nitrogen. In Table 5 the ring-substituted anilines

all contain one or two groups ortho to the amino group. The observed magnitudes of $^{1}J(^{15}N,H)$ in these compounds are compatible with such an interpretation.

However, in the presence of ortho substituents intramolecular hydrogen bonding is an additional factor which may lead to a flattening of the nitrogen pyramid. Evidence for such bonds comes from X-ray diffraction data (40), the amino proton chemical shifts (5-8), as well as from N-H stretching frequencies (41, 42). The relatively large magnitude of 88.6 Hz for $^{1}J(^{15}N,H)$ in 2-aminoacetophenone in toluene solution, compared to 86.4 Hz for 4-nitroaniline in chloroform solution (1), can therefore be regarded as arising from a composite effect: electron withdrawal by the acetyl group, described by 1, together with hydrogen bonding between the N-H and C=O bonds as in 2.

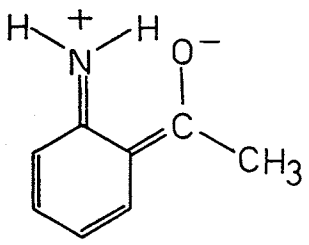

1

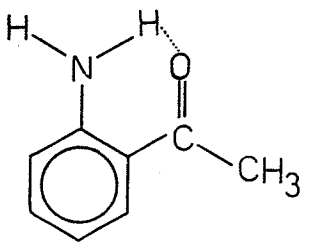

2

Both structures favor an HNH angle larger than the 114° in aniline (33). The linear relationship above yields 35% s character at nitrogen and

an HNH angle of 122° in 2-aminoacetophenone (using $\cos\theta/\cos\theta-1$ = fractional s character), perhaps somewhat large[3] but rather smaller than the 133° deduced from infrared data (41).

In an attempt to provide another measure of the degree of intramolecular hydrogen bonding in aniline derivatives Axenrod and Wieder (43) argue that the difference between the magnitudes of $^1J(^{15}N,H)$ in dimethylsulfoxide solution, where a strong tendency to intermolecular N-H hydrogen bonds to solvent molecules exists, and in chloroform solution, where intramolecular hydrogen bonds are preferred, is a measure of the hydrogen bonding abilities of the ortho substituent. These are deduced as NO_2 > C=O > Br, in reasonable agreement with a priori expectations. The data in Table 5 imply similar hydrogen bonding tendencies for Cl and Br substituents if due allowance is made for their electron withdrawing abilities, also indicated (1) as nearly the same by the $^1J(^{15}N,H)$ magnitudes in the meta and para haloanilines.

b) Computed Data

For ammonia the computed $^1J(^{15}N,H)$ is -42.6 Hz (26, 44) while the experimental value is ±65.1 Hz (45). A similar ratio of the two quantities, -59.5 Hz and -78.9 Hz, is found for aniline in Tables 5 and 8. However, when a planar form is assumed for aniline the computed

---

[3] For acetanilide, $^1J(^{15}N,H)$ is -91.3 Hz in DMSO solution (Table 5) but in view of the known solvent effects (1, 38) it could well be equal to $^1J(^{15}N,H)$ in 2-aminoacetophenone if both compounds were measurable in toluene solution. Planarity of the geometry about the nitrogen atom in 2-aminoacetophenone is therefore not ruled out by this difference in $^1J(^{15}N,H)$.

is larger than the observed magnitude. In this sense the INDO results are in qualitative agreement with the nonplanar geometry of aniline.

For 2-aminoacetophenone one observes -88.6 Hz for $^{1}J(^{15}N,H)$ whereas the average computed value for a planar 2-aminoacetophenone is -93.5 Hz, not strikingly different from the -92.2 Hz calculated for a planar aniline. The relatively good agreement between observed and calculated values is consistent with an almost planar 2-aminoacetophenone but unfortunately cannot be treated as confirmation of this conformation.[4]

Qualitatively the calculated one-bond ^{15}N-H couplings are in accord with the observed trend towards larger magnitudes as the nitrogen pyramid becomes more shallow in ring-substituted anilines.

4. Long-Range Couplings from Amino to Ring Protons

a) Experimental Data

By means of an earlier calibration procedure (22) $^{6}J_{p}^{H,NH}$ was estimated (22) as -0.14 Hz in aniline. Because of problems with intermolecular proton exchange, this parameter was not observable at that time (22) but the prediction is now borne out by the observed value of -0.137 Hz (Table 5). The prediction assumes the geometry of the aniline molecule in the gas phase (33), having an angle ϕ of 20° between the ring plane and the plane defined by the nuclei in the

---

[4] There is a much larger difference between calculated and observed values when the acetyl group is bonded directly to the nitrogen atom, as in acetanilide (Tables 5 and 8). However, it should be noted that in the latter case the calculations were carried out assuming that the planar acetamido group was twisted 38° out of the benzene ring plane (36).

C-N-H fragment (see 3). From the value of -0.108 Hz for $^{6}J_{p}^{H,NH}$ in

3

2-chloroaniline an average ϕ of 17.5° follows. $J_{p}^{H,NH}$ is not observable in 2-aminoacetophenone (Table 5) but an upper limit of 0.06 Hz for this coupling then yields a maximum angle ϕ of 12°. The observed coupling in 2-aminoacetophenone is of course also compatible with ϕ=0° and is an illustration of the unfortunate insensitivity of $J_{p}^{H,NH}$ to small angles of ϕ , a consequence of its proportionality to $\sin^2 \phi$ in the assumed coupling mechanism (22).

The assumption (22) that $J_{p}^{H,NH}$ originates in a hyperconjugative overlap between the N-H bonds and the π electron system of the ring, analogous to the mechanism described for methyl proton interactions in toluene (31, 46), is consistent with its observed values in Table 5. Alternatively, it might have been argued that a decrease in ϕ implies an increase in the conjugation of the nitrogen atom with the π system of the ring. A π electron mechanism operating via the nitrogen atom, i.e., via the partially double C⋯N bond, would then serve to enhance the magnitude of $J_{p}^{H,NH}$ in 2-aminoacetophenone relative to aniline. In fact the opposite occurs, in agreement with the hyper - conjugative model. The application of the model to the conformational problem also assumed the absence of an intrinsic, as distinct from a steric, effect on $J_{p}^{H,NH}$, in line with similar assumptions for other

sidechains (17, 31, 46).[5]

Such an effect is harder to exclude for $^{4}J_{o}^{H,NH}$, other four-bond couplings in unsaturated systems being subject to intrinsic substituent effects (17, 47), but its behaviour in Table 5 is roughly parallel to that of $J_{p}^{H,NH}$. An intrinsic effect on $^{5}J_{m}^{H5,NH}$ is found for the aniline derivatives in Table 5. For example, $J_{m}^{H5,NH}$ is 0.1 Hz smaller than $J_{m}^{H3,NH}$ in 2-aminoacetophenone. This behaviour is reproduced by the molecular orbital calculations.

b) Computed Data

In Table 7 the computed couplings between the amino and ring protons are given for the nonplanar conformation of aniline as well as for the planar forms of aniline and of 2-aminoacetophenone. Their high stereospecificity is of conformational interest. As the experimental values in Table 5 are measured for molecules in which rapid rotation occurs about the C-N bond, they should be compared with the average calculated couplings (indicated by angular brackets) in Table 7.

In as much as INDO considers one-center exchange integrals it includes the π electron contribution to the coupling constants (26). Thus, INDO finds their correct signs for the nonplanar form of aniline, whereas CNDO/2 calculates positive values for $^{4}J_{o}^{H,NH}$ and $^{6}J_{p}^{H,NH}$. On the other hand, INDO tends to overestimate the negative π electron contribution to these two couplings as well as the positive π

---

5 Even when the "substituent" atom forms part of the aromatic ring, as in pyridine, its intrinsic effect on couplings over six bonds is relatively minor (48).

contribution to $^{6}J_{m}^{H,NH}$ (reminiscent of a similar situation in benzaldehyde derivatives(17)). CNDO/2 agrees quantitatively with experiment for $^{5}J_{m}^{H,NH}$, suggesting a dominance of the σ electron contribution to this coupling; and furthermore finds $^{6}J_{p}^{H,NH} = 0.01$ Hz, thereby supporting the assumption that this parameter originates in π electron effects.

The signs of $^{4}J_{o}^{H,NH}$ and $^{6}J_{p}^{H,NH}$ calculated by INDO for the planar form of aniline are opposite to the observed sign. Although their magnitudes are probably again exaggerated, the implied conformational dependence qualitatively confirms the empirical use of the observed couplings in conformational deductions.

For a planar 2-aminoacetophenone the INDO results reproduce the substituent dependence of the two $^{5}J_{m}^{H,NH}$ values but again appear to overestimate the magnitudes of $^{4}J_{o}^{H,NH}$ and $^{6}J_{p}^{H,NH}$. The average coupling between the methyl protons and ring proton H_3 (configuration of the methyl group as given in Table 7) is computed as 0.20 Hz, compared to the observed value of ±0.19 Hz. Couplings of this kind occur when the protons are in close proximity (often called "through-space" couplings) and the comparison indicates that INDO can cope with such interactions (49, 50).

5. Coupling of ^{15}N to Ring Protons

The observed couplings in Table 5 are apparently not closely related to the geometry of the amino group although substituent effects on their magnitudes are present, particularly for $^{4}J(^{15}N,H_m)$. In Table 8 the computed couplings are rather larger than, but roughly in the proportion of, the measured parameters. The computed couplings in

nitrobenzene are not strikingly different from those in aniline derivatives. In nitrobenzene, $^{3}J(^{15}N,H_o)$ is calculated as -3.75 Hz, which may be compared to an observed value of ±2.5 Hz in 1-nitronaphthalene (51).

6. Coupling between Amino Protons

CNDO/2 finds $^{2}J^{H,NH}_{g}$ equal to 1.60 Hz in ammonia and INDO finds -6.37, in qualitative agreement with the experimental value of -10.35 ± 0.8 Hz (45). Similar behaviour is found for aniline in Table 7, CNDO/2 computing 5.70 Hz for this coupling whereas INDO calculates -0.04 Hz. For a planar aniline model the INDO estimate rises to 8.23 Hz. The INDO results are consistent with a nonplanar aniline form because the observed value is 1 to 2 Hz in magnitude. The sign of this coupling is probably negative since in 2-chloroaniline where the nitrogen pyramid is more flattened, $^{2}J^{H,NH}_{g} = 0 \pm 1$ Hz.

INDO computes 7.61 Hz in planar 2-aminoacetophenone. In this respect and also from the view point of the other computed couplings in Table 7 it would be of interest to analyze the spectrum of this compound under conditions where rapid rotation about the C-N bond does not occur.[6]

---

[6] Recently the free energy of activation for hindered rotation about this bond has been reported to be 10.6 ± 0.5 kcal/mol in toluene solution at 233 ± 10 ^{o}K (52) Preliminary low temperature measurements on the ^{15}N isotopomer indicate $^{2}J^{H,NH} \simeq 5$ Hz. Also it is of interest to note that INDO calculates $^{2}J^{H,NH}_{g}$ equal to +3.80 Hz in formamide while the observed value is +2.3 Hz in aqueous solution (53).

CONCLUSIONS

The magnitudes of the coupling constants between amino protons and ^{15}N or ring protons in aniline and some of its derivatives constitute a measure of the degree of flattening at the nitrogen pyramid. In contrast, the coupling constants between ^{15}N and the ring protons are sensitive to the presence of substituents but are not simply related to the geometry of the amino group. The long-range coupling constants computed by molecular orbital theory in the CNDO/2 and INDO approximations are sensitive to the stereochemistry and are in agreement with a nonplanar conformation of aniline.

REFERENCES FOR PART II

1. T. Axenrod, P.S. Pregosin, M.J. Wieder, E.D. Becker, R.B. Bradley, and G.W.A. Milne. J. Am. Chem. Soc. 93, 6536 (1971).
2. G. Binsch, J.B. Lambert, B.W. Roberts, and J.D. Roberts. J. Am. Chem. Soc. 86, 5564 (1964).
3. A.J.R. Bourn and E.W. Randall. Mol. Phys. 8, 567 (1964).
4. M.R. Bramwell and E.W. Randall. Chem. Commun. 250 (1969).
5. H. Suhr. Z. Elektrochem. 66, 466 (1962).
6. L.K. Dyall. Austral. J. Chem. 17, 419 (1964).
7. T. Yonemoto, W.F. Reynolds, H.M. Hutton, and T. Schaefer. Can. J. Chem. 43, 2668 (1965).
8. B.M. Lynch, B.C. Macdonald, and J.K.G. Webb. Tetrahedron 24, 3595 (1968); B.M. Lynch. Tetrahedron Lett. 1357 (1969).
9. H. Rottendorf and S. Sternhell. Austral. J. Chem. 17, 1315 (1964).
10. A.D. Cohen and K.A. McLauchlan. Mol. Phys. 9, 49 (1965).
11. G. Kotowycz and T. Schaefer. Can. J. Chem. 44, 2743 (1966).
12. M.P. Williamson, R.J. Kostelnik, and S.M. Castellano. J. Chem. Phys. 49, 2218 (1968).
13. A.F. Janzen and T. Schaefer. Can. J. Chem. 49, 1818 (1971).
14. G.J. Karabatsos and F.M. Vane. J. Am. Chem. Soc. 85, 3886 (1963).
15. S. Forsén, B. Akermark, and T. Alm. Acta. Chem. Scand. 18, 2313 (1964).
16. D.G. DeKowalewski and S. Castellano. Mol. Phys. 16, 567 (1969).
17. R. Wasylishen and T. Schaefer. Can. J. Chem. 49, 3216 (1971).
18. S. Forsén and R.A. Hoffman. J. Mol. Spectrosc. 20, 168 (1966).

19. R. Freeman. Mol. Phys. 6, 535 (1963).

20. J.A. Weil, A. Blum, A.H. Heiss, and J.K. Kinnaird. J. Chem. Phys. 46, 3132 (1967).

21. T. Schaefer and R. Wasylishen. Can J. Chem. 48, 1343 (1970).

22. R. Wasylishen and T. Schaefer. Can. J. Chem. 48, 1263 (1970).

23. R. Wasylishen and T. Schaefer. Can. J. Chem. 49, 3627 (1971).

24. W.B. Smith, A.M. Ihrig, and J.L. Roark. J. Phys. Chem. 74, 812 (1970).

25. J.A. Pople, J.W. McIver, and N.S. Ostlund. Chem. Phys. Lett. 1, 465 (1967).

26. J.A. Pople and D.L. Beveridge. Approximate molecular orbital theory. McGraw-Hill Book Co., New York, N.Y., 1970.

27. D. Elad. Tetrahedron Lett. 873 (1963).

28. R. Freeman and W.A. Anderson. J. Chem. Phys. 37, 2053 (1962).

29. (a) R.A. Hoffman and S. Forsén. In Progress in nuclear magnetic resonance spectroscopy. Vol. 1. Edited by J.W. Emsley, J. Feeney, and L.H. Sutcliffe. Pergamon Press, Oxford, 1966. (b) W.V. Philipsborn. Angew. Chem. internat. Edit. 10, 472 (1971).

30. C.W. Haigh. In Annual reports on NMR spectroscopy. Vol. 4., p. 311. Edited by E.F. Mooney. Academic Press, New York, 1971.

31. (a) W. McFarlane. Quart. Rev. 23, 187 (1969). (b) C.J. Jameson and H.S. Gutowsky. J. Chem. Phys. 51, 2790 (1969).

32. J.A. Pople and M.S. Gordon. J. Am. Chem. Soc. 89, 4253 (1967).

33. D.G. Lister and J.K. Tyler. Chem. Commun. 152 (1966).

34. J.K. Olsen and S. Kang. Theoret. Chim. Acta (Berl.) 17, 329 (1970).

35. R. Carter. Acta Chem. Scand. 21, 75 (1967).

36. L.E. Sutton, Editor. Chem. Soc. Spec. Publ. No. 11, M1-M19 (1958); No. 18, S1-S23 (1965).

37. A.L. McClellan. Tables of experimental dipole moments. W.H. Freeman and Company, San Francisco, California, 1963.

38. L. Paolillo and E.D. Becker. J. Magn. Resonance 2, 168 (1970).

39. D.M. Grant and W.M. Litchman. J. Am. Chem. Soc. 87, 3995 (1965).

40. D.L. Hughes and J. Trotter. J. Chem. Soc. A, 2181 (1971).

41. P.J. Krueger. Can. J. Chem. 40, 2300 (1962).

42. L.K. Dyall. Austral. J. Chem. 23, 947 (1970).

43. T. Axenrod and M.J. Wieder. J. Am. Chem. Soc. 93, 3541 (1971).

44. J.A. Pople, J.W. McIver, and N.S. Ostlund. J. Chem. Phys. 49, 2965 (1968).

45. R.A. Bernheim and H. Batiz-Hernandez. J. Chem. Phys. 40, 3446 (1964).

46. C.J. Macdonald and W.F. Reynolds. Can. J. Chem. 48, 1002 (1970).

47. M. Barfield. J. Am. Chem. Soc. 93, 1066 (1971).

48. J.B. Rowbotham, R. Wasylishen, and T. Schaefer. Can. J. Chem. 49, 1799 (1971).

49. P.C. Myhre, J.W. Edmonds, and J.D. Kruger. J. Am. Chem. Soc. 88, 2459 (1966).

50. M. Barfield and M. Karplus. J. Am. Chem. Soc. 91, 1 (1969).

51. Y. Kawazoe, M. Araki, S. Sawaki and M. Ohnishi. Chem. Pharm. Bull. (Tokyo) 18, 381 (1970).

52. R. Wasylishen and T. Schaefer. Can. J. Chem. 49, 3575 (1971).

53. R.J. Chuck, D.G. Gillies, and E.W. Randall. Mol. Phys. 16, 121 (1969).

PART III

INDO Molecular Orbital Calculations of Nitrogen-Proton Spin-Spin Coupling Constants over Two and Three Bonds. Effects of Lone-Pair Orientation, of Dihedral Angles and of Protonation

INTRODUCTION

There exists considerable experimental and theoretical interest in the correlation of the signs and magnitudes of nuclear spin-spin coupling constants with molecular structure (1-5). Attention has been focussed on the derivation of empirical relationships between coupling constants and parameters such as the electronegativity and spatial orientation of substituents, the direction of lone-pair electrons[1] as well as bond angles and bond orders. These relationships have proved useful in conformational studies (5). Recently (2, 3) the success of the INDO molecular orbital approximation in the calculation of geminal and vicinal proton-proton coupling constants has been demonstrated (6-9).

Detailed mapping of structural and substituent effects on two-bond and three-bond nitrogen-proton coupling constants has been hampered by experimental difficulties arising from the electric quadrupole moment of ^{14}N (natural abundance of 99.635%). Consequently $J(^{14}N,H)$ is only observable in molecules where the fluctuating electric field gradients at the nitrogen atom are small. The other isotope of nitrogen, ^{15}N, has spin 1/2 but its low natural abundance (0.365%) makes the measurement of $J(^{15}N,H)$ values difficult in unenriched samples. Nevertheless, a considerable body of data is now available (10, 11) for comparison with theory.

---

[1] In this discussion the lone-pair is treated as having directional character, in line with a simple hybridization model.

In the present study the technique of Pople et al. (6, 8) is employed in the study of structural and substituent effects on two-bond and three-bond nitrogen-proton coupling constants. In particular, the dependence of the calculated N,H coupling constants on the orientation of the nitrogen lone-pair, on the NCCH dihedral angle, and on the substituent electronegativity is examined. Computed N,H coupling constants are compared with experimental values when these are available. An attempt is made to compare the angular dependence of the calculated N,H coupling constants with that observed for phosphorus-proton coupling constants in certain molecules. The change in N,H couplings caused by protonation at nitrogen is also calculated and is compared to experiment.

COMPUTATIONAL METHOD

Atomic coordinates (12) and nuclear spin-spin coupling constants (13) were calculated as discussed in the introduction to this thesis. An attempt was made to calculate the N,H coupling constants in nitromethane, methylnitrate, and N,N-dimethylnitrosoamine, but even after 100 SCF cycles the energy and the coupling constants did not converge. Therefore the results of these calculations are not given.

RESULTS AND DISCUSSION

1. Two-Bond Nitrogen-Proton Coupling Constants

In Table 9 calculated two-bond $^{15}N,H$ coupling constants in the ^{15}N-C-H fragment are given for 31 compounds. Available experimental data are presented for comparison. In a few cases, where couplings have been observed for large molecules (greater than 40 valence electrons), comparison is made with values calculated for closely related smaller molecules. To simplify the discussion, the compounds in the first group (1 to 9) contain the $^{15}N(H)C{=}Z$ fragment. In the second group (10 to 15) the carbon atom of the ^{15}N-C-H fragment is bound to four atoms (approximately sp^3 hybridized) or to two atoms (approximately sp hybridized). The compounds in the third group (16 to 31) are either molecules with which one may associate a "localized nitrogen lone-pair" or are their protonated derivatives.

a) Compounds 1 to 9

The observed values of $^2J(^{15}N,H)$ in the 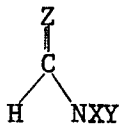 fragment range from -19.0 Hz in formamide (Z=O) through (-)8.3 Hz in N,N-dimethyl-^{15}N-phenyl-formamidine (Z=Nϕ) to ±0.2 Hz in diethylanilino-methene malonate ($Z=CR'_2$). The calculated values are in fair agreement with experiment: -17.23 Hz in formamide, -6.65 Hz in formamidine ($Z=N\langle^{H}$), and 0.23 Hz in vinylamine ($Z=C\langle^{H}_{H}$). This large range of $^2J(^{15}N,H)$ values is analogous to the range of $^2J(H,H)$ values observed and calculated in the $^{H}_{H}\rangle C{=}Z$ fragment (2, 18).

The observed decrease in $^2J(^{15}N,H)$ between $Z=C\langle^{R}_{R}$ and Z=O has

TABLE 9

Observed and calculated two-bond $^{15}N,H$ coupling constants*

EXPERIMENTAL RESULTS				CALCULATED RESULTS		
	COMPOUND	$^2J(^{15}N,H)$ observed	REFERENCE	COMPOUND	$^2J(^{15}N,H)$ calculated	REFERENCE+
1.	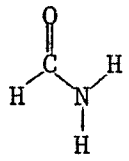	-19.0 (neat liquid)	14.	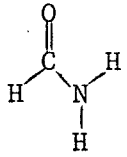	-17.23	a.
		-16.4 (in acetone)	15.		-15.62	b.
		-14.47 (in water, 15M%)	16.			
2.	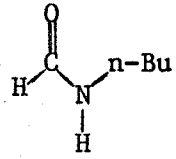	-15.6 (neat liquid)	17.	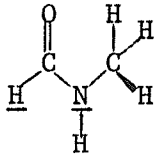	-16.85	c.
3.	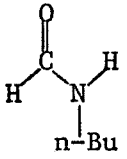	-14.3 (neat liquid)	17.	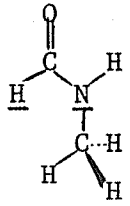	-19.21	c.

EXPERIMENTAL RESULTS			CALCULATED RESULTS		
COMPOUND	$^2J(^{15}N,H)$ observed	REFERENCE	COMPOUND	$^2J(^{15}N,H)$ calculated	REFERENCE[+]
4. 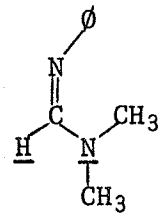	(-)8.3	18.	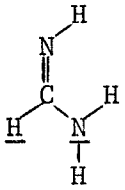	-6.65	b.
5. 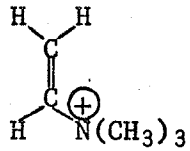	-4.9	19.	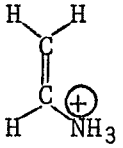	-2.83	d.
6. 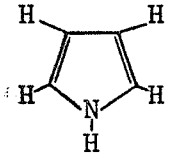	-4.52	20.	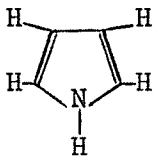	-1.82	e.
7. 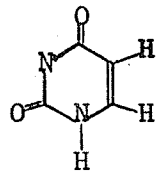	(-)3.50	21.	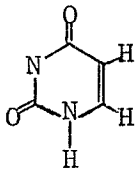	0.67	f.

EXPERIMENTAL RESULTS			CALCULATED RESULTS		
COMPOUND	$^2J(^{15}N,H)$ observed	REFERENCE	COMPOUND	$^2J(^{15}N,H)$ calculated	REFERENCE[+]
8. 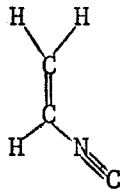	-3.16	19,22	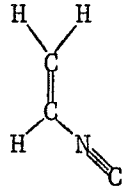	0.52	g.
9. 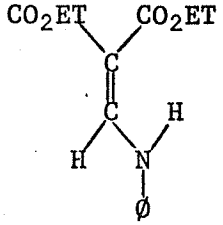	±0.2	18.	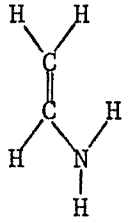	+0.23	b.
10. 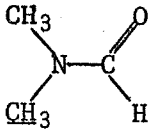	1.10	23.	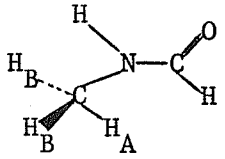	H_A 2.85 H_B 1.49	b.

EXPERIMENTAL RESULTS			CALCULATED RESULTS		
COMPOUND	$^2J(^{15}N,H)$ observed	REFERENCE	COMPOUND	$^2J(^{15}N,H)$ calculated	REFERENCE[+]
11. 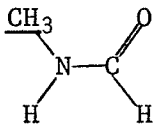	1.20	15.	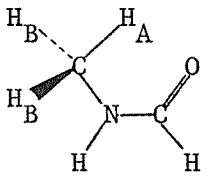	H_A 2.85 H_B 1.49	b.
12. $CH_3CH_2N{\equiv}C$	2.67	24,25.	$CH_3CH_2N{\equiv}C$ (staggered)	+3.90	h.
13. $CH_3N{\equiv}C$	3.23	24.	$CH_3N{\equiv}C$	+4.29	i.
14. $H{-}C{\equiv}N$	8.7	26.	$H{-}C{\equiv}N$	+5.11	j.
15. $H{-}C{\equiv}\overset{\oplus}{N}{-}H$	19.0	27.	$H{-}C{\equiv}\overset{\oplus}{N}{-}H$	+11.39	k.
16. CH_3NH_2	-1.0	28.	CH_3NH_2	-2.70 (average for staggered conformation)	1.

EXPERIMENTAL RESULTS			CALCULATED RESULTS		
	COMPOUND	$^2J(^{15}N,H)$ observed	REFERENCE	COMPOUND	$^2J(^{15}N,H)$ calculated	REFERENCE[+]
17.	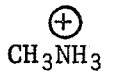	±0.8	29.	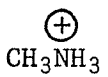	+2.41 (average for staggered conformation)	l.
18.	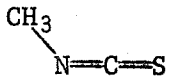	±3.3	29.	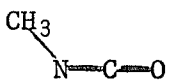	+0.89 (average over all angles)	m.
19.	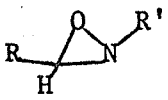	-4.8 to -5.4	30,31.	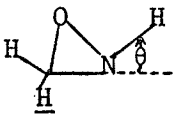 θ=64°	-5.78	n.
20.	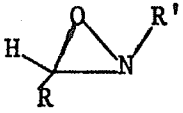	~0.0	30,31.	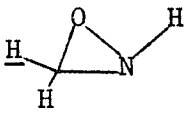 θ=64°	0.95	n.

EXPERIMENTAL RESULTS			CALCULATED RESULTS		
COMPOUND	$^2J(^{15}N,H)$ observed	REFERENCE	COMPOUND	$^2J(^{15}N,H)$ calculated	REFERENCE[+]
21. 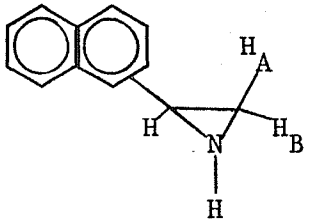	H_A (-)4.9 H_B (-)0.3	32.	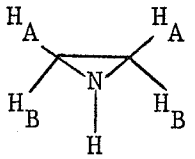 θ=68°	H_A -9.14 H_B 0.62	n.
22. 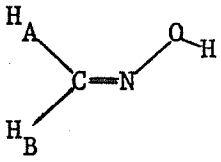	H_A 2.68 H_B -13.88	33.	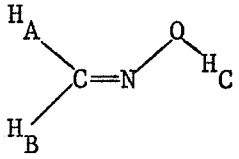	H_A - 0.77 H_B -10.90 H_C - 5.50	o.
			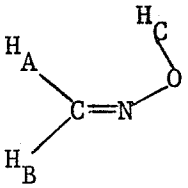	H_A -1.33 H_B -8.53 H_C +6.38	p.
23. 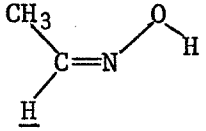	-15.93	33.	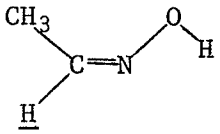	-15.40	q.

EXPERIMENTAL RESULTS			CALCULATED RESULTS		
	COMPOUND	$^2J(^{15}N,H)$ observed	REFERENCE	COMPOUND	$^2J(^{15}N,H)$ calculated	REFERENCE[+]
24.	-			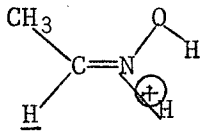	4.66	q.
25.	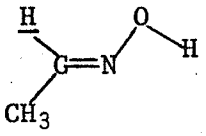	2.93	33.	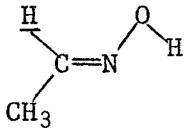	-0.59	q.
26.	-			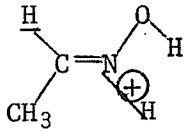	4.43	q.
27.	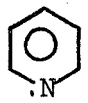	-10.76	34.	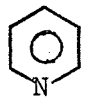	-16.98	r.
28.	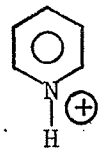	-3.01	34.	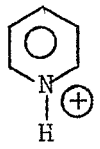	0.48	s.

EXPERIMENTAL RESULTS				CALCULATED RESULTS		
	COMPOUND	$^2J(^{15}N,H)$ observed	REFERENCES	COMPOUND	$^2J(^{15}N,H)$ calculated	REFERENCES+
29.		-15.0	35.	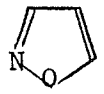	-11.19	t.
30.	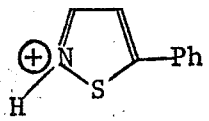	-4.2	35.	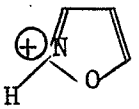	+0.39	t.
31.	-	-	-	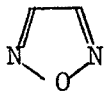	-6.58	u.

* All the coupling constants are $J(^{15}N,H)$ values in Hz; $J(^{14}N,H)$ values have been converted to $J(^{15}N,H)$ values by multiplying by -1.402757 (36).

+ The geometries used for the INDO calculations were taken from the following references:

a) C.C. Costain and J.M. Dowling. J. Chem. Phys. 32, 158 (1960). *b*) Standard geometries were used; J.A. Pople and D.L. Beveridge. Approximate molecular orbital theory. McGraw Book Company. New York, N.Y., 1970. *c*) Standard bond lengths and

(con't)

bond angles (reference *b*) were used for the $NHCH_3$ fragment, while the NCOH fragment was assumed to have the same geometry as that given in reference *a*. *d*) Standard bond lengths and bond angles were used for the vinyl fragment (see reference *b*). The C-N and N-H bond lengths were taken as 1.45 Å and 1.03 Å respectively. *e*) L. Nygaard, J.T. Nielsen, J. Kirchheiner, G. Maltesen, J. Tastrup-Andersen, and G.O. Sørensen. J. Mol. Struct. 3, 491 (1971). *f*) Same as that given for thymine by L.C. Snyder, R.G. Shulman and D.B. Neuman. J. Chem. Phys. 53, 256 (1970) except the methyl group was replaced by a proton with a bond length of 1.086 Å. *g*) The atomic coordinates of the vinyl group were taken from S. Meza and U. Wahlgren. Theoret. Chim. Acta, 21, 323 (1971). The C-N and N≡C bond lengths were assumed to be 1.424 and 1.166 Å respectively (see reference *i*). *h*) The atomic coordinates of the CH CH group were taken from W.J. Jorgensen and L.C. Allen. J. Amer. Chem. Soc., 93, 567 (1971). The C-C≡N fragment was assumed to have the same bond lengths and angles as those given in reference *i*. *i*) C.C. Costain. J. Chem. Phys. 29, 864 (1958). *j*) V.W. Laurie and D.R. Herschback. J. Chem. Phys. 37, 1687 (1962). *k*) This molecule was assumed linear with the following bond lengths: 1.12 Å (H-C), 1.32 Å (C≡N), and 1.04 Å (N-H). *l*) W.H. Fink and L.C. Allen. J. Chem. Phys. 46, 2276 (1967). For protonated methyl amine the following geometry was assumed: N-C bond length = 1.50 Å, C-H bond length = 1.09 Å, N-H bond length = 1.03 Å. All angles were assumed tetrahedral. *m*) R.G. Lett and W.G. Flygare. J. Chem. Phys. 47, 4730 (1967). *n*) J.M. Lehn, B. Munsch, Ph. Millies, and A. Veillard. Theoret. Chim. Acta, 13, 313 (1969). *o*) I.N. Levine. J. Chem. Phys. 38, 2326 (1963). *p*) Same as reference *o*, except that the dihedral angle CNOH was taken as zero degrees. *q*) R.S. Rogowski and R.H. Schwendeman. J. Chem. Phys. 50, 397 (1969). The protonated oximes were assumed to have the same geometry as the unprotonated species. The angle CNH^+ was assumed to be 120° and the N-H bond length was taken as 1.03 Å. *r*) B. Bak, L. Hansen-Hygaard and J. Rastrup-Andersen. J. Mol. Spectrosc.

(con't)

2, 361 (1958). *s*) Same as reference *r*, except for the additional hydrogen atom which was assumed to be 1.03 Å from the pyridine nitrogen atom. *t*) M. Cannas, G. Marongui. Z. Kristallogr. 127, 388 (1968) and S. Biagini, M. Cannas and G. Marongui. J. Hetrocyclic Chem. 6, 901 (1969). The protonated isoxazole was assumed to have the same geometry as the unprotonated species. Angle ONH was assumed to be 127.3° and the N-H bond length was taken as 1.03 Å. *u*) E. Saegebarth and A.P. Cox. J. Chem. Phys. 43, 166 (1965).

been attributed to the higher electronegativity of the oxygen atom as well as to the increase in the π-bond order of the C-N bond (10, 11, 23). In Table 10 calculated values of $^{2}J(^{15}N,H)$ are compared with calculated C-N bond orders and with calculated charge densities at the carbon atom of the NCH fragment. As the electronegativity of Z decreases, the C-N bond orders decrease and the positive charge on the carbon atom of the NCH fragment also decreases, confirming the qualitative arguments (10, 11, 23).

The effect of an electronegative substituent placed β to the carbon atom of the N-C-H fragment was also investigated. In Table 11 the calculated values of $^{2}J(^{15}NCH)$ for three trans-x-vinylamines are

TABLE 11

Effect of substituent electronegativity on $^{2}J(^{15}N,H)$ and $^{2}J(H,H)$*

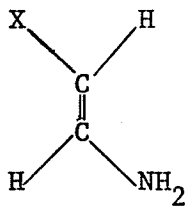

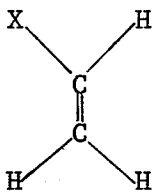

X	$^{2}J(^{15}N,H)$ calc.	$^{2}J(H,H)$ calc.	$^{2}J(H,H)$ obs.
Li	-6.01	13.80	7.1
H	0.23	3.24	2.3
F	1.66	-0.18	-3.2

* Standard geometries (8, 37) were used for all calculations. The C-Li bond length was taken as 2.1 Å (3). Computed and observed values of $^{2}J(H,H)$ are cited from reference (2).

TABLE 10

A comparison of calculated $^{2}J(^{15}NCH)$ values with N-C bond orders and carbon charge densities for compounds 1, 4, and 9.*

Compound	$^{2}J(^{15}N,H)$	Bond Orders $N(p_\pi)$	$C(p_\pi)$	N(s)	C(s)	Total Charge at Carbon (x 10^{+4} electrons)
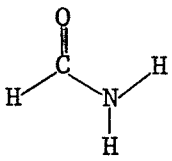	-15.62	0.4412		0.2999		+4382
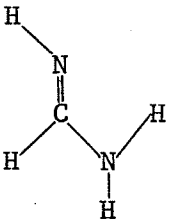	-6.57	0.4043		0.2975		+3018
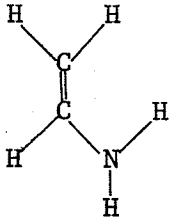	0.23	0.3373		0.2833		+1674

*Standard geometries (8, 37) were used for all calculations.

compared with the calculated and observed $^2J(\underline{H}C\underline{H})$ values in the corresponding substituted ethylenes (2). From Tables 10 and 11, it is apparent that the calculated reduced coupling constants $^2K(\underline{N}C\underline{H})$ show the same trends as the $^2K(\underline{H}C\underline{H})$ values (2, 38).[2]

b) Compounds 10 to 15

In molecules where the carbon atom of the N-C-H fragment is bound to four atoms (compounds 10-13 and 16-21) the known two-bond $^{15}N,H$ coupling constants are usually less than 3.5 Hz in magnitude (10). Exceptions have been observed in cyclic molecules where the relevant dihedral angle[3] is fixed on the n.m.r. time scale (see compounds 19 to 21). In the next section it is shown that when the carbon atom is bound to four groups, one of them being a nitrogen atom with a "localized lone-pair" $^2J(^{15}N,H)$ is predicted to vary over a wide range. However, internal rotation has the consequence that the observed values of these coupling constants are small (see compounds 16 and 18, for example).

Calculated values for compounds 10 to 15 agree fairly well with experiment. Both the calculated and observed $^2J(^{15}N,H)$ increase on going from ethylisocyanide to methylisocyanide. The calculated $^2J(^{15}N,H)$ in protonated hydrogen cyanide is 11.39 Hz, significantly

---

[2] The reduced coupling constant is defined as $K_{AB} = 2\pi J_{AB}/\hbar\gamma_A\gamma_B$. Since $\gamma(^1H)$ and $\gamma(^{15}N)$ are of opposite sign, $K(^{15}N,H)$ and $J(^{15}N,H)$ are also of opposite sign.

[3] In the simple hybridization picture the nitrogen lone-pair has directional character; therefore it is reasonable to define a dihedral angle between the plane containing the NCH fragment and the plane containing the lone-pair, NC fragment.

lower than the observed value of 19.0 Hz (27). This discrepancy is probably due in part to the choice of geometry for the protonated species.

c) Compounds 16 to 31

It is known that the observed two-bond $^{15}N,H$ coupling constants in compounds 19-23, 25, 27, and 29 are stereospecific, depending on the orientation of the nitrogen lone-pair (10, 11, 33). Specifically, if the lone-pair is directed cis to the C-H bond then $^{2}J(^{15}N,H)$ is observed and calculated (see Table 9) to be large and negative; if the nitrogen lone-pair and C-H bond lie trans to one another then the absolute value of $^{2}J(^{15}N,H)$ is small. To test the generality of this rule, the angular dependence of $^{2}J(^{15}N,H)$ was calculated for methylamine, methylisocyanate, methylenimine, and aziridine. The results of these calculations are presented in Figures 9, 10, 11, and 12. In each calculation bond lengths were taken to be the same as those in the ground state conformation (see geometry references in Table 9).

i) Methylamine

In Figure 9, $^{2}J(^{15}N,H)$ is plotted as a function of the angle, θ, defined in 1 and 2. This angle can also be described as the dihedral angle defined by the lone-pair, NC fragment and the NCH fragment.

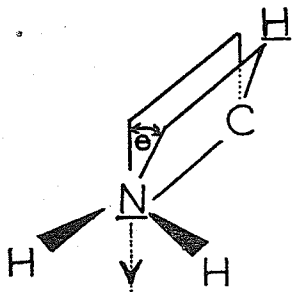

1

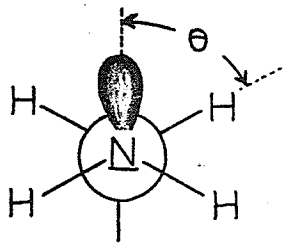

2

Figure 9. A plot of the calculated $^{2}J(^{15}N,H)$ versus the dihedral angle defined by the lone-pair N-C-H fragment in methylamine.

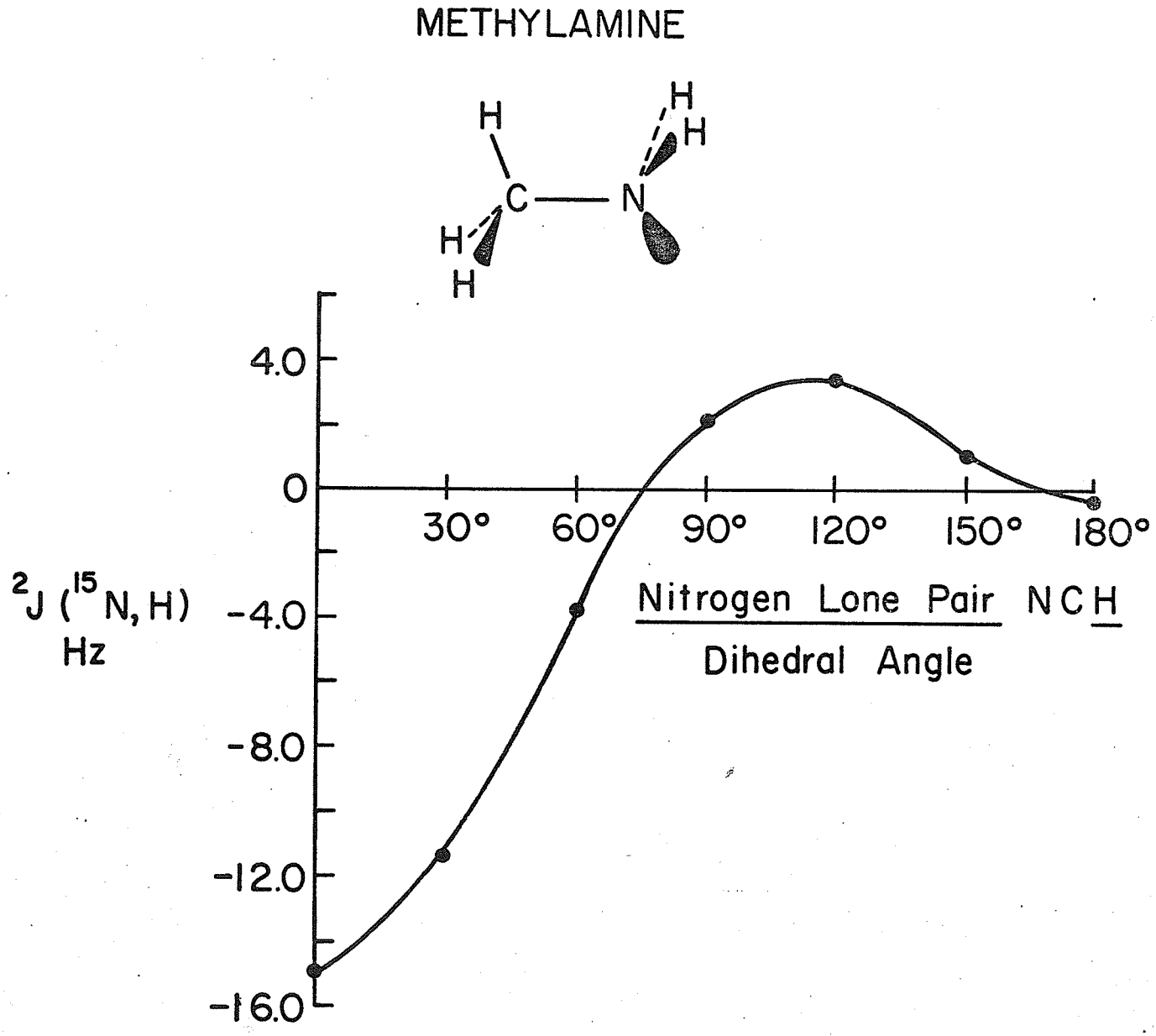
METHYLAMINE
H
H
H
C
N
H
H
4.0
0
-4.0
-8.0
-12.0
-16.0
30°
60°
90°
120°
150°
180°
^{2}J (^{15}N, H) Hz
Nitrogen Lone Pair NCH
Dihedral Angle

For $\theta=0^{\circ}$ one of the C-H bonds eclipses the lone-pair and $^{2}J(^{15}N,H)$ for the proton in that bond is calculated as large and negative, -14.90 Hz. For $\theta=180^{\circ}$, one of the C-H bonds sits trans to the lone-pair and $^{2}J(^{15}N,H)$ is -0.40 Hz. Notice that $^{2}J(^{15}N,H)_{cis}$ and $^{2}J(^{15}N,H)_{trans}$ predicted for methyl amine are similar to those observed for unsaturated compounds such as formaldoxime (compound 22).

To compare experimental and calculated couplings in methyl amine, one need only consider the staggered conformation because the barrier to rotation about the C-N bond is 1.98 kcal/mol (39). For the staggered conformation one calculates an average of -2.70 Hz while the observed value is -1.0 Hz (28) (INDO calculates the barrier to rotation of the methyl group as 1.74 kcal/mol).

Few observations are available for two-bond $^{15}N,H$ coupling constants in saturated systems of fixed geometry. However, it is of some interest to compare calculations for methyl amine with those observed for the saturated 1,3 oxazine(3). Riddel and Lehn (40) measured $^{2}J(^{15}N,H_{2_a})$ and $^{2}J(^{15}N,H_{4_a})$ as approximately zero, while $^{2}J(^{15}N,H_{4_e})$ was about 1.5 Hz. The sign of the latter coupling is almost certainly negative since on protonation of the nitrogen atom these couplings are no longer resolved.[4] Notice that the relevant angle is approximately 180° for H_{2_a} and H_{4_a} while for H_{4_e} it is approximately 60°. For $\theta=180 \pm 5^{\circ}$ and $\theta=60 \pm 5^{\circ}$, INDO calculates $^{2}J(^{15}N,H)$ as -0.4 ± 0.1 Hz and -3.8 ± 1.3 Hz, respectively, for methylamine.

---

[4] The choice of sign is based on the observation that $^{2}J(^{15}N,H)$ usually increases on protonation (33). This observation is supported by the MO calculations. For example, in protonated methylamine INDO calculates $^{2}J(^{15}N,H) = 2.43 \pm 0.05$ Hz, independent of the HNCH dihedral angle.

ii) Methylisocyanate

In Figure 10 the calculated $^{2}J(^{15}N,H)$ in methylisocyanate is plotted as a function of the angle θ, defined in 4. The plot closely resembles that calculated for methylamine. For a given θ, this coupling

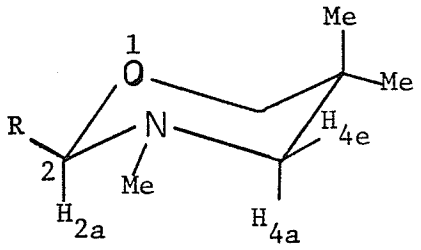

3

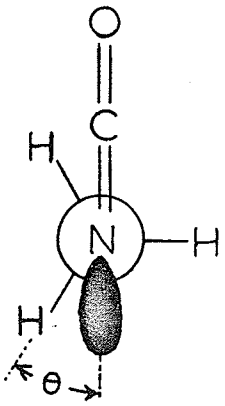

4

in methylisocyanate is calculated to be larger than in methylamine. $^{2}J(^{15}N,H)$ is 5.52 Hz when the C-H bond lies trans to the lone-pair ($\theta=180^{o}$); when the C-H bond lies cis to the lone-pair ($\theta=0^{o}$), $^{2}J(^{15}N,H)$ is -9.93 Hz.

The conformation of lowest energy is calculated as one in which a C-H bond eclipses the nitrogen lone-pair ($\theta=0^{o}$). The barrier to rotation of the methyl group is calculated as 102 cal/mol, in good agreement with the experimental barrier of 83 ± 15 cal/mol (41). Because the barrier is so small, comparison of calculated with experimental coupling constants entails an average over all angles and one finds $^{2}J(^{15}N,H) = 0.88$ Hz. This coupling constant has not been measured in methylisocyanate; in the related compound, methylisothiocyanate, $^{2}J(^{15}N,H) = \pm 3.3$ Hz (29).

Figure 10. A plot of the calculated $^{2}J(^{15}N,H)$ versus the dihedral angle defined by the lone-pair N-C-H fragment in methylisocyanate.

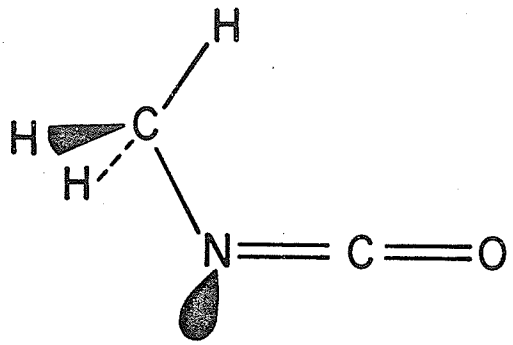
H
H
C
H
N
C
O

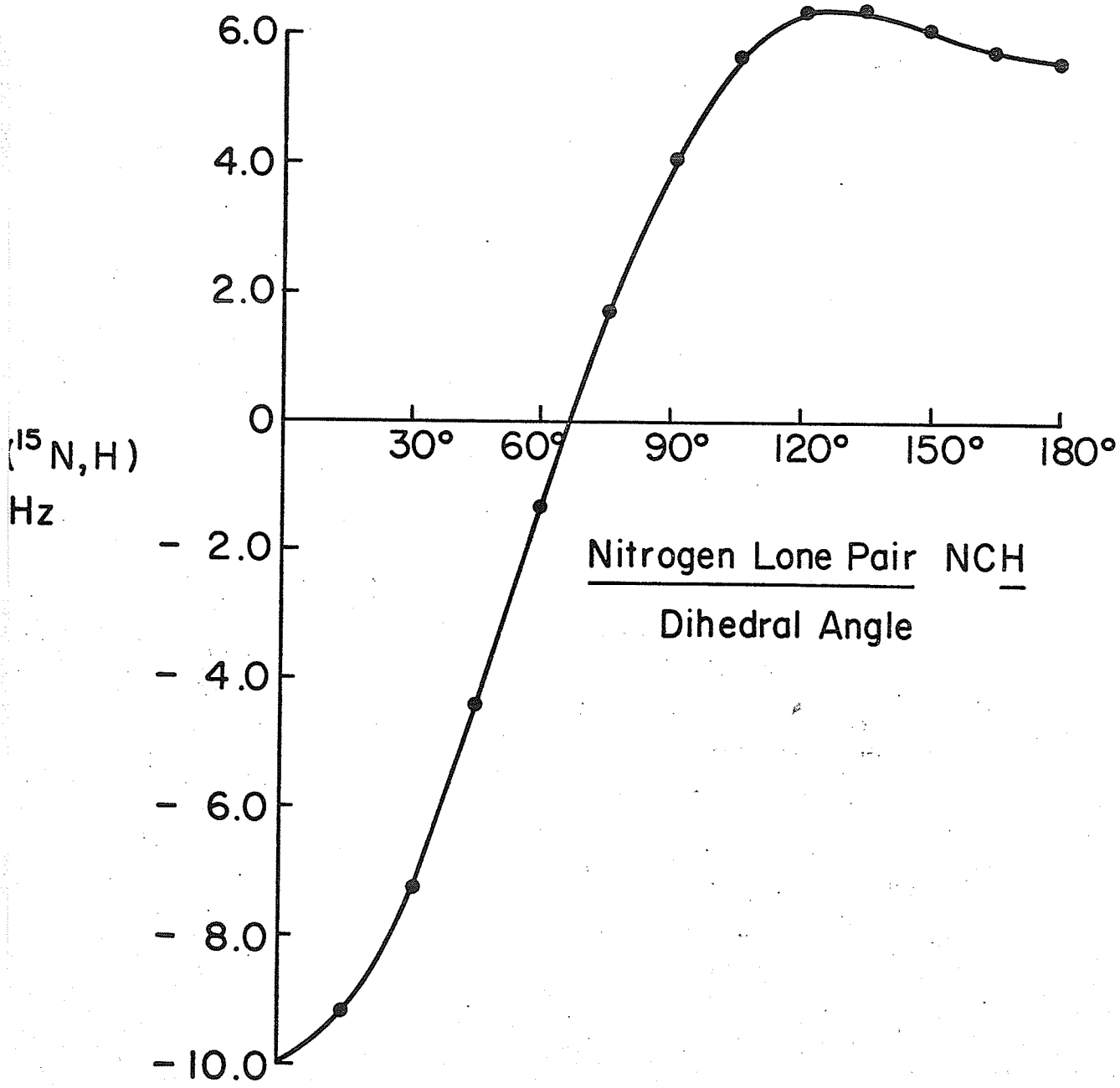
6.0
4.0
2.0
0
- 2.0
- 4.0
- 6.0
- 8.0
- 10.0
30°
60°
90°
120°
150°
180°
(15N,H)
Hz
Nitrogen Lone Pair NCH
Dihedral Angle

iii) Methylenimine

For methylenimine (5), $^{2}J(^{15}N,H)$ is plotted against θ in Figure 11. INDO finds the lowest energy when $\theta \sim 65^{\circ}$. At this angle

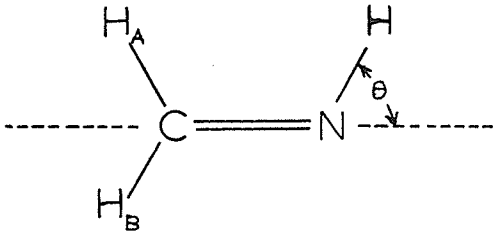

5

$^{2}J(^{15}N,H_A)$ = 4.18 Hz and $^{2}J(^{15}N,H_B)$ = -11.41 Hz.

The barrier to pyramidal inversion is calculated to be 25.5 kcal/mol, in good agreement with the values of 27.9 and 26.2 kcal/mol found by ab initio SCF-LCAO-MO methods (42, 43).

The INDO method was employed to examine substituent effects on $^{2}J(^{15}N,H)$ values in three hypothetical syn- and anti-substituted methylenimines (Table 12). As the electronegativity of X increases,

TABLE 12

Calculated values of $^{2}J(^{15}N,H)$ for some substituted methylenimines*

	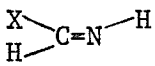	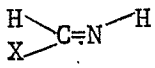
X	$^{2}J(^{15}N,H)$	$^{2}J(^{15}N,H)$
Li †	-17.82	-18.54
H	-9.64	4.27
F	-6.48	10.04

* Standard geometries (8, 37) were used for all calculations.

† The C-Li bond length was taken as 2.1 Å.

Figure 11. A plot of the calculated $^{2}J(^{15}N,H)$ versus the indicated angle θ in methylenimine.

METHYLENIMINE

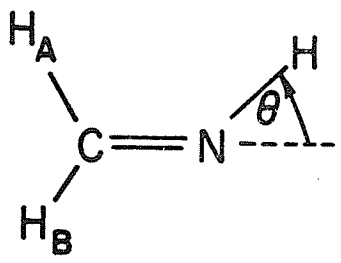

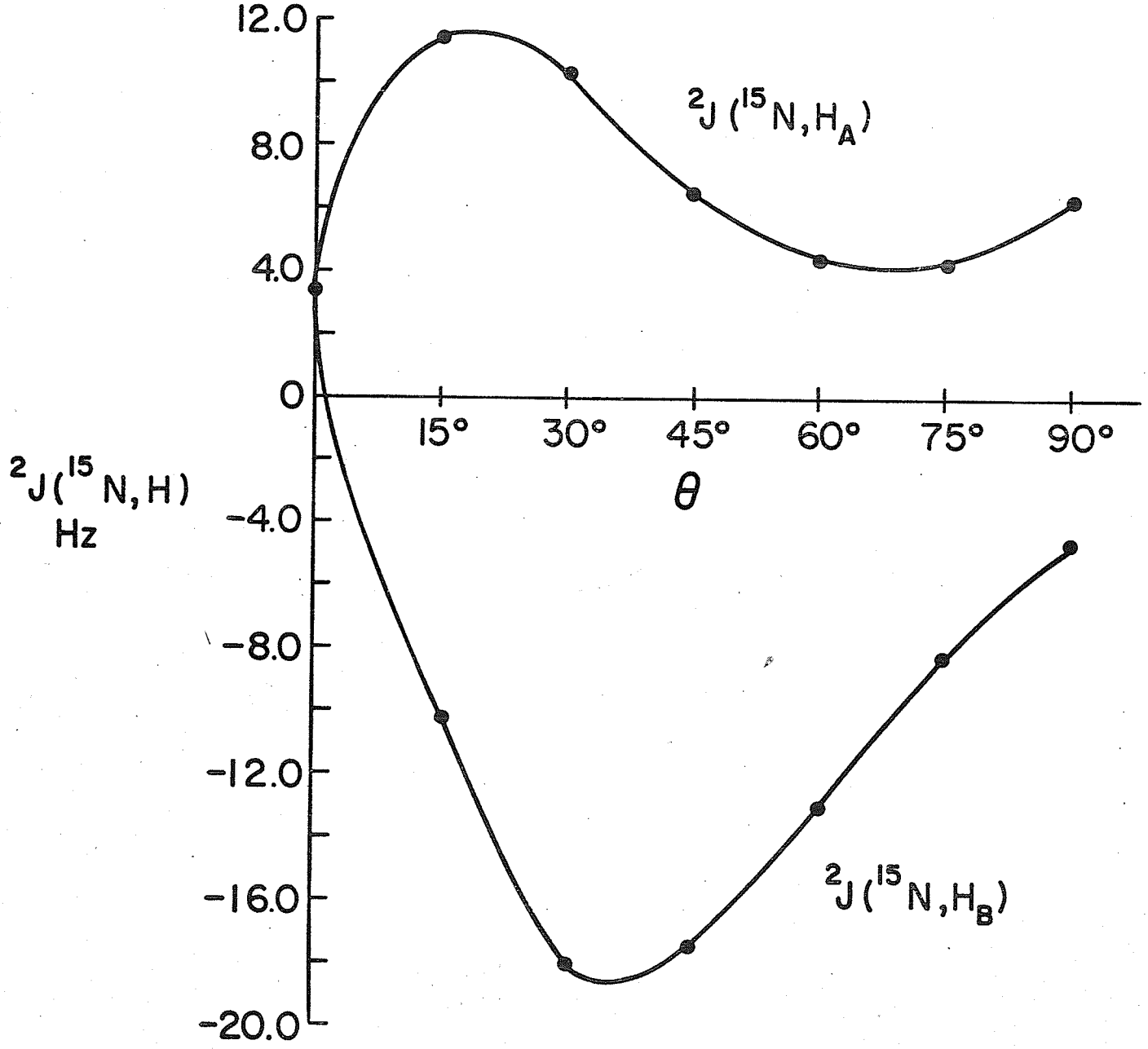

$^2J(^{15}N,H)$ increases for both the syn and anti isomers. Notice that the change in $^2J(^{15}N,H)$ is opposite to the trend observed and calculated in the 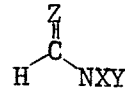 fragment.

iv) Aziridine

In Figure 12 the calculated values of $^2J(^{15}N,H)$ in aziridine (6) are plotted as a function of the angle θ between the bisector of the CNC angle and the N-H bond. INDO finds a minimum energy when $\theta \simeq 68^\circ$, and

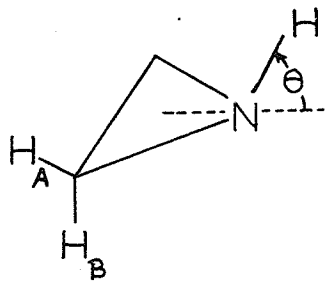

6

then $^2J(^{15}N,H_A) = -0.62$ Hz and $^2J(^{15}N,H_B) = -9.14$ Hz. The barrier to pyramidal inversion is calculated as 24.5 kcal/mol, somewhat larger than the values of 16-19 kcal/mol observed for aziridine derivatives (44).

For oxaziridine (see compounds 19 and 20 in Table 9) $^2J(^{15}N,H)$ was also calculated as a function of θ. Its angular dependence was very similar to that obtained for aziridine although $^2J(^{15}N,H)$ in oxaziridine was more positive than in aziridine. When $\theta \simeq 64^\circ$, $^2J(^{15}N,H_A) = 0.95$ Hz and $^2J(^{15}N,H_B) = -5.78$ Hz, in excellent agreement with the measurements of Becker (30, 31) on some substituted oxaziridines. INDO calculates the barrier to pyramidal inversion to be approximately 10 kcal/mol larger than the 32 kcal/mol (44, 45) observed for oxaziridine derivatives.

Figure 12. A plot of the calculated $^{2}J(^{15}N,H)$ in aziridine versus the angle θ between the N-H bond and the extension of the bisector of the CNC angle.

AZIRIDINE

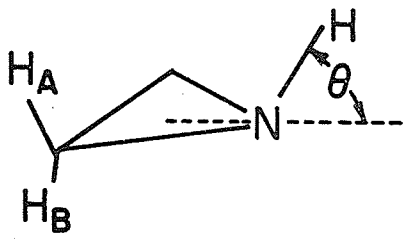
H
H_A
θ
N
H_B

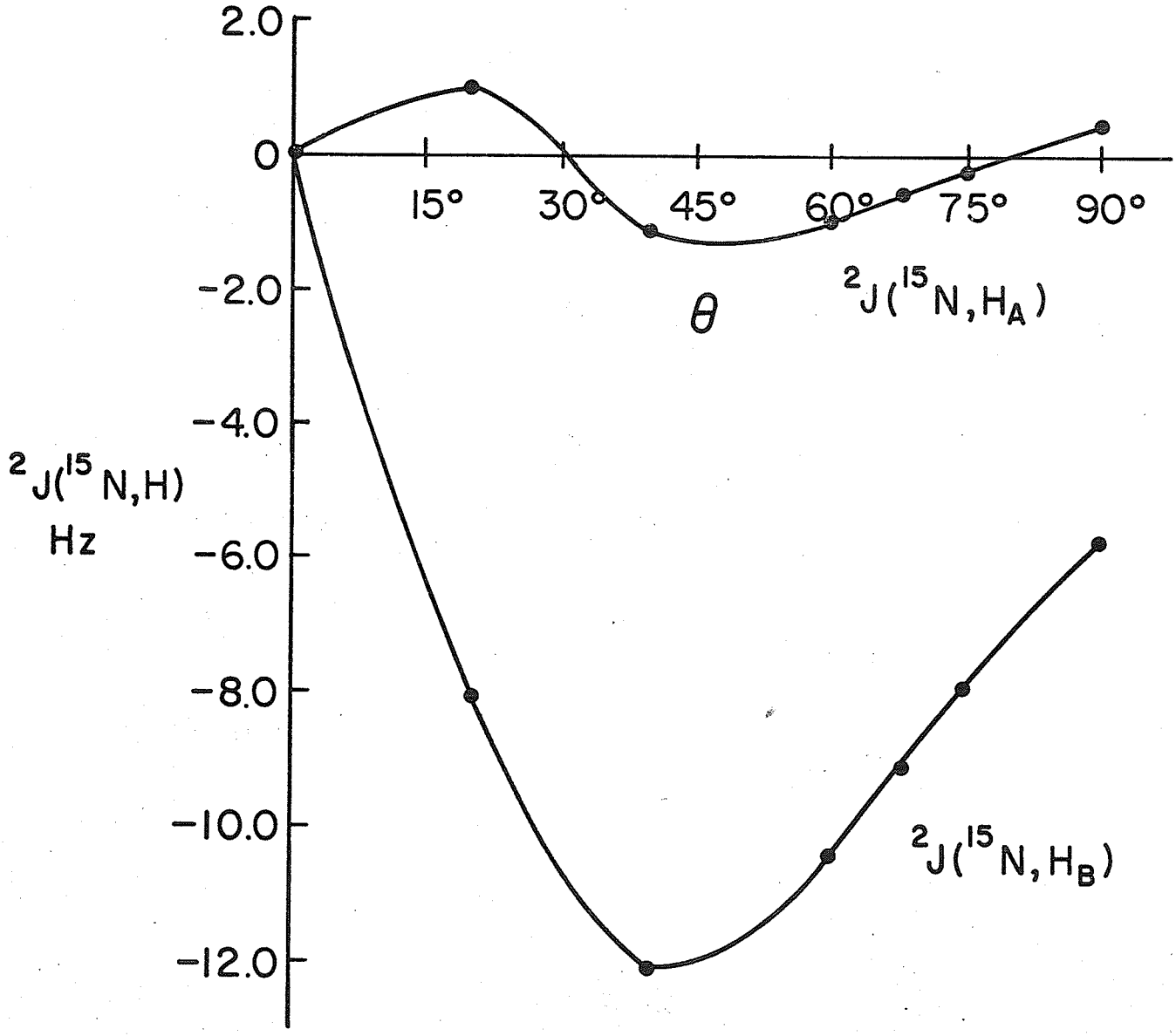
2.0
0
-2.0
-4.0
-6.0
-8.0
-10.0
-12.0
15°
30°
45°
60°
75°
90°
θ
$^2J(^{15}N,H)$
Hz
$^2J(^{15}N,H_A)$
$^2J(^{15}N,H_B)$

From Figures 11 and 12 the very similar calculated angular dependence of $^{2}J(^{15}N,H)$ in methylenimine and aziridine is apparent. In methylenimine and aziridine the hybridization of the nitrogen atom changes with variations in θ. This is not so for methylamine and methylisocyanate in which the hybridization of the nitrogen atom remains essentially unchanged for all values of θ. Because of this difference one does not expect the same angular dependence of $^{2}J(^{15}N,H)$ in methylamine and methylisocyanate as in methylenimine and aziridine.

In summary, the overall agreement between observed and calculated $^{2}J(^{15}N,H)$ values in Table 9 is good. Many experimental trends are reproduced by the calculations. For all compounds (with the exception of vinylamine) nitrogen protonation increases $^{2}J(^{15}N,H)$ in agreement with the experiment. The calculated substituent effects on $^{2}J(^{15}N,H)$ in the $H-\overset{Z}{\underset{\|}{C}}-NXY$ fragment also agree with experiment. The calculated angular dependence of $^{2}J(^{15}N,H)$ in the methylamine and methylisocyanate seems reasonable in view of the values observed in aziridine and oxaziridine derivatives.

2. The Influence of the Phosphorus Lone-Pair on $^{2}J(^{31}P,H)$

The effect of the phosphorus lone-pair on two-bond $^{31}P,H$ coupling constants in tervalent phosphorus compounds has been investigated (46-48). For a series of cyclic phosphines, Albrand et al. (46, 47) plotted the observed $^{2}J(^{31}P,H)$ against the dihedral angle involving the phosphorus lone-pair and the PCH fragment. These data are replotted in Figure 13 along with a plot of $^{2}J(^{15}N,H)$ as

Figure 13. A plot of the observed $^{2}J(^{31}P,H)$ in some tervalent phosphorus compounds (46, 47a) and of the calculated $-^{2}J(^{15}N,H)$ in methylamine versus the dihedral angle defined by the lone-pair X-C-H fragment. See section 2 of the text.

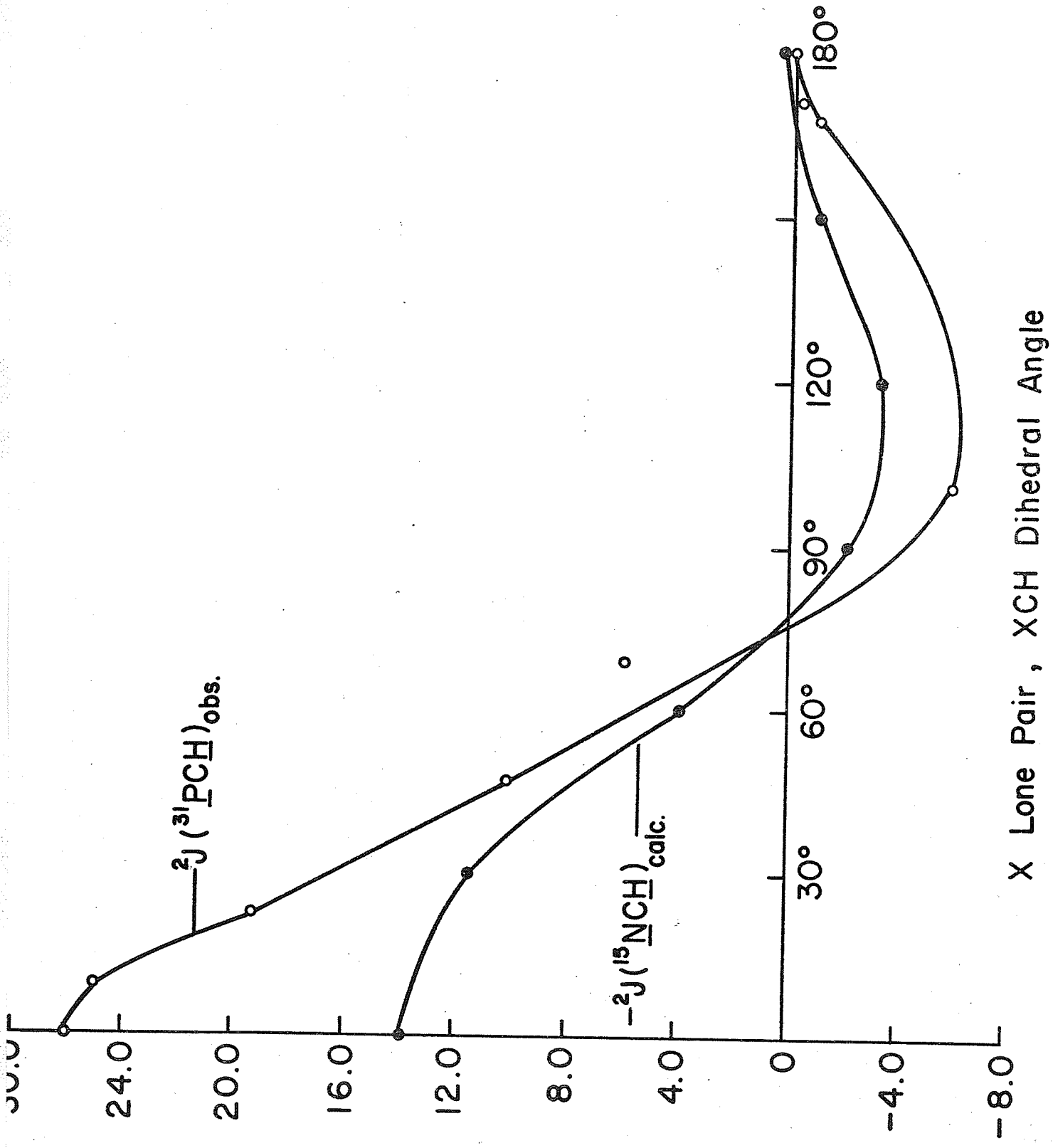
$^2J(^{31}PCH)_{obs.}$
$-^2J(^{15}NCH)_{calc.}$
$^2J(XCH)$ Hz
24.0
20.0
16.0
12.0
8.0
4.0
0
-4.0
-8.0
30°
60°
90°
120°
180°
X Lone Pair, XCH Dihedral Angle

calculated[5] for methylamine in Figure 9. The similar shape of these two curves suggests a similar mechanism by which spin information is transferred between the nuclei.

3. The Influence of the Nitrogen Lone-Pair on $^2J(H,H)$ in an Adjacent Methylene Group

The effect of lone-pairs on geminal proton-proton coupling constants has been calculated for several conformations of methylamine, two of which are shown in 7 and 8. $^2J(H_A,H_B)$ is plotted as a function of θ in Figure 14. According to an earlier MO theory (38) back-donation from the lone-pair into antisymmetrical CH_2 orbitals leads to an increase in $^2J(H,H)$: the present calculations indicate maximum donation for $\theta=30^\circ$ (7) and minimum donation for $\theta=120^\circ$ and $\theta=300^\circ$ (8).

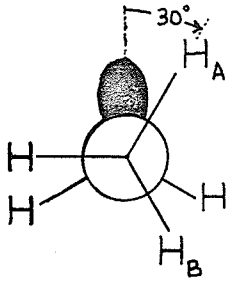

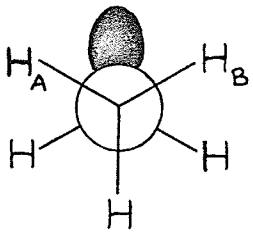

$\theta=30^\circ$, $^2J(H_A,H_B)=-0.85$ Hz

7

$\theta=300^\circ$, $^2J(H_A,H_B)=-4.79$ Hz

8

In Table 13 the calculated angular dependence of $^2J(H,H)$ is compared with the experimental values for a series of compounds with bridge-head nitrogen atoms (49, 50). The calculated values of $^2J(H,H)$ are obviously too large (2), although the relative values are in fair agreement with experiment. Chivers and Crabb (49) predict $^2J(H,H)$ as most positive when $\theta=0^\circ$ but INDO calculates $^2J(H,H)_{\theta=30^\circ} > {}^2J(H,H)_{\theta=0^\circ}$.

[5] In comparing the angular dependence of $^2J(^{15}N,H)$ and $^2J(^{31}P,H)$ it is convenient to multiply either parameter by -1 because the magnetogyric ratios of ^{15}N and ^{31}P have opposite sign.

Figure 14. A plot of the calculated $^{2}J(HCH)$ in methylamine versus the lone-pair N-C-H dihedral angle.

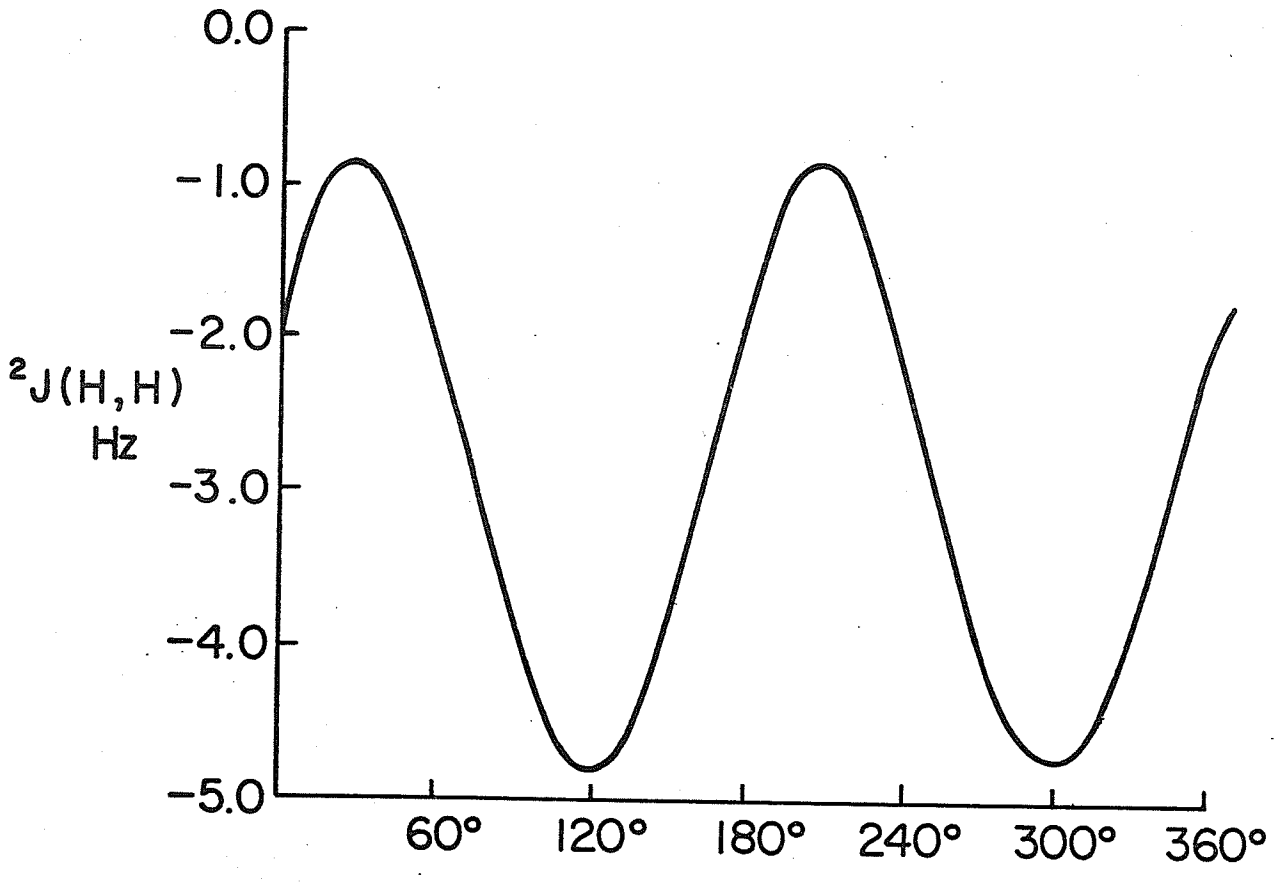

Nitrogen Lone Pair NCH Dihedral Angle

TABLE 13

Calculated and observed (49) influence of nitrogen lone-pair orientation on $^2J(HCH)$ values in an adjacent methylene group

θ	^2J obs.	Δ^* obs.	^2J calc.	Δ^* calc.
30°	-8.5	4.9	-0.85	4.0
60°	-11.0	2.5	-1.92	2.9
300°	-13.6	0.0	-4.79	0.0

* $\Delta \equiv J_\theta - J_{300°}$

To show that the observed variations in $^2J(H\underline{C}H)$ are due to lone-pair effects, $^2J(H\underline{N}H)$ was calculated for the staggered conformation, $^2J(HNH) = -6.57$ Hz, and for the eclipsed conformation, $^2J(HNH) = -7.10$ Hz. The difference was only 0.53 Hz.

4. Three-Bond Nitrogen-Proton Coupling Constants, $^3J(N,H)$

In Table 14 the calculated $^3J(^{15}N,H)$ are presented for 15 compounds with rigid geometries. The paucity of experimental data makes a critical evaluation of the calculated $^3J(^{15}N,H)$ values difficult. However, several experimental trends appear to be reproduced by the calculations. On protonation of the nitrogen atom, $^3J(^{15}N,H)$ is predicted to decrease, (see compounds 1 and 2, 3 and 4, 7 and 8, and 11 and 12) in line with an experimental rule (33): on quaternization of the nitrogen atom, $^3J(^{15}N,H)$ decreases. In vinyl isocyanide $^3J(^{15}N,H_{trans})$ is calculated as approximately twice $^3J(^{15}N,H_{cis})$, in good agreement

TABLE 14

Calculated and observed three-bond $^{15}N,H$ coupling constants*

Compound		$^3J(^{15}N,H)$ calc.	$^3J(^{15}N,H)$ obs.
1.	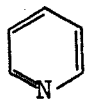	-0.59	-1.53
2.	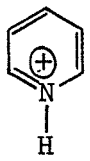	-7.51	-3.98
3.	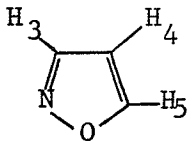	H_4 -0.74 H_5 2.14	— —
4.	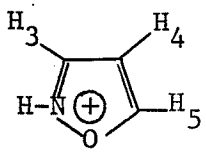	H_4 -5.45 H_5 -17.27	— —
5.	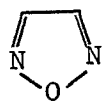	-3.19	—
6.	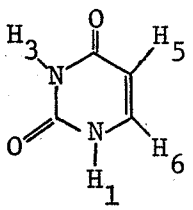	N_1H_3 -7.30 N_1H_5 -8.10 N_3H_1 -7.01 N_3H_5 -7.73	— — — —

Compound		$^3J(^{15}N,H)$ calc.	$^3J(^{15}N,H)$ obs.
7.	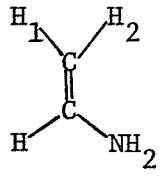	H_1 -11.17	—
		H_2 -4.56	—
8.	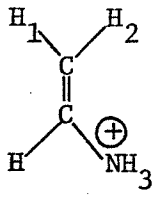	H_1 -13.56	—
		H_2 -6.76	—
9.	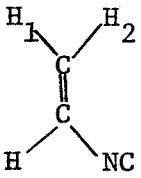	H_1 -11.96	-8.68
		H_2 -5.19	-4.26
10.	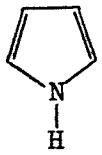	-10.93	-5.40
11.	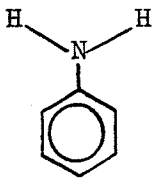	-2.52	-1.94
12.	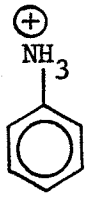	-5.00	—
13.	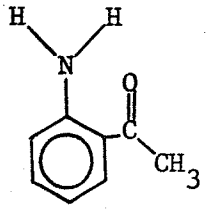	-3.90	-2.46

Compound	$^3J(^{15}N,H)$ calc.	$^3J(^{15}N,H)$ obs.
14. 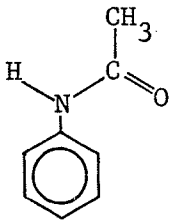	-3.86	-1.85
15. 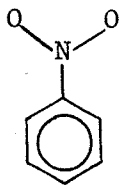	-3.75	2.5[+]

* References to the geometries and observed coupling constants for the first ten molecules are given in Table 9. The geometries used, and the experimental values observed for compounds 11, 13, and 14 are given in Part II. For the anilinium ion, standard geometries (8, 37) were used to calculate the atomic coordinates of the atoms in the benzene ring fragment. The C-N and N-H bond lengths were taken as 1.431 and 1.03 Å respectively (5). All CNH and HNH angles were taken as 109.47°.

+ This is the experimental value of $^3J(^{15}N,H)$ in α-nitronapthalene. See Y. Kawazoe, M. Araki, S. Sawaki, and M. Ohnishi. Chem. Pharm. Bull. (Tokyo) 18, 381 (1970).

with experiment. For aniline, 2-aminoacetophenone, acetanilide, and nitrobenzene, the calculated $^3J(^{15}N,H)$ values range from -2.52 to -3.90 Hz. If $^3J(^{15}N,H)$ in nitrobenzene is negative the observed $^3J(^{15}N,H)$ values fall between -1.85 and -2.5 Hz, in fair agreement with the calculated values. With the exception of $^3J(^{15}N,H_5)$ in isoxazole, all $^3J(^{15}N,H)$ coupling constants are correctly calculated as negative.

TABLE 15

Effect of substituent electronegativity on $^3J(^{15}N,H)$ and $^3J(H,H)$*

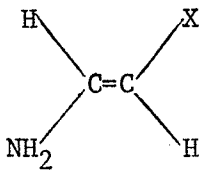

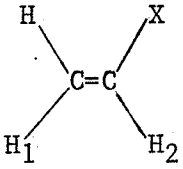

X	$^3J(^{15}N,H_{cis})$ calc.	$^3J(H_1,H_2)$ calc.	$^3J(H_1,H_2)$ obs.
Li	-13.04	23.03	19.3
H	-6.76	9.31	11.5
F	-1.99	4.74	4.65

* Standard geometries (8, 37) were used for all calculations. The C-Li bond length was taken as 2.1 Å. Computed and observed values of $^3J(H_1,H_2)$ are cited from reference (3).

In Table 15 the $^3J(^{15}N,H)$ values calculated for three vinylamines are compared with $^3J(H,H)$ calculated in three ethylene derivatives (3). As the electronegativity of X increases, $^3J(^{15}N,H)$ increases while $^3J(H,H)$ decreases. Thus for the vinyl fragment the reduced

coupling constants, $^{3}K(N,H)_{cis}$ and $^{3}K(H,H)_{cis}$, show similar substituent effects.

To anticipate future experiments, the angular dependence of $^{3}J(^{15}N,H)$ was evaluated for ethylamine, protonated ethylamine, ethylisocyanide, cis- and trans-acetaldoxime, and protonated cis- and trans-acetaldoxime. Since the experimental plots (52) present $^{3}J(^{14}N,H)$ versus the NCCH dihedral angle, the same convention will be followed here. This facilitates a comparison between $^{3}J(^{14}N,H)$ and the analogous couplings $^{3}J(H,H)$, $^{3}J(F,H)$, and $^{3}J(P,H)$, all these nuclei having positive gyromagnetic ratios.

a) The Angular Dependence of $^{3}J(^{14}N,H)$ in the $^{N}\!\!\diagdown C-C\!\!\diagup^{H}$ fragment

i) Ethylamine

In Figure 15 the NCCH dihedral angle θ, in ethylamine is plotted against calculated $^{14}N,H$ coupling constants. Two conformations of the amino group are considered; in the E conformation (9) the N-H bonds and the C-H bonds of the adjacent methylene group are eclipsed, while in the S conformation (10) they are staggered.[6] Note that in the E conformation

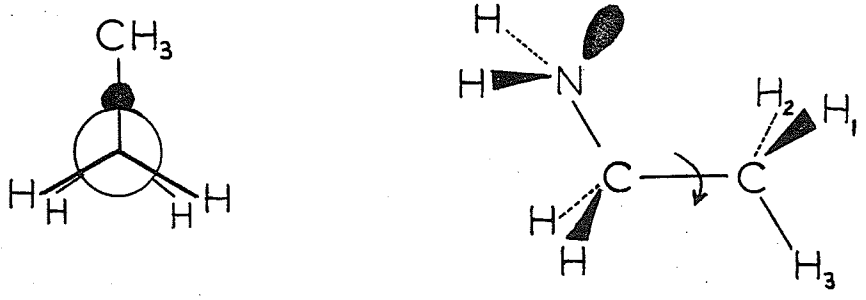

E conformation

$\theta = 180^{\circ}$ (H_3), 60° (H_1 and H_2)

9

[6] In this discussion, E and S denote eclipsed and staggered conformations respectively.

Figure 15. A plot of the calculated $^{3}J(^{14}N,H)$ versus the NCCH dihedral angle for the E and S conformations of ethylamine. The E and S conformations are depicted in 9 and 10 of the text.

ETHYLAMINE

$CH_3\ CH_2NH_2$

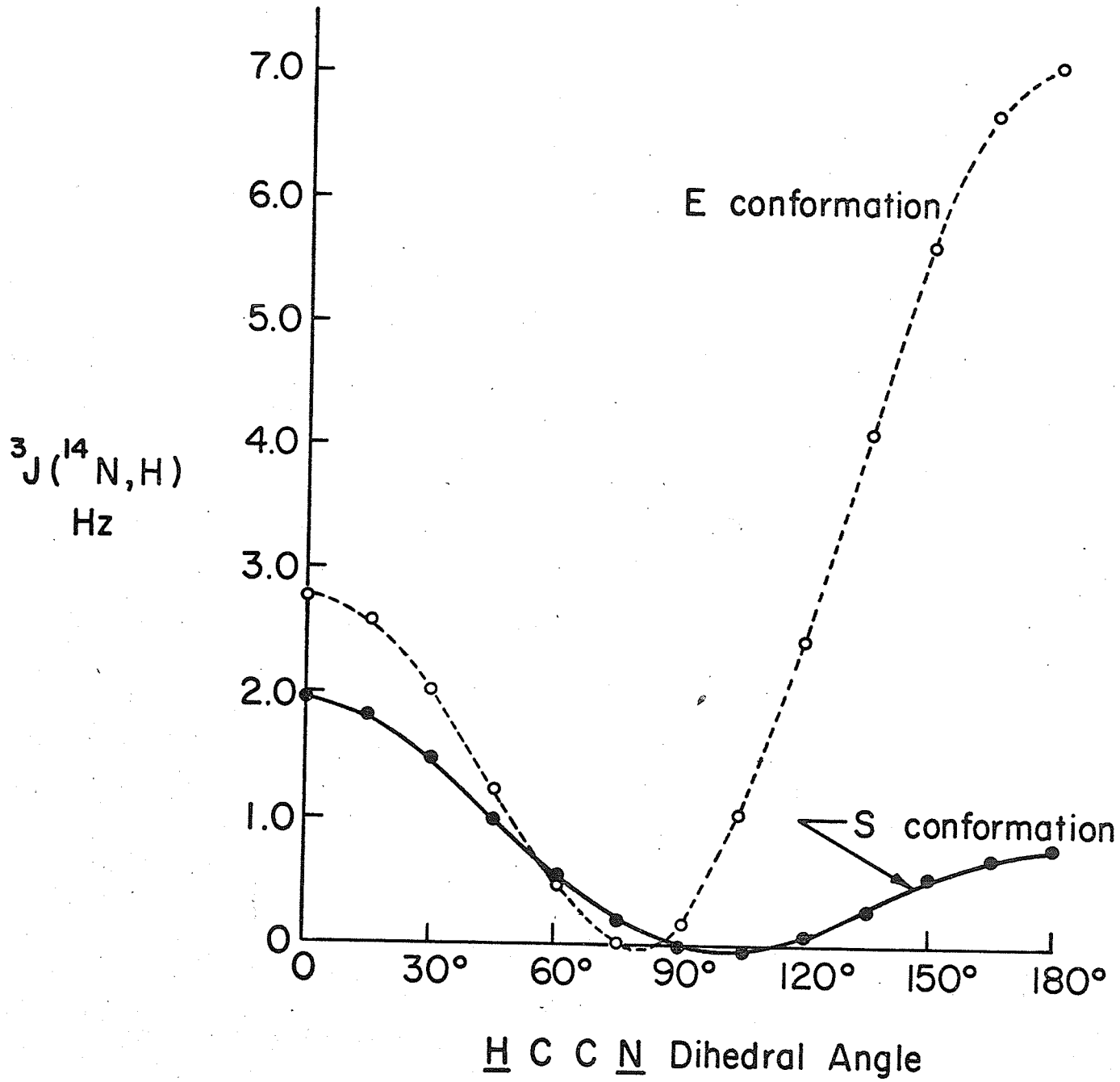

the nitrogen lone-pair lies cis to the methyl group while in the S conformation it lies trans to the methyl group. The E conformation is

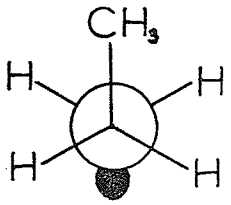

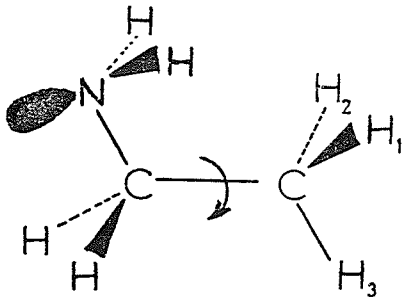

S conformation

$\theta = 180^{\circ}$ (H_3), 60° (H_1 and H_2)

10

calculated to be more stable than the S conformation for all angles θ.

From Figure 15 it is apparent that $^{3}J(^{14}N,H)$ is dependent both on the orientation of the nitrogen lone-pair and on the NCCH dihedral angle. Both the E and S conformations of ethylamine are most stable when the C-H bonds of the methyl and methylene groups are staggered, i.e., for $\theta = 60^{\circ}$ (H_1 and H_2) and 180° (H_3). Then $^{3}J(^{14}N,H)_{ave}$ is 2.65 Hz for the E conformation, and is 0.61 Hz for S. In rigid compounds a similar dependence of $^{3}J(N,H)$ on lone-pair orientation is observed (53-56). For example, in N,N-dimethylnitrosamine (11), $^{3}J(^{15}N,H) = \pm 2.2$ Hz when the methyl group lies cis to the lone-pair while $^{3}J(^{15}N,H) = \pm 0.8$ Hz when the methyl group lies trans to the lone-pair (53).

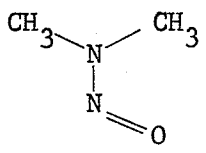

11

The coordinates of the amino group nuclei were calculated assuming equal C-N and N-H bond lengths in ethylamine and methylamine (reference 7 in Table 9). In addition, the following bond angles were assumed: angle HNC = 109.47° and dihedral angles HNCC = 120° (E conformation) and ±60° (S conformation). The atomic coordinates of the ethyl group were taken from the literature (57).

$^3J(^{31}P,H)$ in aminophosphines depends on the orientation of the phosphorus lone-pair (58-60). Below -120 °C the p.m.r. spectrum of methylaminobis (trifluoromethyl) phosphine, $CH_3NH{\cdot}P(CF_3)_2$, indicates the presence of two rotational isomers (12a) and (12b). The most

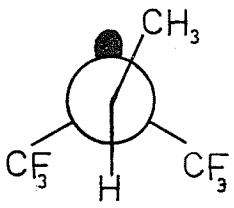

12a

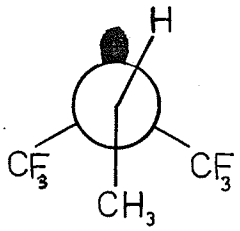

12b

abundant isomer is assigned to 12a where $^3J(^{31}P,H)$ = 13.9 Hz while in 12b, $^3J(^{31}P,H) \simeq 4$ Hz (58). In phosphines and in nitrogen compounds containing a lone-pair, $^3J(^{31}P,H)$ and $^3J(^{14}N,H)$ apparently display a similar dependence on the orientation of the lone-pair.

ii) Protonated Ethylamine

In Figure 16, $^{3}J(^{14}N,H)$ in protonated ethylamine is plotted against the dihedral angle in the fragment $^{\oplus}NCCH$. Both the E (13) and S (14) conformations of the amino group are considered. The atomic

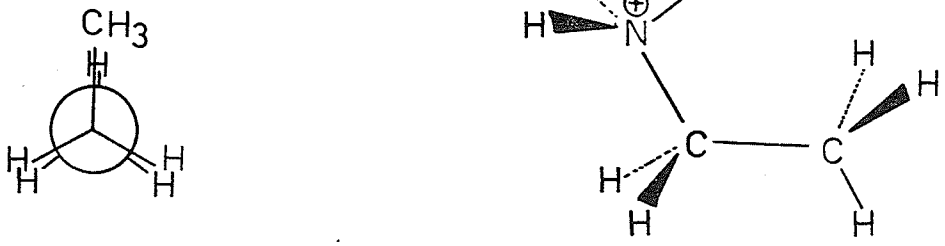

13

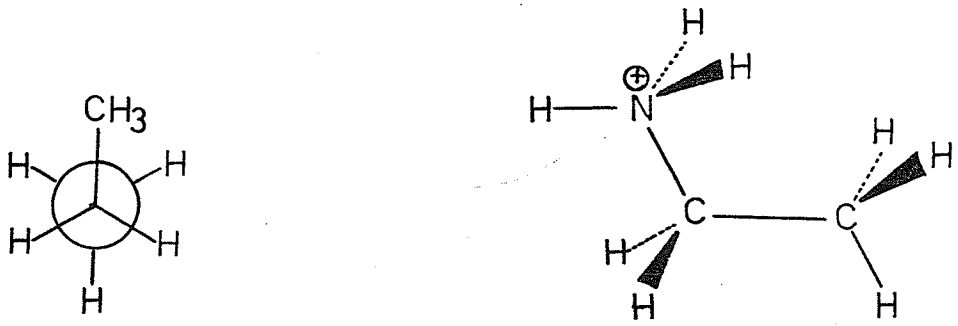

14

Figure 16. A plot of the calculated $^{3}J(^{14}N,H)$ versus the dihedral angle of the NCCH fragment in the E and S conformations of protonated ethylamine.

PROTONATED ETHYLAMINE

$CH_3 CH_2 \overset{\oplus}{N}H_3$

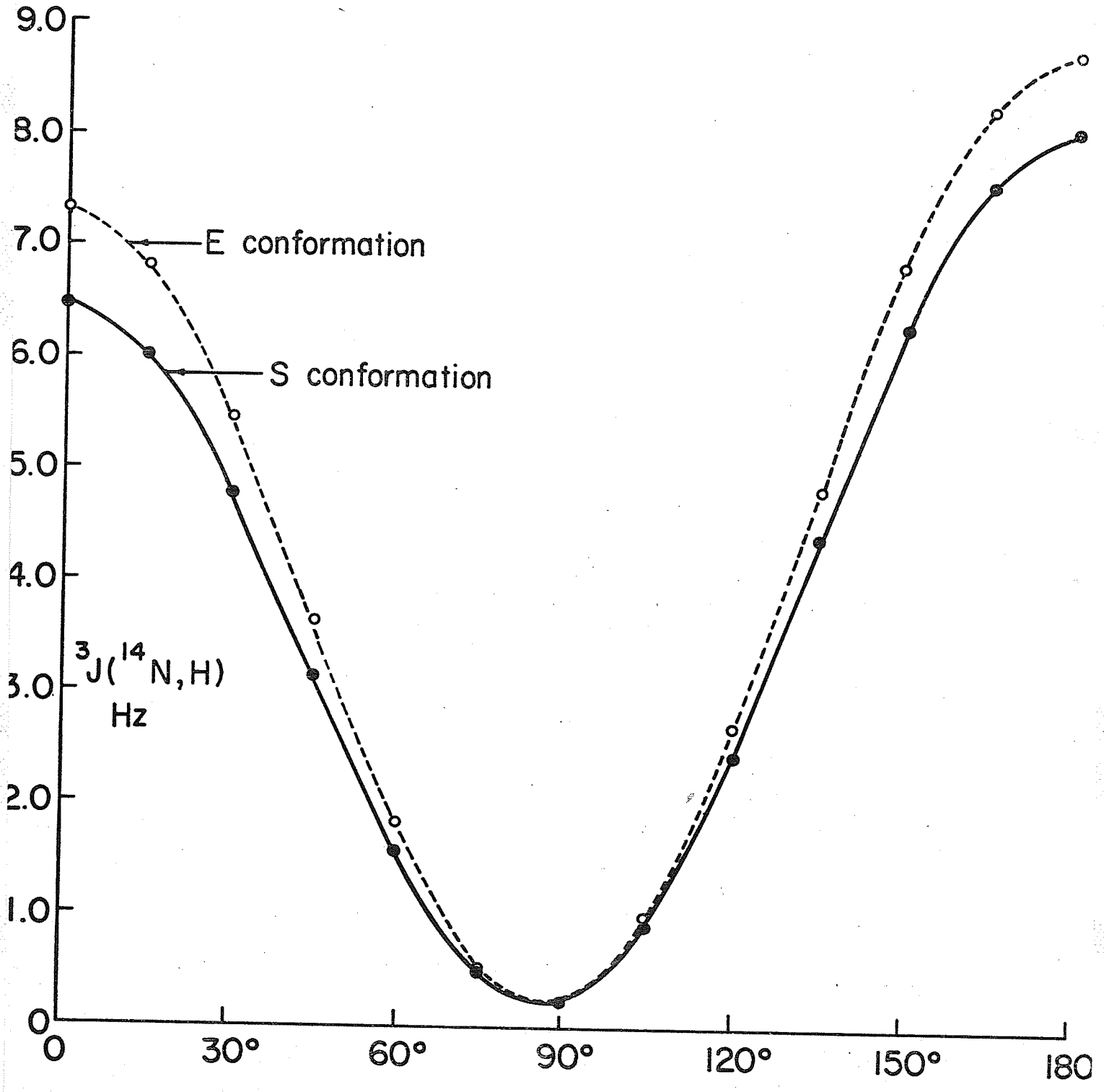

coordinates for protonated ethylamine were essentially the same as those used for the unprotonated species. All H-N-X angles were taken as 109.47° and the N-H bond length was assumed to be 1.03 Å. For every angle θ the S conformation (14) was more stable than the E conformation (13).

The curves of $^{3}J(^{+}NCCH)$ versus θ in Figure 16 are very similar, in contrast to those of the unprotonated molecules (Figure 15). Note the increase in $^{3}J(^{14}N,H)$ over its values in the unprotonated species.

iii) Ethylisocyanide

In Figure 17 the curve depicting the calculated angular dependence of $^{3}J(^{14}N,H)$ closely resembles the rough experimental curves assembled by Bothner-By and Cox (52). INDO finds 2.345 kcal/mol as the barrier to rotation about C-C bond. Therefore it is best to use the calculated average $^{14}N,H$ couplings in the staggered conformation. One has $^{3}J(^{14}N,H)_{ave}$ = 2.81 Hz and $^{2}J(^{14}N,H)_{ave}$ = -2.78 Hz. Maher (25) and MacFarlane (24) observe $^{3}J(^{14}N,H)$ = 2.5 Hz and $^{2}J(^{14}N,H)$ = -2.0 Hz.

The bond lengths and angles in the C-N≡C and the ethyl fragments were taken as those in methylisocyanide and ethane, respectively (reference i and h in Table 9).

b) The Angular Dependence of $^{3}J(^{14}N,H)$ in the $^{N}\!\!\diagdown\!\!=C-C\!\!\diagup^{H}$ Fragment

i) Cis-Acetaldoxime and Protonated Cis-Acetaldoxime

In Figure 18 the calculated $^{3}J(^{14}N,H)$ in 15 and 16 is plotted versus the N=C-C-H dihedral angle. The maximum occurs at an angle of 90° indicating the importance of the π orbitals of the C=N bond in the transmission of the spin information.

The structure used to calculate the atomic coordinates in 15 was that of Rogowski and Schwendeman (61). With the exception of the

Figure 17. A plot of the calculated $^{3}J(^{14}N,H)$ versus the NCCH dihedral angle in ethylisocyanide.

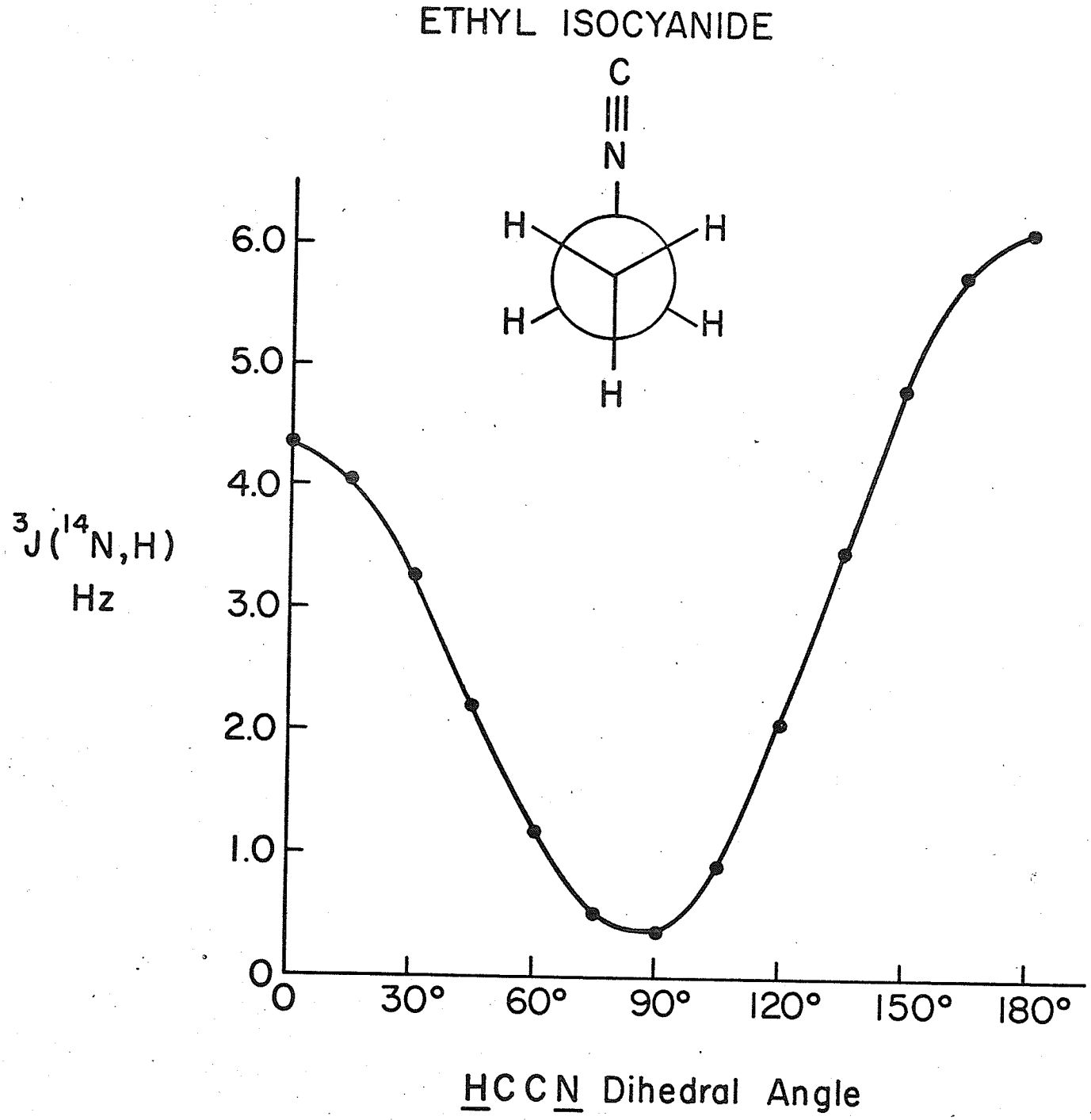
ETHYL ISOCYANIDE
C
N
H
H
H
H
H
6.0
5.0
4.0
3.0
2.0
1.0
0
$^3J(^{14}N,H)$
Hz
0
30°
60°
90°
120°
150°
180°
HCCN Dihedral Angle

Figure 18. A plot of the calculated $^{3}J(^{14}N,H)$ versus the NCCH dihedral angle in cis-acetaldoxime and in protonated cis-acetaldoxime.

CIS - ACETALDOXIME

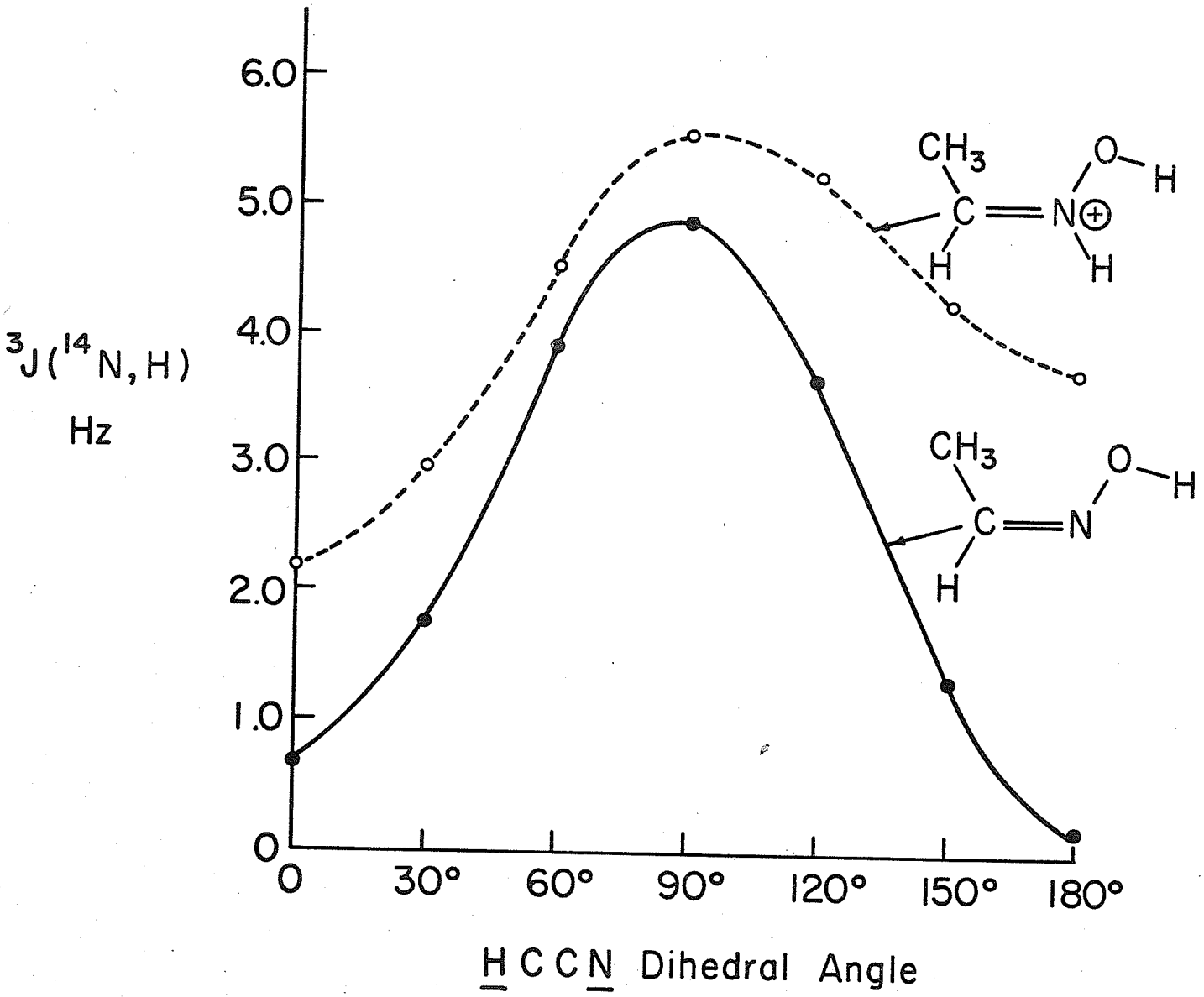

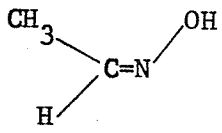

15

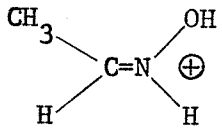

16

methyl group, the protonated species was assumed planar, with all bond angles and bond lengths the same as those used for the unprotonated species; the N-H bond length was taken as 1.03 Å and the CNH angle as 120°. INDO calculates the barrier to rotation of the methyl group to be 208 cal/mol while the observed barrier is 373 cal/mol (61). The barrier in the protonated species is calculated to be slightly larger, 363 cal/mol.

Averaging over all angles yields $^{3}J(^{14}N,H)$ as 2.65 Hz and 4.22 Hz, respectively, for cis-acetaldoxime and protonated cis-acetaldoxime.

ii) Trans-Acetaldoxime and Protonated Trans-Acetaldoxime

In Figure 19 the H-C-C=N dihedral angle in 17 and 18 is plotted against the calculated $^{3}J(^{14}N,H)$.

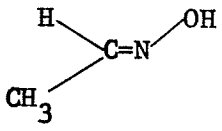

17

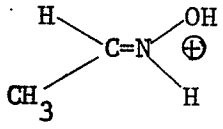

18

The structural parameters for trans-acetaldoxime were obtained from Rogowski and Schwendeman (61). Except for the additional proton, the protonated species was assumed to have the same structure as the unprotonated species: the N-H bond length was taken as 1.03 Å, the CNH bond angle as 120° and the CCNO dihedral angle as 180°.

Figure 19. A plot of the calculated $^{3}J(^{14}N,H)$ versus the NCCH dihedral angle in trans-acetaldoxime and in protonated trans-acetaldoxime.

TRANS - ACETALDOXIME

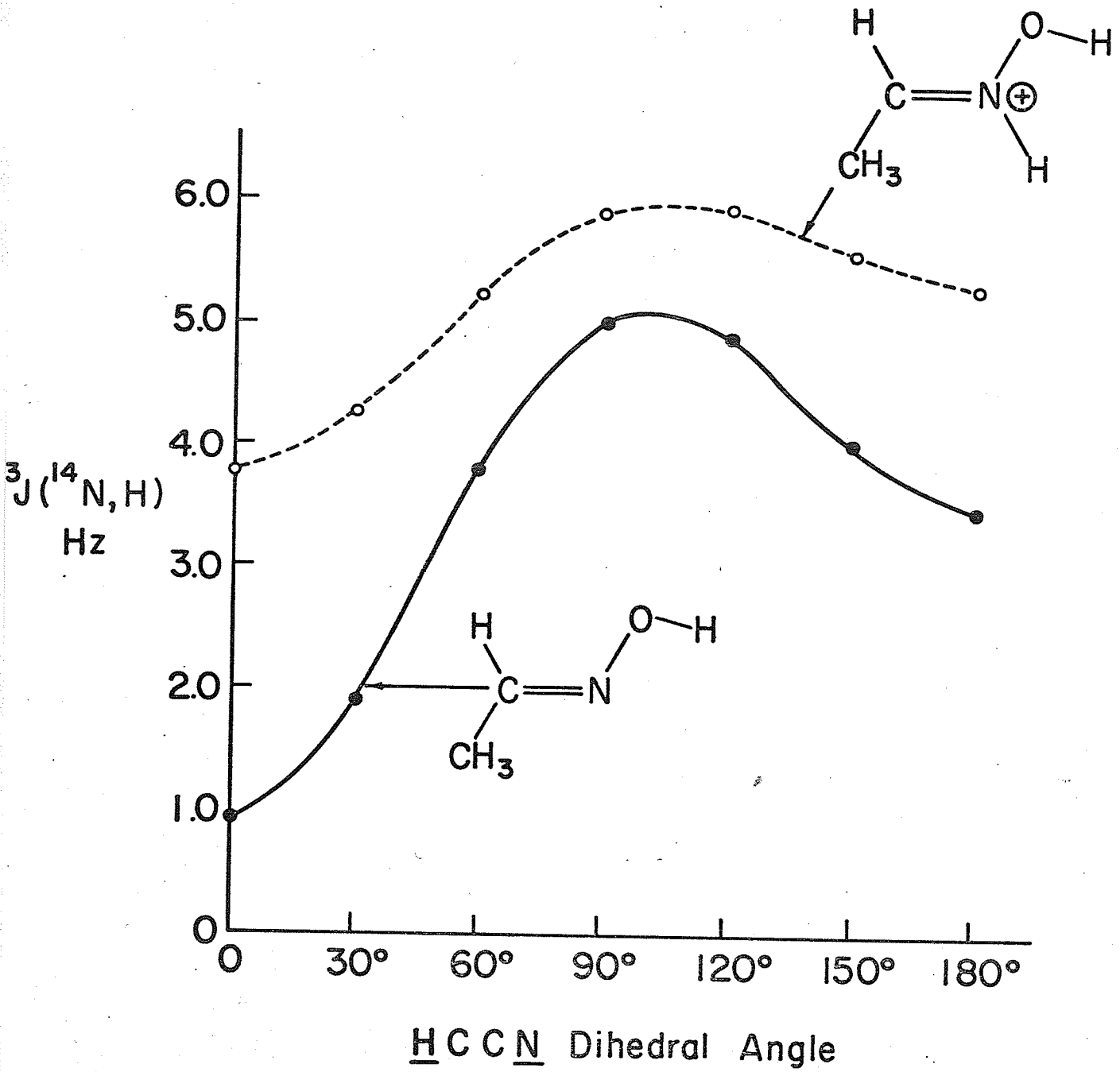

INDO finds the barrier to rotation of the methyl group to be 1080 cal/mol while the experimental barrier is 1835 cal/mol (61). The barrier in the protonated species was calculated as 1185 cal/mol. Since the observed barrier is greater than 3kT one can compare the calculated and observed coupling constants by considering only the most stable conformation. The average values of $^{3}J(^{14}N,H)$ for the most stable conformations are 3.57 Hz and 5.25 Hz for trans-acetaldoxime and protonated trans-acetaldoxime, respectively.

Notice that in the trans isomer (17) the nitrogen lone-pair is cis to the methyl group and $^{3}J(^{14}N,H)$ is calculated to be larger than in the case where the methyl group is trans (15) to the lone-pair. This is in good agreement with experiment. For the oxime (19) $^{3}J(^{14}N,CH_3(A))$ is 1.57 Hz and $^{3}J(^{14}N,CH_3(B))$ is 2.86 Hz (33). When 19 is studied in trifluoroacetic acid, each of the $^{14}N,H$ coupling constants becomes larger:

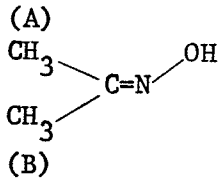

19

$^{3}J(^{14}N,CH_3(A))$ is 2.36 Hz and $^{3}J(^{14}N,CH_3(B))$ is 3.27 Hz (33). Although all the calculated coupling constants are a little too large, their relative values agree with experiment.

In summary, SCF calculations at the INDO level predict a dihedral angle dependence of $^{3}J(^{14}N,H)$ in the N-C-C-H fragment similar to that observed for $^{3}J(H,H)$ (1,3,5), for $^{3}J(^{19}F,H)$ (62, 63) and for $^{3}J(^{31}P,H)$ (52, 64) in the saturated X-C-C-H fragments. The angular dependence of $^{3}J(^{14}N,H)$ in the N=C-C-H fragment is computed as different from that in the saturated fragment.

5. The Effect of Protonation on J(N,H) in Pyridine, Aniline, Ammonia, and Methylamine

In Tables 16 and 17 the calculated and observed $^{15}N,H$ couplings are given for pyridine and the pyridinium ion, and for aniline and the anilinium ion. In Table 18, $^{1}J(^{15}N,H)$ is presented for ammonia, the ammonium ion, methylamine, and protonated methylamine.

INDO predicts a decrease in $^{1}J(^{15}N,H)$ on protonation, in agreement with experiment for ammonia and methylamine but not for aniline, where uncertainty about the geometry of the amino group may be the cause of the disagreement. Thus, a planar amino group entails a calculated $^{1}J(^{15}N,H)$ of -92.5 Hz (50).

TABLE 16

Calculated and observed $^{15}N,H$ coupling constants for pyridine and the pyridinium ion *

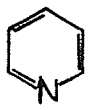

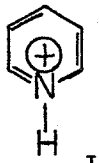

	$J_{calc.}$	$J_{obs.}$ (34)	$J_{calc.}$	$J_{obs.}$ (34)
$^{2}J(^{15}N,H)$	-16.98	-10.76	0.47	-3.01
$^{3}J(^{15}N,H)$	-0.59	-1.53	-7.51	-3.98
$^{4}J(^{15}N,H)$	0.54	0.21	1.73	±0.69

* The geometries used for these calculations are given in Table 9.

TABLE 17

Calculated and observed $^{15}N,H$ coupling constants for aniline and the anilinium ion *

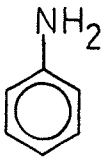

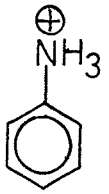

	$J_{calc.}$	$J_{obs.}$ (see Part II)	$J_{calc.}$	$J_{obs.}$ (65)
$^{1}J(^{15}N,H)$	-59.53	-78.875	-72.36	-76.0 ± 0.5
$^{3}J(^{15}N,H)$	-2.52	-1.935	-5.00	—
$^{4}J(^{15}N,H)$	-1.06	-0.476	-1.04	—
$^{5}J(^{15}N,H)$	+0.18	0.009	-1.34	—

* The geometries used for these calculations are given in Table 14.

TABLE 18

Calculated and observed $^{1}J^{15}N,H)$ in ammonia and methylamine *

Compound	$^{1}J(^{15}N,H)$ calc.	$^{1}J(^{15}N,H)$ obs.	Reference
NH_3	-42.64	-61.2	66
$\oplus NH_4$	-73.52	-73.2	29
CH_3NH_2	-34.78	-65.0	28
$CH_3\overset{\oplus}{N}H_3$	-75.38	-75.6	29

* Standard geometries (8, 37) were used to calculate the atomic coordinates of ammonia. The N-H bond length was taken as 1.03 Å for ammonia. The geometries used for methylamine and protonated methylamine are given in Table 9.

On protonation, the calculations predict an increase in $^{2}J(^{15}N,H)$ in pyridine, a decrease in $^{3}J(^{15}N,H)$ in aniline and pyridine, an increase in $^{4}J(^{15}N,H)$ in pyridine, and a decrease in $^{5}J(^{15}N,H)$ in aniline. Such an alternating effect due to protonation has been observed by Crépaux, Lehn and Dean (33).

CONCLUSIONS

A comparison of theoretical with the available experimental two-bond and three-bond nitrogen-proton spin-spin coupling constants encourages their combined use in conformational and structural work.[7]

---

[7] After completion of this work, a paper (69) appeared giving the results of CNDO/2 and INDO calculations on N,H; C,H; and H,H coupling constants in several of the molecules discussed above. There are some large discrepancies in the two sets of N,H couplings. The calculations presented in this thesis are in exact agreement with previous data for $^{1}J(^{14}N,H)$ in ammonia (7, 8), $^{1}J(^{15}N,^{13}C)$ in methyl cyanide (70) and $^{1}J(^{13}C,N)$ in methylenimine (71).

REFERENCES FOR PART III

1. (a) A.A. Bothner-By. Advan. Magn. Resonance, 1, 195 (1965).
   (b) T. Yonezawa, I. Moroshima, K. Fukuta, and Y. Ohmori. J. Mol. Spectrosc. 31, 341 (1969).
2. G.E. Maciel, J.W. McIver, Jr., N.S. Ostlund, and J.A. Pople. J. Am. Chem. Soc. 92, 4151 (1970).
3. G.E. Maciel, J.W. McIver, Jr., N.S. Ostlund, and J.A. Pople. J. Am. Chem. Soc. 92, 4497 (1970).
4. G.E. Maciel, J.W. McIver, Jr., N.S. Ostlund, and J.A. Pople. J. Am. Chem. Soc. 92, 4506 (1970).
5. L.M. Jackman and S. Sternhell. Applications of nuclear magnetic resonance spectroscopy in organic chemistry. Pergamon Press, Oxford, 1969.
6. J.A. Pople, J.W. McIver, Jr., and N.S. Ostlund. Chem. Phys. Letter, 1, 465 (1967).
7. J.A. Pople, J.W. McIver, Jr., and N.S. Ostlund. J. Chem. Phys. 49, 2960, 2965 (1968).
8. J.A. Pople and D.L. Beveridge. Approximate molecular orbital theory. McGraw-Hill Book Company, New York, N.Y., 1970.
9. J.A. Pople, D.L. Beveridge, and P.A. Dobosh. J. Chem. Phys. 47, 2026 (1967).
10. E.W. Randall and D.G. Gillies. In Progress in nuclear magnetic resonance spectroscopy. Edited by J.W. Emsley, J. Feeney, and L.H. Sutcliffe. Vol. 6, p. 119. Pergamon Press. Oxford, 1971.

11. R.L. Lichter. In Determination of organic structures by physical methods. Edited by F.C. Nachod and J.J. Zuckerman. Vol. 4, p. 195. Academic Press, New York, N.Y., 1971.

12. Program 135. Quantum chemistry program exchange. Indiana University, Bloominton, Indiana.

13. Program 141. Quantum chemistry program exchange. Indiana University, Bloomington, Indiana.

14. B. Sunners, L.H. Piette, and W.G. Schneider. Can. J. Chem. 38, 681 (1960).

15. A.J.R. Bourn and E.W. Randall. Mol. Phys. 8, 568 (1964).

16. R.J. Chuck, D.G. Gillies, and E.W. Randall. Mol. Phys. 16, 121 (1969).

17. M.T. Rogers and L.A. LaPlanche. J. Phys. Chem. 69, 3648 (1965).

18. A.K. Bose and I. Kugajevsky. Tetrahedron, 23, 1489 (1967).

19. M. Ohtsuru, K. Tori, J.M. Lehn, and R. Seher. J. Am. Chem. Soc. 91, 1187 (1969).

20. E. Rahkamaa. Mol. Phys. 19, 727 (1970).

21. B.W. Roberts, J.B. Lambert, and J.D. Roberts. J. Am. Chem. Soc. 87, 5439 (1965).

22. D.S. Matteson and R.A. Bailey. J. Am. Chem. Soc. 90, 3761 (1968).

23. A.J.R. Bourn and E.W. Randall. J. Mol. Spectrosc. 13, 29 (1964).

24. W. McFarlane. J. Chem. Soc. A, 1660 (1967).

25. J.P. Maher. J. Chem. Soc. A, 1855 (1966).

26. G. Binsch and J.D. Roberts. J. Phys. Chem. 72, 4310 (1968).

27. G.A. Olah and T.E. Kiovsky. J. Am. Chem. Soc. 90, 4666 (1968).

28. L. Paolillo and E.D. Becker. J. Mag. Res. 3, 200 (1970).

29. G. Binsch, J.B. Lambert, B.W. Roberts, and J.D. Roberts. J. Am. Chem. Soc. 86, 5564 (1964).

30. D.M. Jerina, D.R. Boyd, L. Paolillo, and E.D. Becker. Tetrahedron Letters. 18, 1483 (1970).

31. E.D. Becker. Private communication.

32. M. Ohtsuru and K. Tori. Tetrahedron Letters. 47, 4043 (1970).

33. D. Crépaux, J.M. Lehn, and R.R. Dean. Mol. Phys. 16, 225 (1969).

34. R.L. Lichter and J.D. Roberts. J. Am. Chem. Soc. 93, 5218 (1971).

35. J.P. Kintzinger and J.M. Lehn. Chem. Commun. 660 (1967).

36. E.D. Becker, R.B. Bradley, and T. Axenrod. J. Mag. Res. 4, 136 (1971).

37. J.A. Pople and M. Gordon. J. Am. Chem. Soc. 89, 4254 (1967).

38. J.A. Pople and A.A. Bothner-By. J. Chem. Phys. 42, 1339 (1965).

39. T. Nishikawa, T. Itoh, and K. Shimoda. J. Chem. Phys. 23, 1735 (1955).

40. F.B. Riddell and J.M. Lehn. J. Chem. Soc. B, 1224 (1968).

41. R.G. Lett and W.H. Flygare. J. Chem. Phys. 47, 473 (1967).

42. J.M. Lehn and B. Munsch. Theor. Chim. Acta, 12, 91 (1968).

43. J.M. Lehn, B. Munsch, and P. Millié. Theor. Chim. Acta, 16, 351 (1970).

44. J.M. Lehn, B. Munsch, P. Millié, and A. Veillard. Theor. Chim. Acta, 13, 313 (1969).

45. F.A.L. Anet, J.C. Jochims, and C.H. Bradley. J. Am. Chem. Soc. 92, 2557 (1970).

46. J.P. Albrand, D. Gagnaire, and J.B. Robert. Chem. Commun. 1469 (1968).

47. J.P. Albrand, D. Gagnaire, J. Martin, and J.B. Robert. Bull. Soc. Chim. France. 40 (1969).

48. H. Goldwhite and D.G. Rowsell. Chem. Commun. 1665 (1968).

49. P.J. Chivers and T.A. Crabb. Tetrahedron. 26, 3389 (1970).

50. R. Cahill and T.A. Crabb. Org. Magn. Resonance. 4, 259 (1972).

51. D.G. Lister and J.K. Tyler. Chem. Commun. 152 (1966).

52. A.A. Bothner-By and R.H. Cox. J. Phys. Chem. 73, 1830 (1969).

53. W.J. Jorgensen and L.C. Allen. J. Am. Chem. Soc. 93, 567 (1971).

54. T. Axenrod, P.S. Pregosin, and G.W.A. Milne. Chem. Commun. 702 (1968).

55. T. Axenrod, M.J. Wieder, and G.W.A. Milne. Tetrahedron Letters. 6, 401 (1969).

56. T. Axenrod, M.J. Wieder, and G.W.A. Milne. Tetrahedron Letters. 18, 1397 (1969).

57. T. Axenrod. Spectroscopy Letters. 3, 263 (1970).

58. A.H. Cowley, M.J.S. Dewar, W.R. Jackson, and W.B. Jennings. J. Am. Chem. Soc. 92, 1085 (1970).

59. A.H. Cowley, M.J.S. Dewar, W.R. Jackson, and W.B. Jennings. J. Am. Chem. Soc. 92, 5206 (1970).

60. J. Nelson, R. Spratt, and B.J. Walker. Chem. Commun. 1509 (1970).

61. R.S. Rogowski and R.H. Schwendeman. J. Chem. Phys. 50, 397 (1969).

62. K.L. Williamson, Y.L. Hsu, F.H. Hall, S. Swager, and M.S. Coulter. J. Am. Chem. Soc. 90, 6717 (1968).

63. M.S. Gopinathan and P.T. Narasimham. Mol. Phys. 21, 1141 (1971).

64. D.W. White and J.G. Verkade. J. Mah. Res. 3, 111 (1970).

65. T. Axenrod, M.J. Wieder, G. Berti, and P.L. Barili. J. Am. Chem. Chem. Soc. 92, 6066 (1970).

66. R.A. Bernheim and H. Batiz-Hernandez. J. Chem. Phys. 40, 3446 (1964).

67. W.A. Anderson and R. Freeman. J. Chem. Phys. 39, 1518 (1963).

68. J.E. Lancaster. Spectrochim. Acta, 23A, 1449 (1967).

69. M.S. Gopinathan and P.T. Narasimham. Mol. Phys. 22, 473 (1971).

70. G.E. Maciel, J.W. McIver, Jr., N.S. Ostlund, and J.A. Pople. J. Am. Chem. Soc. 92, 11 (1970).

71. G.E. Maciel, J.W. McIver, Jr., N.S. Ostlund, and J.A. Pople. J. Am. Chem. Soc. 92, 1 (1970).

PART IV

INDO Molecular Orbital Calculations On the Conformational Dependence of Long-Range Spin-Spin Coupling of Methyl Protons in Toluene, p-Fluorotoluene and the Xylenes

INTRODUCTION

The "methyl group replacement" technique (1, 2) is often used (2-7) in estimating the π electron contribution to spin-spin coupling constants between protons and protons or other nuclei in conjugated systems. It is based on the idea (2), derived from arguments about proton-electron hyperfine coupling in organic radicals, that a replacement of a hydrogen atom in a C-H bond by a methyl group (under conditions where approximately free rotation of the methyl group occurs) yields a new coupling constant of the same magnitude as, but of different sign to, the original coupling of the replaced proton. This will be roughly true if a π electron mechanism operates to the exclusion of a σ electron mechanism of coupling. For example, in toluene the coupling over six bonds between the methyl protons and the para ring proton, $^{6}J_{p}^{H,CH_3}$ is -0.62 ± 0.02 Hz (8) while it is 0.62 ± 0.03 Hz in a derivative of p-xylene (6).

Such a result is encouraging but extension to the coupling between methyl and ring protons over four and five bonds is problematical in that a σ electron contribution is now more difficult to exclude on theoretical grounds (9-11). Another view (8) holds that the ring-methyl proton coupling constants are transmitted by a mechanism independent of that operating to couple the ring protons themselves. This view is based on the fact that coupling between ring protons is markedly substituent dependent while this is not true of the ring-methyl proton couplings. It is then held that the methyl-ring couplings are propagated by a π electron mechanism.

The general success of the INDO molecular orbital calculations of nuclear spin-spin coupling constants (12-15), particularly in reproducing the observed substituent dependence of ring proton couplings in monosubstituted benzenes (15), encourages their extension to ring-methyl proton couplings in toluene and to the fluorine-methyl proton coupling in p-fluorotoluene for which accurate experimental data (7, 8) are available. Experimental methyl-methyl proton couplings are also known for derivatives of the xylenes (6). In this study such couplings are computed as a function of the rotational angle of the methyl group with the intention of elucidating to some extent the mechanism of coupling and in the hope of their use in future conformational studies by n.m.r.

The discussion takes the view that computed numbers shall be related as closely as possible to the common concepts of the experimentalist, such as the separability of σ and π electron systems, conjugation, hyperconjugation and the like; which are used, for example, in the interpretation of chemical shifts, intensities of infrared spectra of benzene derivatives and of nuclear quadrupole frequencies (16). The INDO formulation, of course, treats all valence electrons on an equal footing but this is not to say that the semiquantitative concepts are no longer necessary or at least useful.

COMPUTATIONAL PROCEDURE

1. Toluene and p-Fluorotoluene

Standard geometries (17, 18) are used to calculate atomic coordinates. The finite perturbation method (12, 18) at the INDO level of approximation (18, 19) is employed with the convergence requirement that for all i

$$10^{-5} < (\rho_{ii}^{old} - \rho_{ii}^{new}) \; / \; \rho_{ii}^{old} \qquad (1)$$

where ρ_{ii} are diagonal elements of the spin density matrix.

When convergence is not reached in 90 SCF cycles, 100 cycles are carried out and the coupling constants are usually not changing by more than 10^{-3} Hz per cycle at that stage. It is felt that the present convergence criterion is more stringent (but also more costly) than one using all elements of the spin density matrices.

All coupling constants are computed in Hz for the conformations 1, 2, and 3 of the methyl group (the dashed lines representing the

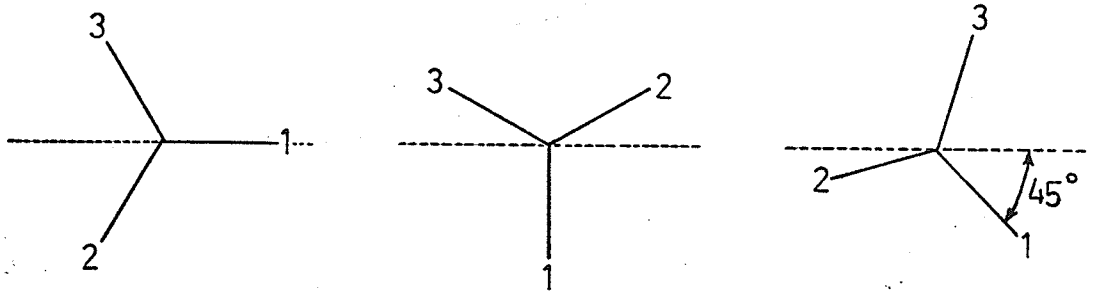

1 2 3

plane of the aromatic ring). The method can be checked by computing

all coupling constants to one of the ring protons situated ortho to the methyl group. Satisfactory agreement with literature values is found (15).

In Table 19 the coupling constants are given as a function of the angle θ, defined as the $H_1C_4C_5C_6$ dihedral angle in 4a and 4b.

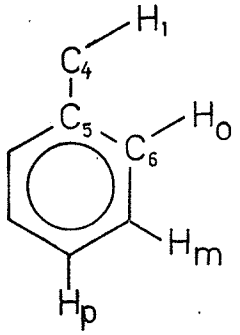

4a (θ=0°)

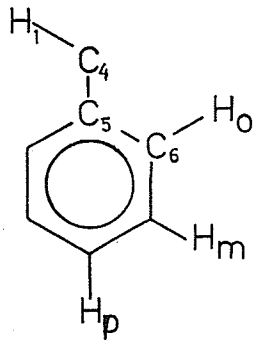

4b (θ=180°)

TABLE 19

Computed long-range coupling constants in Hz of the methyl protons in toluene, A, and in p-fluorotoluene, B

θ, degrees	$^4J^{H,CH_3}_o$		$^5J^{H,CH_3}_m$		$^6J^{H,CH_3}_p$	$^6J^{F,CH_3}_p$
	A	B	A	B		
0	-0.345	-0.343	0.234	0.242	-0.075	-0.008
15	-0.414	-0.416	0.266	0.276	-0.151	0.117
30	-0.606	-0.617	0.358	0.373	-0.357	0.463
45	-0.875	-0.898	0.493	0.515	-0.642	0.935
60	-1.154	-1.189	0.646	0.673	-0.929	1.406
75	-1.370	-1.412	0.786	0.816	-1.141	1.750
90	-1.467	-1.511	0.889	0.918	-1.219	1.872
105	-1.424	-1.464	0.943	0.964		
120	-1.264	-1.294	0.946	0.956		
135	-1.036	-1.052	0.917	0.912		
150	-0.806	-0.807	0.876	0.857		
165	-0.637	-0.627	0.843	0.814		
180	-0.575	-0.562	0.831	0.798		

2. The Xylenes

Again, standard geometries are employed but the convergence parameter in Equation 1 is changed from 10^{-5} to 10^{-4}. Because of computional costs the coupling constants are calculated for a limited number of conformations, given in Tables 20 to 23.

TABLE 20

Computed long-range coupling constants in Hz of the methyl protons in p-xylene

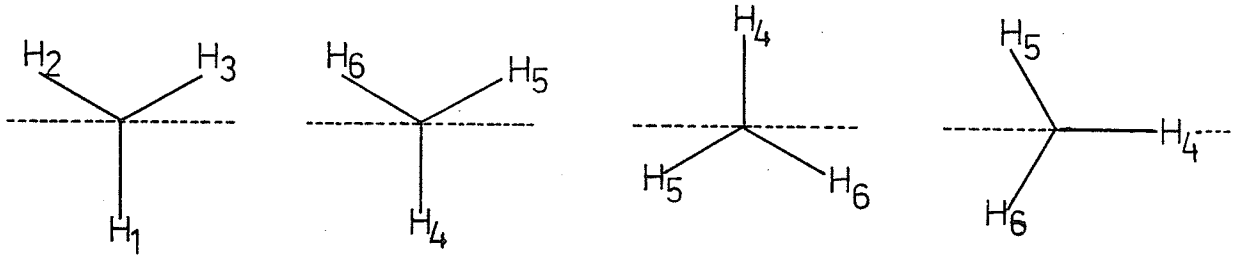

Coupling*	5	6	7
$^{4}J_{o}^{H_1,H}$	-1.484 -1.484	-1.483 -1.483	-1.491 -1.476
$^{5}J_{m}^{H_1,H}$	0.920 0.921	0.931 0.931	0.924 0.927
$^{7}J^{H_1,H_4}$	2.881	2.914	0.141
$^{7}J^{H_1,H_5}$	0.834	0.815	2.218
$^{7}J^{H_1,H_6}$	0.836	0.814	2.187

* The couplings to the ring protons over four and five bonds can be compared to those in Table 19 for $\theta=90^{o}$. The plane of the aromatic ring lies perpendicular to the plane of the paper and is indicated by dashed lines in 5, 6, and 7.

TABLE 21

Computed long-range coupling constants in Hz of the methyl protons in m-xylene

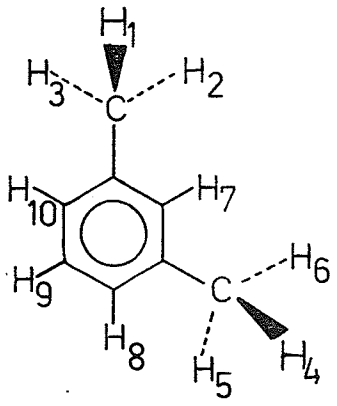

8

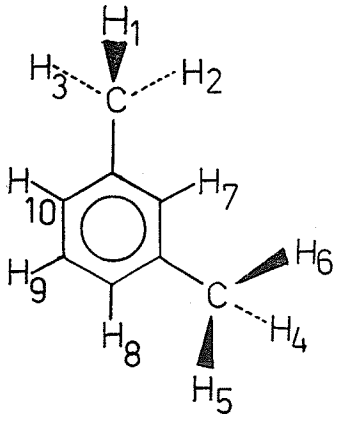

9

Coupling*	8	9
$^{4}J_{o}^{H_1,H_7}$	-1.501	-1.502
$^{4}J_{o}^{H_1,H_{10}}$	-1.484	-1.483
$^{5}J_{m}^{H_1,H_9}$	0.897	0.899
$^{6}J_{p}^{H_1,H_8}$	-1.246	-1.243
$^{6}J^{H_1,H_4}$	-1.936	-1.927
$^{6}J^{H_1,H_5}$	-0.582	-0.596
$^{6}J^{H_1,H_6}$	-0.584	-0.580

* In both 8 and 9, C-H_1 and C-H_4 lie in a plane perpendicular to the plane of the ring. In 8, C-H_4 lies above the plane and lies below the plane in 9. The couplings to the ring protons can be compared with those for $\theta=90^{o}$ in Table 19.

TABLE 22

Computed long-range coupling constants in Hz of the methyl protons in o-xylene for two conformations

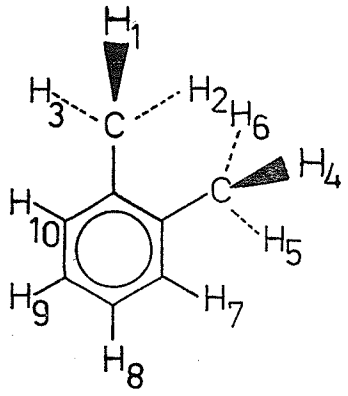

10

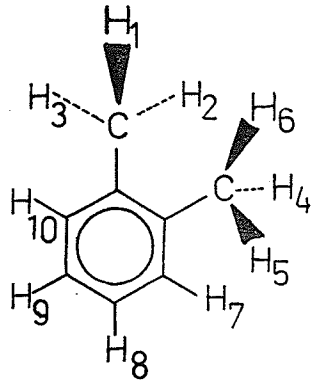

11

Coupling*	X= 1	2	3	1	2	3
$^{4}J_{o}^{H_x,H_{10}}$	-1.479	-0.800	-0.626	-1.473	-0.802	-0.629
$^{5}J_{m}^{H_x,H_9}$	0.913	0.908	0.358	0.919	0.901	0.361
$^{5}J_{m}^{H_x,H_7}$	0.910	0.405	0.881	0.901	0.390	0.899
$^{6}J_{p}^{H_x,H_8}$	-1.223	-0.360	-0.364	-1.221	-0.358	-0.366
$^{5}J^{H_x,H_4}$	2.714	0.931	0.773	2.727	0.701	0.874
$^{5}J^{H_x,H_5}$	0.773	0.214	0.256	0.875	0.033	0.283
$^{5}J^{H_x,H_6}$	0.931	-0.164	0.214	0.700	-0.259	0.277

* The conformations of the methyl groups are as described in Table 21.

TABLE 23

Computed long-range coupling constants in Hz of the methyl protons in o-xylene for three conformations in which two of the methyl protons lie in the plane of the benzene ring

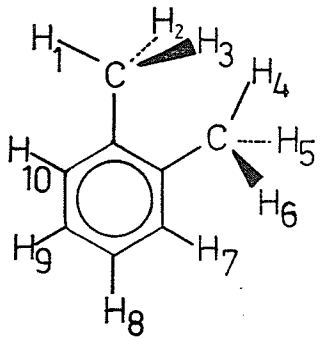

12

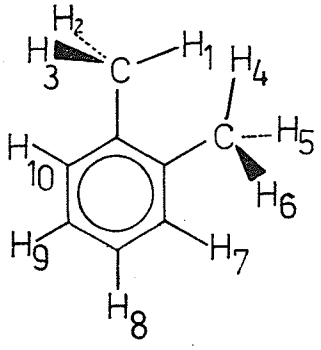

13

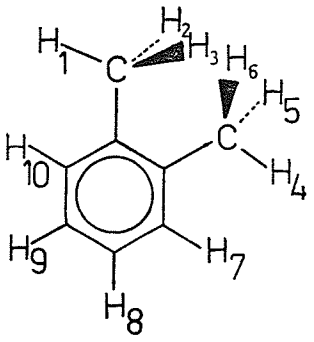

14

Coupling*	X=	1	2	1	2	1	2
$^{4}J_{o}^{H_X,H_{10}}$		-0.380	-1.256	-0.557	-1.179	-0.356	-1.269
$^{5}J_{m}^{H_X,H_9}$		0.277	0.976	0.861	0.662	0.226	0.974
$^{5}J_{m}^{H_X,H_7}$		0.841	0.672	0.280	0.965	0.841	0.673
$^{6}J_{p}^{H_X,H_8}$		-0.091	-0.923	-0.069	-0.936	-0.086	-0.936
$^{5}J^{H_X,H_4}$		-0.400	-0.297	-0.691	0.040	0.060	0.135
$^{5}J^{H_X,H_5}$		0.121	1.740	0.040	1.605	0.135	1.448
$^{5}J^{H_X,H_6}$		0.121	1.529	0.040	1.649	0.135	1.883

* The C-H_1 and C-H_4 bonds lie in the plane of the aromatic ring in each of 12, 13, and 14.

RESULTS AND DISCUSSION

The computed couplings in the tables are quoted to three decimal places in accord with the convergence criteria; experimental values are known to a precision of a few hundredths of a Hz. Note that there are checks on the internal consistency of the calculations; thus conformations 5 and 6 in Table 20 should and do show almost identical couplings from H_1 to the ring protons. Similar checks can be found in the other tables.

Note also that a second methyl group does not appreciably change the magnitude of the ring-methyl proton couplings: compare, for example, Tables 19 and 20. This result may be in part due to the use of standard geometries but is also consistent with the observed insensitivity (3, 6, 8, 20, 21) of the ring-methyl proton coupling constants to substituent effects.

1. Ring-Methyl Proton Couplings in terms of a π Electron Mechanism

By analogy to the McConnell-Heller equation (22) for the hyperfine interaction of methyl protons with the unpaired spin density in the π orbital of the contiguous carbon atom in the conjugated system, a π electron mechanism for the ring-methyl proton coupling suggests that the coupling may be written as

$$J = J_0 + J_1 \sin^2 \theta \qquad (2)$$

The angle θ is defined in 4 and J_0 is presumably small compared to J_1. Therefore J has its largest magnitude when the C-H bond of the methyl group containing the coupled proton lies in a plane perpendicular to the aromatic ring. For free rotation of the methyl group one has $\langle \sin^2 \theta \rangle = 1/2$, a good assumption for toluene (and by implication for

meta and para xylene) in which the barrier to rotation of the methyl group is 0.014 kcal/mol in the gas phase (23). J_1 is known from the computed value of J at $\theta=90^o$ (J_o small).

a) Toluene and p-Xylene

Considering now $^6J^{H,CH_3}_p$ one has from Table 19 that its average value is $-1.22/2 = -0.61$ Hz, in excellent agreement with the known value of -0.62 Hz (8). Alternatively, $<^6J^{H,CH_3}_p> = \{-1.219 - (-0.075)\}/2 - 0.075 = -0.65$ Hz if one assumes that -0.075 Hz($\theta=0^o$) corresponds to a J_0 term in Equation 2, present at all angles θ. Note also that the computed values of $^6J^{H,CH_3}_p$ in Table 19 quite closely obey a $\sin^2\theta$ dependence.

It follows that in p-xylene (Table 20) the coupling between the protons in the two different methyl groups should be $<^7J^{CH_3,CH_3}> = 0.25\ (2.881 + 2.914)/2 = 0.72$ Hz where the mean is taken of the computed values at $\theta=90^o$ for conformations 5 and 6. Or, in terms of a J_0 term, $<^7J^{CH_3,CH_3}> = 0.25\ (2.898 - 0.141) + 0.140 = 0.83$ Hz (note that $0.141 \sim 2|0.075|$). The experimental value in p-xylene itself is unknown but in a p-xylene derivative it is 0.62 ± 0.03 Hz (6).

b) Toluene and m-Xylene and o-Xylene

From the values of $^4J^{H,CH_3}_o$ and $^5J^{H,CH_3}_m$ for toluene in Table 19 it is likely that the computations are not in agreement with a sole π mechanism for these couplings. Each should then have equal magnitudes at $\theta=90^o$ and 180^o - they do not - and they should have a maximum magnitude at $\theta=90^o$; but $^5J^{H,CH_3}_m$ has a maximum near 120^o.

Nevertheless, application of the same argument as for p-xylene yields $<^5J^{H,CH_3}_m> = 0.889/2 = 0.45$ Hz (Table 19) and $<^6J^{CH_3,CH_3}_m>=$

$-1.931/4 = -0.48$ Hz for m-xylene (Table 21). Similarly, $\langle {}^4J_o^{H,CH_3} \rangle = -1.467/2 = -0.73$ Hz (Table 19) and $\langle {}^5J_o^{CH_3,CH_3} \rangle = 2.720/4 = 0.68$ Hz for o-xylene (Table 22). These numbers compare with ${}^4J_o^{H,CH_3} = -0.75$ Hz and ${}^5J_m^{H,CH_3} = 0.36$ Hz observed in toluene (8) and ${}^5J_o^{CH_3,CH_3} = 0.40$ Hz and ${}^6J_m^{CH_3,CH_3} = -0.19$ Hz found in xylene derivatives (6).

One may conclude that on the basis of the "methyl group replacement" model and taking only those conformations where $\theta=90^o$, the computations imply a π electron mechanism for the ring-methyl proton couplings insofar[1] as $-\langle {}^4J_o^{H,CH_3} \rangle \sim \langle {}^5J_o^{CH_3,CH_3} \rangle$ and $-\langle {}^5J_m^{H,CH_3} \rangle \sim \langle {}^6J_m^{CH_3,CH_3} \rangle$, remembering that these averages are obtained by taking $\langle \sin^2\theta \rangle = 1/2$. The experimental data, on the other hand, imply that only a fraction of ${}^4J_o^{H,CH_3}$ and ${}^5J_m^{H,CH_3}$ are accounted for by a π mechanism.

One may now find the mean values over θ of the ring-methyl coupling constants in Table 19, a reasonable approximation to the true mean because numbers are given at 15^o intervals. In this way one finds ${}^6J_p^{H,CH_3} = -0.64$ Hz, ${}^5J_m^{H,CH_3} = 0.69$ Hz, and ${}^4J_o^{H,CH_3} = -0.92$ Hz. Comparison of these close approximations to the true calculated mean with those obtained from $\theta=90^o$ indicates agreement of the computations with a sole π electron mechanism for ${}^6J_p^{H,CH_3}$ but disagreement for the other two couplings. It also suggests that the computed approximate equalities in the magnitudes of the ring-methyl and methyl-methyl proton couplings ($\theta=90^o$) are fortuitous for o-xylene and m-xylene. The observed values of the methyl-methyl proton couplings also imply as much. The matter is discussed further in sections 2 and 3.

---

[1] Valence bond studies (11), when calibrated on the experimental value of ${}^6J_p^{H,CH_3}$ in toluene, give precisely these equalities for a π electron mechanism.

c) Ratio of Q_{CH} and Q_{CCH} from $^6J_p^{H,CH_3}$ and $^7J_p^{CH_3,CH_3}$

The McConnell formulation of π electron coupling between ring and methyl protons predicts that (24, 25)

$$J^{\pi} \alpha Q_{CH}Q_{CCH} \tag{3}$$

where Q_{CH} and Q_{CCH} are isotropic hyperfine coupling constants corresponding to the interaction between a π electron in carbon atomic orbital and the ring and methyl protons, respectively. If $^6J_p^{H,CH_3}$ and $^7J_p^{CH_3,CH_3}$ are dominated by π electron propagation of spin information then one may write

$$Q_{CH}/Q_{CCH} = (^6J_p^{H,CH_3}/^7J_p^{CH_3,CH_3})_{\theta=90^o} = -1.219/1.449 = -0.84$$

from the computations in Tables 19 and 20 and as

$$Q_{CH}/Q_{CCH} = {}^6J_p^{H,CH_3}/{}^7J_p^{CH_3,CH_3} = -0.62/0.62 = -1.0$$

from experimental coupling. The e.s.r. data (26-29) suggest the former ratio as more reasonable, however. INDO methods are markedly successful in calculating unpaired spin distributions in free radicals (30). Of course, the ratios above assume the invariance of other parameters like mobile bond order to the insertion of a second methyl group into toluene.

d) Methyl Proton Couplings in p-Fluorotoluene

An inappreciable substituent effect on $^4J_o^{H,CH_3}$ and $^5J_m^{H,CH_3}$ may be inferred from the computed values in Table 19 and these parameters are indeed equal to within experimental error in toluene (8) and p-fluorotoluene (7).

The mean value of $^6J_p^{F,CH_3}$ is 0.94 Hz in Table 19 while a mechanism ($\theta=90^o$) yields 1.872/2 = 0.94 Hz, hence in correspondence

with such a mechanism. The experimental value is 1.15 ± 0.02 Hz (7). As the theory takes into account only the contact contribution to spin-spin coupling, the close agreement between experiments and theory suggests a minor contribution from magnetic dipole-dipole and orbital-dipole interactions between electron and nucleus.

2. Angular Dependence of $^{5}J_{m}^{H,CH_3}$

Available experimental evidence (31-36) indicates that a proton on a sidechain, for example, an amino, hydroxyl, or aldehydic group, couples by 0.5 to 0.8 Hz over five bonds to a ring proton when $\theta=180^{o}$ as in 15a but does not couple by more than 0.1 Hz when $\theta=0^{o}$ as in 15b. For the methyl group itself no direct evidence is available

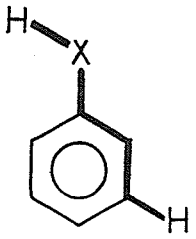

15a ($\theta=180^{o}$)

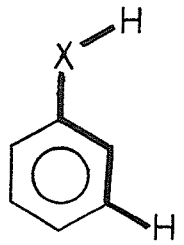

15b ($\theta=0^{o}$)

of course, but in 16, $^{5}J_{m}^{H,H}$ is 0.5 to 0.6 Hz while in 17, $^{5}J_{m}^{H,H}$ is less than 0.1 Hz (37, 38).

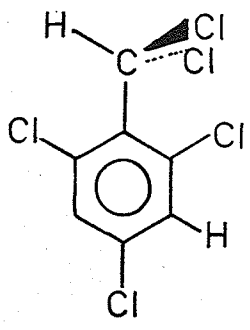

16

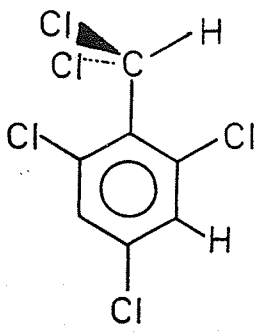

17

$^{5}J_{m}^{H,CH_3}$ in Table 19 is computed as 0.234 Hz when $\theta=0^{o}$, suggesting an overestimate of about 0.2 Hz. A similar situation is found for benzaldehyde (36) where $^{5}J_{m}^{H,CHO}$ is calculated to be 0.20 Hz when $\theta=0^{o}$. Subtraction of 0.234 Hz from the computed value at $\theta=180^{o}$ yields 0.597 Hz, in better agreement with what is known experimentally. Subtraction of 0.234 Hz from each of the values of $^{5}J_{m}^{H,CH_3}$ in Table 19 yields a mean coupling of 0.46 Hz, considerably closer to the experimental value of 0.36 Hz than the mean of 0.69 Hz found without the subtraction.

These considerations allow a reasonable if somewhat arbitrary estimate of the actual angular dependence of $^{5}J_{m}^{H,CH_3}$ and, by implication, of the analogous coupling for protons on other sidechains. In Figure 20 the empirically adjusted $^{5}J_{m}^{H,CH_3}$ numbers are plotted as a function of θ(closed circles) and it is clear that about 70% of the mean value of the coupling is accounted for by the region between 90^{o} and 180^{o} (this is also true, of course, for the unadjusted numbers). A reasonable check of the plot in Figure 20 is available from data (39) on 18,

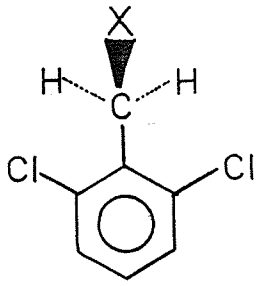

18

where $^{5}J_{m}^{H,CH_2X}$ is almost independent of the nature of X and has a value of 0.35 Hz, the same as in toluene. From Figure 20 the predicted value of 0.39 Hz is extracted, the average of $^{5}J_{m}^{H,CH_3}$ at $\theta=30^{o}$ and 150^{o}, to which the experimental value in 18 corresponds.

Figure 20. The coupling over five bonds between ring and methyl protons in toluene $^{5}J_{m}^{H,CH_3}$, as adjusted by the procedure described in section 2 of the text, is plotted as closed circles versus the dihedral angle θ defined in 4a and b of the text. The open circles give the π electron contribution to $^{5}J_{m}^{H,CH_3}$ as estimated in the text. The crosses give the resultant σ electron contribution to the coupling.

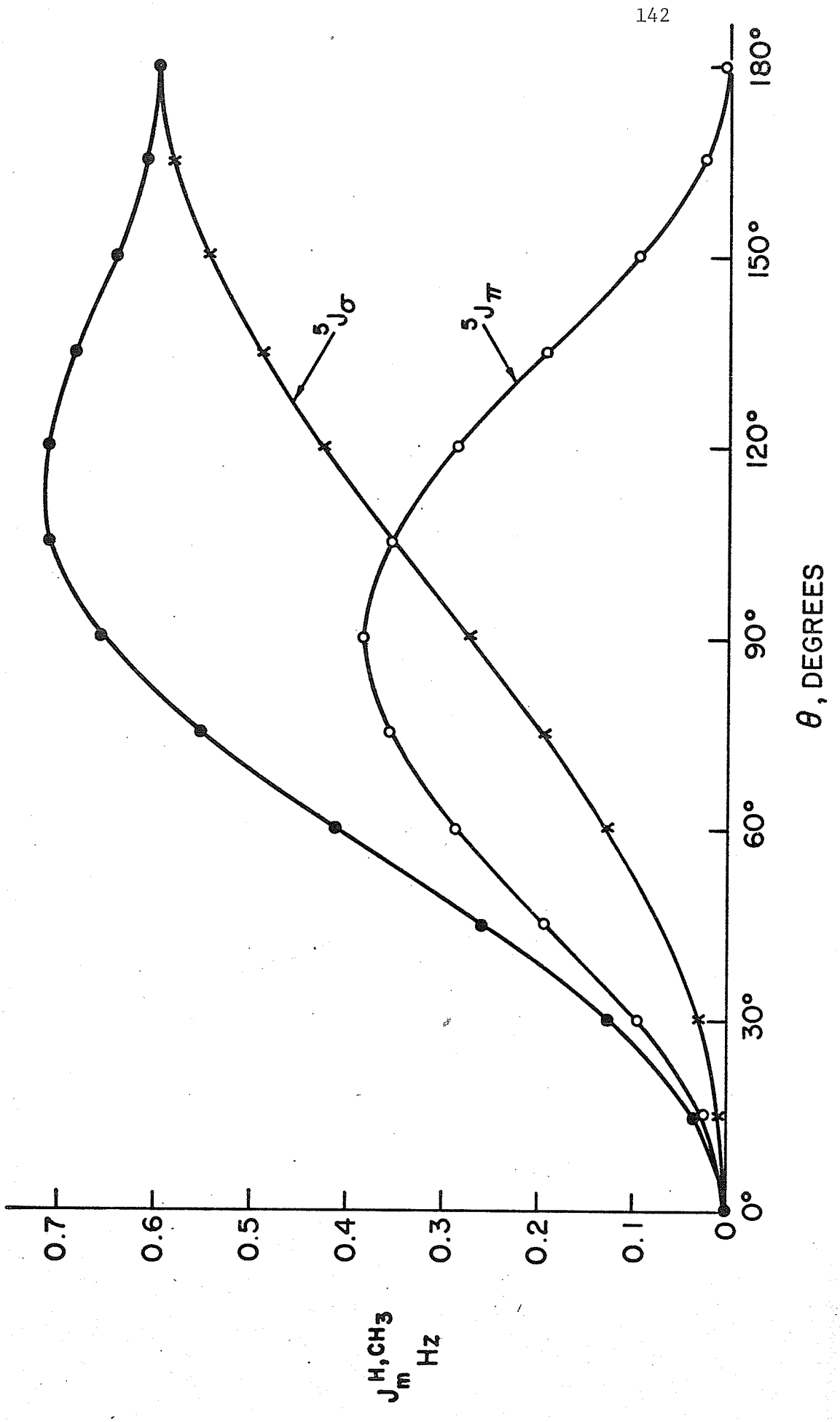
0.7
0.6
0.5
0.4
0.3
0.2
0.1
0
0°
30°
60°
90°
120°
150°
180°
θ, DEGREES
J_m^{H,CH_3} Hz
$^5J_\sigma$
$^5J_\pi$

The shape of the plot in Figure 20 is compatible with π mechanism ($\sin^2\theta$ curve) superimposed on a σ mechanism. An attempt at decomposing this plot into those of the two mechanisms could be undertaken by use of the data in Table 21 on $^6J_m^{CH_3,CH_3}$ were it not for the high probability that they would yield an overestimate of the π contribution (see section 1b). Consequently we take the experimental value of $^6J_m^{CH_3,CH_3}$ = 0.19 Hz in an m-xylene derivative (6) and write $^5J^{H,CH_3}$ = 0.38 $\sin^2\theta$. This function is plotted in Figure 20 as open circles. The σ electron dependence of the coupling is obtained by difference and is the plot consisting of crosses. Its period is twice that of the dependence and it quite closely follows a $\sin^2(\theta/2)$ function. Such a dependence has not been predicted for coupling over five bonds in saturated systems (10).

3. Angular Dependence of $^6J_m^{CH_3,CH_3}$

The computed coupling over six bonds between methyl protons in m-xylene is dominated by a π electron mechanism (Table 21) as can be seen from its θ dependence. Thus $^6J_m^{CH_3,CH_3}$ = -0.585 Hz when $\theta=90^\circ$ and $\theta_2=30^\circ$ for the two methyl groups. Therefore 4 x 0.585 = -2.340 Hz, not much larger than the -1.931 Hz for consistency with a π mechanism the latter representing 80% of the former. Apparently theory overestimates the magnitude of the coupling substantially but qualitatively agrees with the "methyl group replacement" model.

4. Angular Dependence of $^4J_o^{H,CH_3}$

Although in contrast to $^5J_m^{H,CH_3}$ the computed magnitude of $^4J_0^{H,CH_3}$ reaches a maximum at $\theta=90^\circ$ and although -1.47/2 = -0.73 Hz coincides with the measured datum in toluene, the substantial and

different magnitudes at $\theta=0^{o}$ and 180^{o} again indicate that a π mechanism is modified by a σ electron contribution, albeit to a lesser extent than for $^{5}J^{H,CH_3}_{m}$. The mean value for $^{4}J^{H,CH_3}_{o}$ of -0.92 Hz in Table 19 can be brought into agreement with the observed value of 0.75 Hz by subtraction of -0.17 Hz from each calculated value. This may well be a reasonable procedure but there exists no unequivocal experimental data with which to test the computed values at $\theta=0^{o}$ and 180^{o}. The only data are for 19 and 20 where $^{4}J^{H,CHCl_2}_{o}$ is -0.4 Hz (40), corresponding to $\theta=180^{o}$ and consistent with a subtraction of -0.17 Hz from

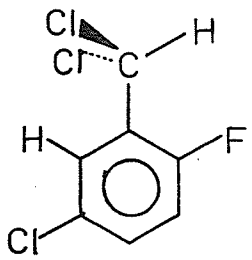

19

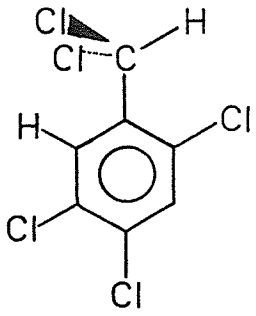

20

the computed value. However, there probably exists an appreciable substituent effect from the chlorine atoms on the sidechain. In addition there probably occurs an appreciable torsional oscillation of the dichloromethyl group about the indicated conformation.

In any event the σ electron contribution to $^{4}J^{H,CH_3}_{o}$ is apparently negative at all angles θ but its numerical angular dependence depends on whether one takes the π contribution as $-2.720/2 = -1.36$ Hz from $\theta=90^{o}$ (o-xylene in Table 22) or as $-0.40 \times 2 = -0.80$ Hz from $\theta=90^{o}$ using the measured value of $^{5}J^{CH_3,CH_3}_{o}$ in an o-xylene derivative. One

objection to these estimates recognizes the possibility of a significant σ contribution to the methyl-methyl proton coupling over five bonds, as implied by four different values of the computed coupling between H_1 and H_5 or H_6 in Table 22, ranging from 0.70 to 0.93 Hz. These couplings should be nearly equal in the event of a π mechanism, as is found in Table 21 for $^6J_m^{CH_3,CH_3}$. Another objection to the estimates cites an appreciable barrier of 2kcal/mol to rotation of the methyl group (41) in o-xylene, arising from mutual hindrance of the two groups and thereby vitiating a simple averaging procedure based on free rotation.

It therefore appears unwise to attempt a numerical separation into σ and π mechanisms in the manner undertaken above for $^5J_m^{H,CH_3}$. One may note, however, that the computed curve implies a dominant π mechanism and, when adjusted by subtraction of -0.17 Hz from each value, predicts significant couplings for $\theta=0^o$ and 180^o. This contrasts with $^6J_p^{H,CH_3}$ and implies that a π mechanism operation by spin polarization, that is, along the H-C-C fragment and then into the π system by a one-center two-electron exchange interaction, is unimportant for nuclear spin-spin coupling in toluene derivatives. The hyperconjugative π electron mechanism, involving interaction of the C-H bond of the methyl group with the π system and obeying a $\sin^2\theta$ relationship, is therefore implied by the INDO fomulation. In consequence the computed values of $^4J_o^{H,CH_3}$ values at $\theta=0^o$ and 180^o may be accepted as σ electron effects.

5. Comparison of the Computed $^4J_o^{H,CH_3}$ in toluene and propene

It is interesting to compare $^4J_o^{H,CH_3}$ in toluene in Table 19 with the analogous cisoid allylic coupling in propene, recently computed in the INDO approximation (42). Both couplings display a maximum magnitude at $\theta=90^o$ but the asymmetry about $\theta=90^o$ in propene is the reverse of that in toluene (Table 4 and Figure 4 of reference 42) in that the magnitude at $\theta=0^o$ is larger than at $\theta=180^o$ for propene. In addition the allylic coupling in propene is calculated to be larger in magnitude at all angles than is $^4J_o^{H,CH_3}$ in toluene, confirming the valence bond results (43) which characterize the aromatic π electron system as less effective than a linear polyene in transmitting spin information, as found experimentally (8, 44).

6. Coupling Mechanism of $^5J_o^{CH_3,CH_3}$ in o-Xylene

In addition to the propagation of coupling via some or all of the intervening bonds, the close proximity of two methyl protons in some conceivable conformations of o-xylene can lead to "direct" interactions in the sense that only the two C-H bonds containing the coupled protons are involved. Normally such interactions are important in coupling over two or three bonds (10). If the proximity is high enough a "through-space" mechanism, proportional to an interaction integral between the two hydrogen 1s orbitals, also becomes possible (10). These two mechanisms need not be considered in the other compounds of this section and they introduce a further complication into the use of $^5J_o^{CH_3,CH_3}$ as a measure of the π electron contribution to $^4J_o^{H,CH_3}$.

Consequently three other conformations of o-xylene, shown in Table 23, were examined in the hope of elucidating the matter. In each of 12, 13, and 14 two of the methyl protons (H_1 and H_4) lie in the plane of the aromatic ring and the coupling is computed between two protons on one methyl group and the three protons on the other group. For symmetry reasons this yields six couplings for each conformation. The striking points about the computed couplings in 10 to 14 are that:

(i) they have a maximum when the C-H bonds containing the coupled protons lie in planes perpendicular to the ring, for example, 2.7 Hz in 10 and 11;

(ii) they have a minimum and are often almost zero when one or both of the coupled protons are situated in the ring plane, for example, $J^{H1,H4}$ is 0.1 Hz in 14 but

(iii) they may also be negative when both coupled protons lie in the aromatic plane or if they are spatially proximate, for example, $J^{H2,H6}$ is -0.2 Hz in 10 and 11; $J^{H2,H4}$ is -0.3 Hz in 12;

(iv) the most negative coupling occurs when the coupled protons are nearest one another, viz., $J^{H1,H4}$ is -0.7 Hz in 13.

Now the π mechanism does not operate if one of the coupled protons is coplanar with the ring. By analogy with the available valence bond formulation for a saturated hydrocarbon (10) a maximum positive σ contribution to the coupling between H_1 and H_4 is expected in 14, the magnitude evidently being independent of the dihedral angle about the aromatic C-C bond (10). Yet $J^{H1,H4}$ is computed as only

0.06 Hz in 14. Therefore the observed negative couplings can probably be attributed to the "direct" and/or the "through-space" mechanisms.[2] Their actual magnitude in o-xylene remains in doubt because unknown and unconsidered distortion of the molecule could in fact bend the methyl groups significantly away from a regular geometry.

In general the computed couplings in Tables 22 and 23 support the dominance of the π mechanism in the methyl-methyl couplings in o-xylene (points i and ii), but in any event overestimate their magnitude. Thus the average of 45 values known from the calculations is 0.75 Hz whereas the observed value is 0.40 Hz in a derivative of o-xylene.

There remains the question whether such a simple averaging procedure is justified for o-xylene. Hot bands in the ultraviolet spectrum of o-xylene (41), heat capacities in the gas phase (45),

---

[2] An exception may be the coupling of -0.4 Hz between H_1 and H_4 in 12 where the C-H_4 bond might interact with C-H_3 and C-H_2. As a point of interest, INDO calculations in which we bring a hydrogen or methane molecule to within van der Waals distances of a methane molecule predict negative couplings between protons in different molecules and imply that these two mechanisms yield negative couplings, at least for some configurations.

neutron scattering results (46), far infrared spectra (47a), and carbon-13 spin relaxation times (47b) agree in finding a barrier of 2kcal/mol to rotation of the methyl group. The equilibrium structure is not known although 14 is assumed in the ultraviolet work. According to INDO the most stable of the five conformations, 10 to 14, is indeed 14, being more stable than 12 by 0.9 kcal/mol and more stable than 10 and 11 by 1.1 kcal/mol, while conformation 13 is less stable than 14 by 4.8 kcal/mol. At room temperature 14 is therefore weighted about 4 to 1 relative to 10, 11, or 12 while 13 need not be considered, probably because of strong nonbonded repulsion between H_1 and H_4. Perusal of the data in Tables 22 and 23, however, demonstrates that this weighing procedure will not change the computed $^5J_o^{CH_3,CH_3}$ appreciably from that obtained by a simple average. Even if 14 is more stable than all other conformations by 2 kcal/mol this conclusion stands.

7. Barrier to Methyl Group Rotation in Toluene

The present calculations predict that 1 is lower in energy than 2 by 0.013 kcal/mol and that 3 is of intermediate stability. The experimental barrier is 0.014 kcal/mol (23). For p-fluorotoluene the calculations similarly give 0.0138 kcal/mol in exact agreement with the experimental barrier (48). The chemical shifts of the alkyl protons in a series of alkylarenes are best interpreted in terms of a preferred conformation in which a C-H bond of the sidechain eclipses the aromatic plane, in qualitative agreement with the INDO predictions(49).

8. Geminal Couplings between Methyl Protons, $^2J_g^{H,H}$

The experimental value of $J_g^{H,H}$ in methane is -12.4 Hz (50) while INDO calculates -6.13 Hz (18). In toluene $J_g^{H,H}$ is expected to

depend on the conformation of the molecule (51). Present calculations are summarized in 21 and 22 where dashed lines indicate the plane of the ring and, for example, $J^{H_2H_3}$ is -7.5 Hz in 21. Relative to methane

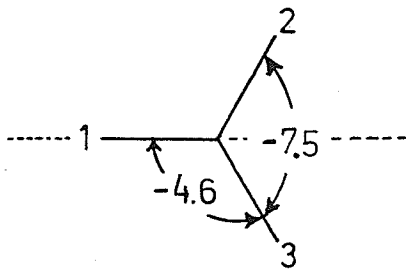

21

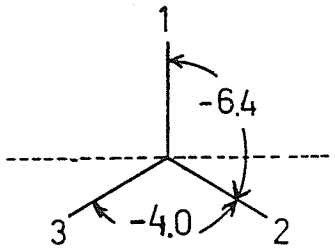

22

a positive shift in the calculated J_g occurs when the line joining the coupled protons is parallel to the ring plane or when one of the coupled protons lies in this plane. A negative shift occurs when the joining line is perpendicular to the ring plane or when one of the C-H bonds containing the proton lies in a plane perpendicular to the ring. Experimental data (52) suggest that the observed negative shift in J_g in the presence of a π system is largest when the joining line is perpendicular to the ring plane, qualitatively bearing out the calculated value of -7.5 Hz in 21.

In terms of an earlier MO theory (51) the negative shift in J_g arises from hyperconjugative withdrawal of electrons from the methyl group by the aromatic nucleus. The INDO calculations predict that the charge in the hydrogen orbital of the C-H bond of the methyl group decreases by 0.01 electron units (from -0.024 to -0.013 units) as θ goes from 0° to 90°, this change accurately following a $\sin^2\theta$

dependence and in agreement with a hyperconjugative effect. The earlier theory is not in qualitative agreement with the calculated coupling of -4.6 Hz between H_1 and H_3 in 21 because it predicts a negative shift from the methane value when one proton is situated in the ring plane. On the other hand, the earlier theory agrees with the positive shift calculated for the coupling between H_2 and H_3 in 22.

SUMMARY AND CONCLUSIONS

The calculations by molecular orbital theory in the INDO approximation are in quantitative agreement with experiment for $^{6}J_{p}^{H,CH_3}$ in toluene and are in accord with a π mechanism for the propagation of the spin information; similarly for $^{6}J_{p}^{F,CH_3}$ in p-fluorotoluene. The calculations for $^{5}J_{m}^{H,CH_3}$ can be interpreted in terms of a predominant σ electron mechanism which, however, apparently makes a much smaller relative contribution to the calculated $^{4}J_{o}^{H,CH_3}$.

The calculated methyl-methyl proton couplings in the xylenes are dominated by a π electron mechanism but are rather larger in magnitude than the observed values in xylene derivatives. The computations indicate the likelihood of negative values for $^{5}J_{o}^{CH_3,CH_3}$, caused by "direct" or even "through space" mechanisms, in conformations where the coupled protons are in close proximity.

An earlier MO theory of the conformational dependence of geminal proton coupling in the methyl group of toluene is in rough qualitative agreement with the INDO formulation.

The calculated barriers to rotation of the methyl group in toluene and p-fluorotoluene are in quantitative accord with experiment. The preferred conformation is one in which a C-H bond of the methyl group eclipses the plane of the aromatic nucleus.

REFERENCES FOR PART IV

1. R.A. Hoffman. Mol. Phys. 1, 326 (1958).
2. R.A. Hoffman and S. Gronowitz. Acta Chem. Scand. 13, 1477(1959).
3. D.J. Blears, S.S. Danyluk, and T. Schaefer. J. Chem. Phys. 47, 5037 (1967).
4. J.B. Rowbotham, R. Wasylishen, and T. Schaefer. Can. J. Chem. 49, 1799 (1971).
5. R. Hoffman and S. Gronowitz. Arkiv Kemi, 16, 471 (1960).
6. C.J. Macdonald and W.F. Reynolds. Can. J. Chem. 48, 1002 (1970).
7. R. Wasylishen and T. Schaefer. Can. J. Chem. 49, 94 (1971).
8. M.P. Williamson, R. Kostelnik, and S.M. Castellano. J. Chem. Phys. 49, 2218 (1968).
9. H. Frischleder and G. Bär. Mol. Phys. 11, 359 (1966).
10. M. Barfield and M. Karplus. J. Am. Chem. Soc. 91, (1969).
11. M. Barfield and B. Chakrabarti. J. Am. Chem. Soc. 91, 4346 (1969).
12. J.A. Pople, J.W. McIver, Jr., and N.S. Ostlund. J. Chem. Phys. 49, 2960, 2965 (1968).
13. G.E. Maciel, J.W. McIver, Jr., N.S. Ostlund, and J.A. Pople. J. Am. Chem. Soc. 92, 1 (1970).
14. M. Barfield, C.J. Macdonald, I.R. Peat, and W.F. Reynolds. J. Am. Chem. Soc. 93, 4195 (1971).
15. G.E. Maciel, J.W. McIver, Jr., N.S. Ostlund, and J.A. Pople. J. Am. Chem. Soc. 92, 4506 (1970).
16. A.R. Katritzky and R.D. Topsom. Angew. Chem. Int. Ed. 9, 87 (1970).
17. J.A. Pople and M.S. Gordon. J. Am. Chem. Soc. 89, 4253 (1967).

18. J.A. Pople and D.L. Beveridge. Approximate molecular orbital theory. McGraw-Hill Book Company, New York, N.Y., 1970.

19. P.A. Dobosh. Program number 141. Quantum chemistry program exchange. University of Indiana, Bloominton, Indiana.

20. G. Kotowycz and T. Schaefer. Can. J. Chem. 44, 2743 (1966).

21. D. Gagnaire and Trinh-Huu-Ich. Bull. Chem. Soc. Fr. 3763 (1966).

22. C. Heller and H.M. McConnell. J. Chem. Phys. 32, 1535 (1960).

23. H. Rudolph, H. Dreizler, A. Jaeschke, and P. Wendling. Z. Naturforsch. 22a, 940 (1967).

24. H.M. McConnell. J. Chem. Phys. 30, 126 (1959).

25. M.J.S. Dewar and R.C. Fahey. J. Am. Chem. Soc. 85, 2704 (1963).

26. J.V. Acrivos. Mol. Phys. 5, 1 (1962).

27. R.A. Hoffman. Arkiv Kemi, 17, 1 (1961).

28. A.D. McLachlan. Mol. Phys. 2, 223 (1959).

29. T.M. McKinney and D.H. Geske. J. Am. Chem. Soc. 89, 2806 (1967).

30. J.A. Pople, D.L. Beveridge, and P.A. Dobosh. J. Am. Chem. Soc. 90, 4201 (1968).

31. J.A. Weil, A. Blum, A.H. Heiss, and J.K. Kinnaird. J. Chem. Phys. 46, 3132 (1967).

32. R. Wasylishen and T. Schaefer. Can. J. Chem. 48, 1263 (1970).

33. S. Forsén and R.A. Hoffman. J. Mol. Spectrosc. 20, 168 (1966).

34. T. Schaefer and G. Kotowycz. Can. J. Chem. 46, 2865 (1968).

35. G.J. Karabatsos and F.M. Vane. J. Am. Chem. Soc. 85, 3886 (1963).

36. R. Wasylishen and T. Schaefer. Can. J. Chem. 49, 3216 (1971).

37. T. Schaefer, R. Schwenk, C.J. Macdonald, and W.F. Reynolds. Can. J. Chem. 46, 2187 (1968).

38. B.J. Fuhr, B.W. Goodwin, H.M. Hutton, and T. Schaefer. Can. J. Chem. 48, 1558 (1970).

39. A.F. Janzen and T. Schaefer. Can. J. Chem. 49, 1818 (1971).

40 H.M. Hutton, J.B. Rowbotham, B.H. Barber, and T. Schaefer. Can. J. Chem. 49, 2033 (1971).

41. K.C. Ingham and S.J. Strickler. J. Chem. Phys. 53, 4313 (1970).

42. M. Barkield. J. Am. Chem. Soc. 93, 1066 (1971).

43. M. Barfield and B. Chakrabarti. Chem. Rev. 69, 757 (1969).

44. A.A. Bothner-By and C. Naar-Colin. J. Am. Chem. Soc. 83, 231 (1961).

45. W.J. Taylor, D.D. Wagman, M.G. Williams, K.S. Pitzer, and F.D. Rossini. J. Res. Natl. Bur. Std. 37, 95 (1946).

46. J.J. Rush. J. Chem. Phys. 47, 3936 (1967).

47. (a) G.W.F. Pardoc, S.J. Larson, H.A. Gebbie, S.J. Strickler, K.C. Ingham, and D.G. Johnson. J. Chem. Phys. 52, 6426 (1970).
(b) K.F. Kuhlmann and D.M. Grant. J. Chem. Phys. 55, 2998 (1971).

48. H.D. Rudolph and H. Seiler. Z. Naturforsch. 20a, 1682 (1965).

49. R.J. Ouellette, B.K. Sinha, J. Stolfo, C. Levin, and S. Williams. J. Am. Chem. Soc. 92, 7145 (1970).

50. M. Karplus, D.H. Anderson, T.C. Farrar, and H.S. Gutowsky. J. Chem. Phys. 27, 597 (1957).

51. J.A. Pople and A.A. Bothner-By. J. Chem. Phys. 42, 1339 (1965).

52. M. Barfield and D.M. Grant. J. Am. Chem. Soc. 85, 1899 (1963).

APPENDIX

The transmission of spin information by a π-electron system and by the σ-π exchange interaction is nicely illustrated by INDO calculations on conformation 1 of toluene. Figure A1 shows the result

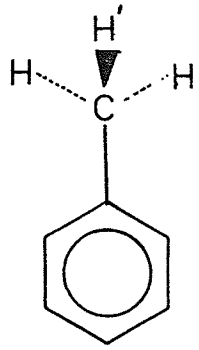

1

of perturbing, that is, adding a finite unpaired electron spin to the 1s orbital of the methyl proton, H', which is perpendicular to the aromatic ring plane. Notice that approximately 10% of the unpaired spin density at H' is transferred into the π orbitals of the aromatic ring system.

The effect of perturbing a proton in the aromatic ring plane, H'', in 2 is illustrated in Figure A2. In this case notice that INDO

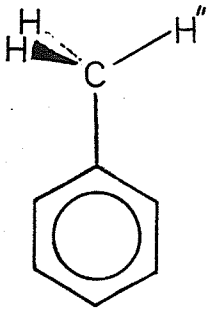

2

predicts that less than 1% of the unpaired spin density at H'' is transferred into the π system.

Finally the results of a CNDO/2 calculation on conformation 1 of toluene is of interest. The effect of perturbing the methyl proton H' is shown in Figure A3. Notice that although approximately 10% of the unpaired spin density is transferred effectively into the aromatic π system, this information is not transferred efficiently to the 1s orbitals of the ring hydrogen atoms. This is in part due to the neglect of σ-π exchange integrals in the CNDO formalism.

The unpaired spin densities in the 1s ring proton orbitals can be converted to nuclear-spin-nuclear-spin coupling constants, in units of Hz, by the following expression,

$$J(H_{methyl}, H_{ring}) = 105.044724\rho/h.$$

Figure A1. The transmission of spin information from the methyl group proton, H_1', in toluene 1. All spin densities were calculated using INDO and are in units of $\rho/h_{H'}$ where $h_{H'}=10^{-3}$ hartrees. The x-y plane corresponds to the aromatic ring plane; the y-axis passes through H_{13}, C_8, C_5, and C_4.

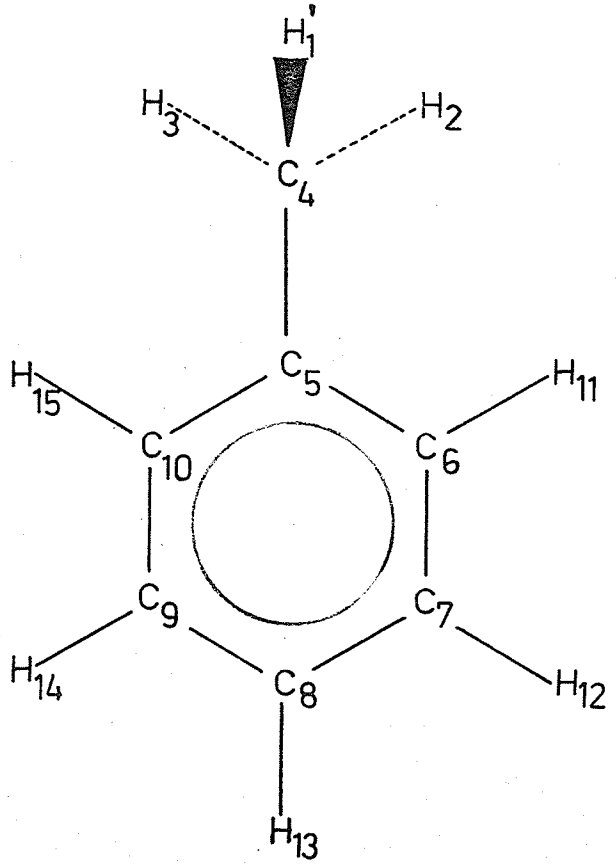

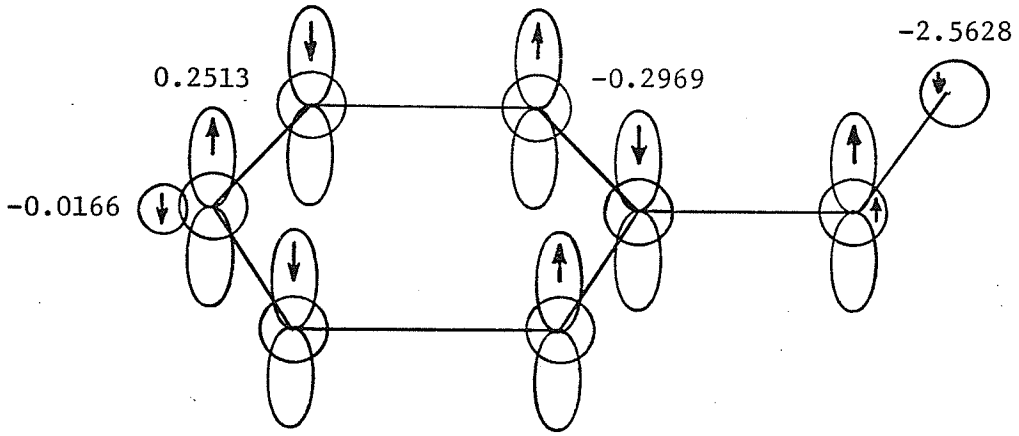

Atom	Orbital	Unpaired Spin Density (ρ/h)
H_1'	1s	-2.5628
C_4	2s	0.4217
	$2p_x$	0.0891
	$2p_y$	0.3236
	$2p_z$	1.7386
C_5	2s	-0.0285
	$2p_x$	-0.0184
	$2p_y$	-0.0439
	$2p_z$	-0.2969
C_6	2s	0.0176
	$2p_x$	0.0145
	$2p_y$	0.0143
	$2p_z$	0.2829
C_7	2s	-0.0125
	$2p_x$	-0.0098
	$2p_y$	-0.0128
	$2p_z$	-0.1779
C_8	2s	0.0143
	$2p_x$	0.0120
	$2p_y$	0.0102
	$2p_z$	0.2513
H_{11}	1s	-0.0139
H_{12}	1s	0.0085
H_{13}	1s	-0.0116

Figure A2. The transmission of spin information from the methyl group proton, H'', in toluene 2. All spin densities were calculated using INDO and are in units of $\rho/h_{H''}$ where $h_{H''}=10^{-3}$ hartrees. The x-y plane corresponds to the aromatic ring plane; the y-axis passes through H_{13}, C_8, C_5, and C_4.

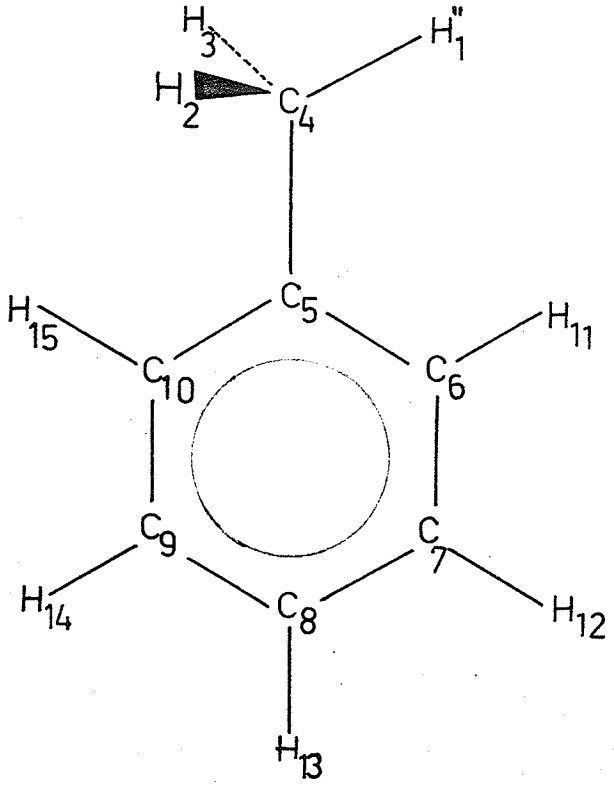

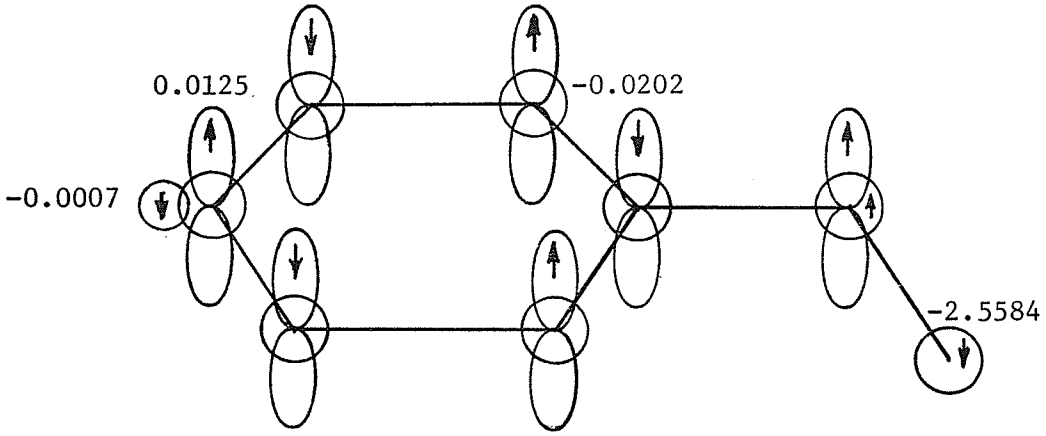

Atom	Orbital	Unpaired Spin Density (ρ/h)
H_1	1s	-2.5584
C_4	2s	0.4259
	$2p_x$	1.7873
	$2p_y$	0.3193
	$2p_z$	0.0817
C_5	2s	-0.0207
	$2p_x$	-0.0297
	$2p_y$	-0.0398
	$2p_z$	-0.0202
C_6	2s	0.0170
	$2p_x$	0.0138
	$2p_y$	0.0115
	$2p_z$	0.0166
C_7	2s	-0.0012
	$2p_x$	-0.0014
	$2p_y$	-0.0018
	$2p_z$	-0.0126
C_8	2s	0.0008
	$2p_x$	0.0008
	$2p_y$	0.0006
	$2p_z$	0.0125
C_9	2s	+0.0016
	$2p_x$	-0.0027
	$2p_y$	+0.0034
	$2p_z$	-0.0125
C_{10}	2s	0.0283
	$2p_x$	0.0291
	$2p_y$	0.0199
	$2p_z$	0.0188
H_{11}	1s	-0.0033
H_{12}	1s	0.0022
H_{13}	1s	-0.0007
H_{14}	1s	0.0079
H_{15}	1s	-0.0055

Figure A3. The transmission of spin information from the methyl group proton, H_1', in toluene 1. All spin densities were calculated using CNDO/2 and are in units of $\rho/h_{H'}$, where $h_{H'}=10^{-3}$ hartrees. The x-y plane corresponds to the aromatic ring plane; the y-axis passes through H_{13}, C_8, C_5, and C_4.

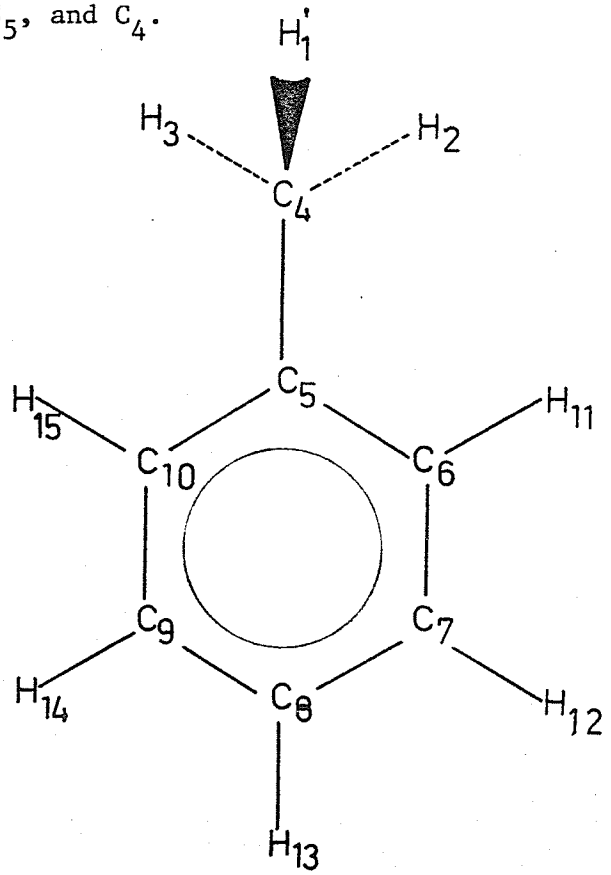

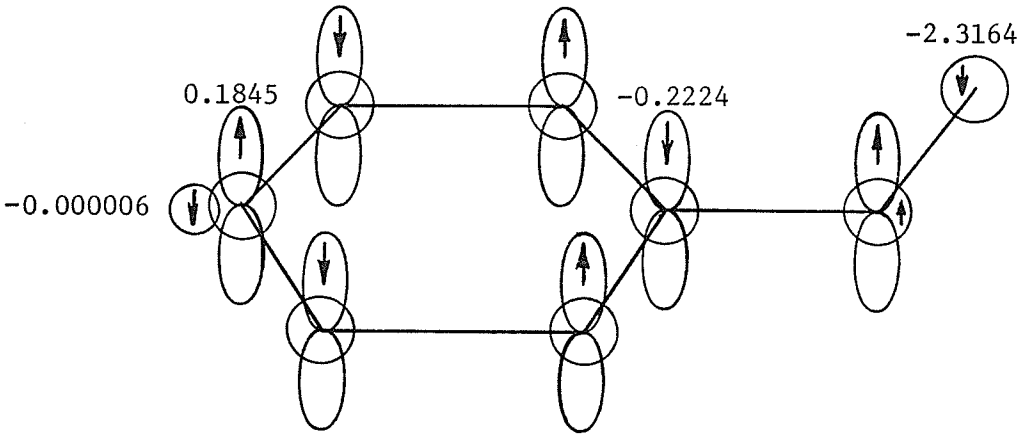

Atom	Orbital	Unpaired Spin Density (ρ/h)
H_1	1s	-2.3164
C_4	2s	0.3205
	$2p_x$	-0.0038
	$2p_y$	0.2206
	$2p_z$	1.6008
C_5	2s	-0.0002
	$2p_x$	-0.0001
	$2p_y$	0.0044
	$2p_z$	-0.2224
C_6	2s	0.0000
	$2p_x$	0.0003
	$2p_y$	-0.0001
	$2p_z$	0.2116
C_7	2s	0.0001
	$2p_x$	-0.0001
	$2p_y$	0.0002
	$2p_z$	-0.1166
C_8	2s	0.0000
	$2p_x$	-0.0000
	$2p_y$	0.0000
	$2p_z$	0.1845
H_{11}	1s	0.00035
H_{12}	1s	0.00016
H_{13}	1s	-0.000006